THE EXPLOSIVE DECOMPOSITION OF ETHYLENE OXIDE VAPOUR

A thesis submitted

for the

DEGREE OF DOCTOR OF PHILOSOPHY

in the

UNIVERSITY OF LONDON

by

RICHARD LEE, B.Sc. (Eng.)., A.C.G.I.

Department of Chemical Engineering
and Chemical Technology,
Imperial College of Science and Technology,
London, S.W.7.

October, 1964.

ABSTRACT.

To assess the hazards involved in the handling of ethylene oxide vapour in plant where a source of ignition may exist, an investigation has been made of the explosive decomposition of this material at temperatures in the range 20° to 100°C and pressures up to 135 PSIA. Analysis of the products of decomposition showed that the formation of ethylene is favoured at low initial pressures whereas that of methane is favoured at higher pressures. The maximum explosion pressure developed during the decomposition explosion is influenced greatly by the rate of heat loss from the flame to the vessel wall; this is especially so with explosions at low initial pressures in vessels of large surface area to volume ratios. At an initial vapour temperature of 100°C, thermochemical calculations indicate that the ratio of the maximum explosion pressure to the initial pressure should not exceed ten at high initial pressures in vessels of large volume to surface area ratio. The decomposition explosion is capable of suppression by inert diluents and the use of nitrogen, in this connection, was studied in detail. The results indicate that previous work is in error and revised data for the safe handling of the vapour are presented. The effect of other diluents such as steam, carbon dioxide, methanol, ammonia and propylene oxide was also investigated. Steam, carbon dioxide and ammonia act as inert diluents, whereas methanol and

propylene oxide are chemically active in the decomposition flame. The effect of pressure on the burning velocities of the ethylene oxide decomposition flame were estimatedand a mechanism for the decomposition reaction is proposed.

Acknowledgements

I am indebted to Dr. K.E. Bett for the supervision of this work, and for his valuable guidance and advice.

I wish to express my gratitude to Dr. J.H. Burgoyne for his interest, and helpful suggestions which he has made during the course of this work.

I am grateful to my wife and parents for their encouragements and endless patience during the course of the research, and for their valuable assistance.

Thanks are due to Mr. A.M. Alger and members of the departmental workshop in modifying and maintaining the apparatus, and to Shell Chemicals Ltd. for financial assistance and for sponsoring of the work.

C O N T E N T S

NOMENCLATURE.

Principal symbols used.

A	Arrhenius constant	
a_o	Initial reactant concentration	g/cc
c_p	Specific heat at constant pressure	cals/g/^oK
C_p	Molar specific heat at constant pressure	cals/mole/^oK
c_v	Specific heat at constant volume	cals/g/^oK
C_v	Molar specific heat at constant volume	cals/mole/^oK
D_j	Diffusion coefficient of j^{th} species	cm^2/s
D	Diameter of vessel	ins. or cms.
E	Activation energy	cals/mole
h	Heat transfer coefficient	$cals/s/cm^2$
ΔH	Enthalpy	cal/mole
ΔH_c	Heat of combustion at constant pressure	cals/mole
ΔH_D	Heat of decomposition at constant pressure	cals/mole
k	Reaction rate constant, 1^{st} order	s^{-1}
L	Length of vessel	ins. or cms.
M	Molecular weight	
N	Number of molecules per cc.	
N_I	Mole fraction of reactant in initial mixture	
N_o	Mole fraction of oxygen in initial mixture	

n_e	Total number of moles at equilibrium condition	
n_i	Total number of moles of initial ethylene oxide	
n_f	Total number of moles of final products	
n_j	Number of moles of j^{th} species	
P^*	Pressure	atm.
$\triangle P'$	Pressure drop due to heat loss	PSI
P_E	Maximum explosion pressure	PSIA
P_{EO}	Maximum explosion pressure for 100% decomposition	PSIA
P'_{EO}	Maximum explosion pressure for 100% decomposition with no heat loss	PSIA
P_F	Final pressure	PSIA
P_{FO}	Final pressure for 100% decomposition	PSIA
P_{FT}	Total final pressure	PSIA
P_I	Initial pressure of ethylene oxide	PSIA
P_{IT}	Total initial pressure	PSIA
Q	Heat loss per second	cals/s
Q'	Heat of reaction of 1 gm of initial mixture	cals/g
R	Gas constant	
S	Surface area	cm^2
S_u	Burning Velocity	cm/s
t	time	s
T_f	Adiabatic equilibrium flame temperature	^oK
T_{fL}	Limit flame Temperature	^oK

T_E	Mean maximum explosion temperature	^oK
T_i	Initial temperature	^oK
$\triangle U_D$	Heat of decomposition at constant volume	cals/mole
$\triangle U_j$	Internal energy of j^{th} species	cals/mole
$\triangle U_{DIS}$	Heat of dissociation	cal/mole
V	Volume of vessel	cm^3
w	rate of chemical reactions	gm/cc/s
α	Molar Ratio of diluent to ethylene oxide, or dimensionless concentration	
β	Fraction of ethylene oxide decomposed	
θ	Dimensionless temperature	
λ	Thermal conductivity	cals/s/^oK/cm.
ρ	Density	g/cc
μ	viscosity	poises
η	Heat loss fraction.	

CHAPTER I

INTRODUCTION.

Ethylene oxide first assumed some commercial importance as a fumigant for the control of insect pests in foodstuffs. However, during the last twenty years, its widespread use as a chemical intermediate has raised its status to that of a 'heavy' organic chemical. It has been reported (64), in recent years, that its production in the United States has exceeded 1300 million pounds per annum; in 1960, it was estimated that the production capacity in the United Kingdom exceeded 100 million pounds per annum.

At atmospheric pressure all mixtures of ethylene oxide in air containing more than 3% ethylene oxide are capable of being ignited. Following the occurrence of several explosions during fumigation, consideration was given some years ago to reducing the flammability of ethylene oxide in air. The effect of carbon dioxide on the limits of its flammability in air was studied by several investigators, (27,28,29) which concluded that all possible mixtures of ethylene oxide in air can be made non-flammable at atmospheric temperature and pressure by adding at least 7.15 volumes of carbon dioxide to each volume of ethylene oxide present.

Ethylene oxide can undergo explosive decomposition in the absence of air and this leads to explosion hazards in chemical plants. The use of an inert gas to maintain a non-explosive vapour mixture is the only reliable method to obviate the hazard and one of the primary objects of this investigation was to study the amount of inert diluent required to suppress the explosive decomposition of ethylene oxide vapour under various conditions of temperature and pressure. Diluent gases such as nitrogen, carbon dioxide, steam, methanol, ammonia and propylene oxide were used in this investigation because of their widespread use in the chemical industry. For example, ethylene oxide/water, ethylene oxide/methanol, ethylene oxide/ammonia and ethylene oxide/propylene oxide mixtures are employed for the manufacture of glycols, glycol ethers, ethanolamines and epoxy-polymers respectively. The flammability limits for ethylene oxide/steam mixtures are also important in assessing the hazards that may be involved in the manufacture of ethylene oxide by the direct oxidation process, since steam is used in the separation and purification units. Data for nitrogen and carbon dioxide are of importance in reducing the hazards involved in the storage of ethylene oxide.

The second object of this investigation was to measure the rate of pressure rise and the maximum explosion pressure developed during an ethylene oxide decomposition explosion. This information is needed to facilitate the safe design of plant and explosion relief equipment.

The third object of this investigation was to analyse the products of the decomposition reaction and to measure the burning velocity of the decomposition flame under various pressure conditions in order to obtain information about the mechanism and kinetics of the reaction.

CHAPTER II.

REVIEW OF PREVIOUS WORK.

II A. Thermal decomposition of ethylene oxide vapour.

II A(1) Low temperature range (380 - 450° C).

The homogeneous, non-explosive thermal decomposition of ethylene oxide vapour in the temperature range 380 - 450° C has been studied by a number of investigators. (5-10) From measurements of the rates of pressure increase during decomposition at different initial pressures, the reaction appears to be approximately first order at initial pressures greater than 250 m.m Hg. (5-10) Furthermore, the rates of decomposition and the apparent activation energy of the overall reaction determined by infra-red spectroscopy (11) and those determined by pressure measurements are in good agreement. The activation energies reported (5-10) varied from 52 to 53 kcals per mole of ethylene oxide decomposed. However, rather conflicting conclusions were drawn as to the nature of the decomposition mechanism.

In 1929, Heckert and Mack, (5) proposed that since the isomerisation of ethylene oxide to acetaldehyde is exothermic to the extent of 23 kcals per mole and the activation energy is 52 kcals per mole, an excited species $(CH_3.CHO)^*$ having an excess energy of 75 kcals per mole was produced during the decomposition. Since the first order rate constant for the pyrolysis of acetaldehyde was known to give an activation energy of 46 kcals per mole, it was concluded that the

excited species $(CH_3 \cdot CHO)^{*}$ splits directly into the final products CH_4, CO, C_2H_6 and H_2, although some collisional quenching will also occur. The proposed mechanism for the decomposition was

$$C_2H_4O \longrightarrow (CH_3 \cdot CHO)^{*} \begin{cases} \longrightarrow CH_4 + CO \\ \searrow \tfrac{1}{2} C_2H_6 + CO + \tfrac{1}{2} H_2 \end{cases} \qquad \text{II (1)}$$

Fletcher and Rollefson [7] dismissed Heckert and Mack's conclusion on the grounds that acetaldehyde could not split directly to methane and carbon monoxide and they postulated that although the main reaction of ethylene oxide when heated to 410° C was isomerisation to acetaldehyde, free radicals were also formed simultaneously which decomposed the acetaldehyde by the following chain mechanism:-

$$C_2H_4O \longrightarrow H \cdot CHO + \dot{C}H_2 \qquad \text{II (2)}$$

$$C_2H_4O \longrightarrow CH_3 \cdot CHO \qquad \text{II (3)}$$

$$:CH_2 + C_2H_4O \longrightarrow 2\ \dot{C}H_3 + CO \qquad \text{II (4)}$$

$$\dot{C}H_3 + CH_3 \cdot CHO \longrightarrow CH_4 + \dot{C}H_3 + CO \qquad \text{II (5)}$$

$$2\ \dot{C}H_3 + (M) \longrightarrow C_2H_6 + (M) \qquad \text{II (6)}$$

The authors did not express an opinion as to whether the acetaldehyde formed by equation II (3) was in an excited state.

More recently, the decomposition has been studied by Mueller and Walters [9, 10] in greater detail. Whereas previous investigators relied on the changes in pressure to indicate the extent of the decomposition, these workers carried out an analysis for ethylene oxide at all stages of the reaction and thus were able to base their results on the actual rate of disappearance of ethylene oxide. The reaction was studie

between 350 - 440° C and from 180 - 440 m.m. Hg pressure. The first order rate constant was expressed as

$$k = 1{\cdot}5 \times 10^{13} \; e^{-52,700/RT} \; SEC^{-1} \qquad II\ (7)$$

They also studied the rate of the decomposition in the presence of mercury dimethyl, $Hg(CH_3)_2$, and propylene. The mercury dimethyl was found to increase the reaction rate slightly, indicating the susceptibility of the ethylene oxide to free radical attack. Propylene was found to inhibit the decomposition reaction which showed that free radicals were produced during the reaction. The most interesting aspect of their work was that propylene was found to inhibitcarbon monoxide but increase acetaldehyde formation. Also, mercury dimethyl was found to enhance ketene formation whereas propylene inhibited it. From these findings, Mueller and Walters (9, 10) concluded that the major part of the reaction proceeds through the formation of $CH_3 \cdot CHO$ which undergoes chain sensitised decomposition as in equation II (5). Although, ethylene oxide will give ketene when attacked by methyl radicals, no ketene was detected with a mixture of acetaldehyde and mercury dimethyl. Hence, the authors concluded that ketene does not arise from the radical sensitised decomposition of acetaldehyde and proposed the following mechanisms:-

$$\dot{C}H_3 + C_2H_4O \longrightarrow CH_4 + \dot{C}_2H_3O \qquad II\ (8)$$

$$\dot{C}_2H_3O \xrightarrow{R} \begin{cases} CH_2 = CO + H \\ RH + CH_2 = CO \end{cases} \qquad II\ (9)$$

These authors doubted that reaction II (2) suggested by Fletcher and Rollefson [7] was the main initiation reaction for the following reasons. Firstly, because formaldehyde was found only in minute quantities and secondly because the addition of propylene had no effect on the formaldehyde formation. They believed that the primary process responsible for the production of most of the free radicals in the decomposition of ethylene oxide was as follows:-

$$C_2H_4O \longrightarrow (\text{Intermediate}) \longrightarrow \dot{C}H_3 + H\dot{C}O \qquad \text{II (10)}$$

However, Mueller and Walters [9, 10] did not specify the nature of the intermediate compound or whether the acetaldehyde came from the quenching of an excited species, $(CH_3 \cdot CHO)^*$ or directly from the isomerisation of ethylene oxide. In fact, their work merely indicated some of the important reactions such as those given by equations II (5), II (8), II (9) which take part in the decomposition mechanism of ethylene oxide.

In a recent theoretical treatment of the pyrolysis of ethylene oxide vapour, Benson [12] proposed that the ethylene oxide molecule is initially isomerised to an excited $(CH_3 \cdot CHO)^*$ molecule which may be quenched to give acetaldehyde or decomposed to give free radicals. He estimated the isomerisation rate by similarity with the cyclopropane system as

$$k_{II} = 10^{14.5}\ 10^{-57/\theta}\ \text{sec}^{-1} \qquad \text{II (11)}$$

where $\theta = 4.575\ T$ kcal/mole. This compares well with the first order rate constant reported by Mueller and Walters [9, 10] and is given by equation

II (12) for the pyrolysis of ethylene oxide in the presence of propylene in such quantity that further addition will not reduce the decomposition rate.

$$k_f = 10^{14.34}\ 10^{-57.4/\theta} \qquad \text{II (12)}$$

Benson also compared the half life of the excited $(CH_3 \cdot CHO)^*$ molecule with the time of collision betwen an excited $(CH_3 \cdot CHO)^*$ molecule and an ethylene oxide molecule and concluded that at pressures above $\frac{1}{2}$ atmosphere and at a temperature of 450° C, most of the $(CH_3 \cdot CHO)^*$ will be quenched to give acetaldehyde. This conclusion is in accord with the original suggestion by Heckert and Mack [5] except that these authors put forward an incorrect mechanism for the subsequent decomposition of acetaldehyde. The detection of acetaldehyde by Mueller and Walters [9,10] together with their suggestion that the acetaldehyde also undergoes chain sensitised decomposition further supports Benson's conclusion that most of the excited $(CH_3 \cdot CHO)^*$ molecules are quenched.

II A (2) Higher temperature range (900 - 1300°K).

Only two investigations have been carried out to study the decomposition of ethylene oxide in the temperature range 900 - 1300° K. Crocco, Glassman, Smith [13], employed a flow reactor in which the temperature profile in the exhaust were used as a measure of the extent of the reaction. They worked at atmospheric pressure with a carrier gas (argon, nitrogen or carbon dioxide) containing 2 - 10% by volume of ethylene oxide. The isomerisation of ethylene oxide to acetaldehyde liberates 28 kcal per mole while the pyrolysis of acetaldehyde to methane and carbon

monoxide only liberates 4.5 kcals per mole. Thus the main increase in temperature occurs as a result of the isomerisation process. They observed that the different inert carrier gases employed had no effect on the reaction rate and reported a first order rate constant

$$k_1 = 10^{11} \quad 10^{-42/\theta} \quad sec^{-1} \qquad II\ (13)$$

The activation energy of 42 kcal/mole obtained by Crocco et al [13] is low compared to the value of 52.7 kcals per mole obtained by Mueller and Walters [9,10] at a lower temperature of 440° C. The crudeness of the method for the rate measurement employed by Crocco et al probably accounts for the descrepancy in these values.

Lossing, Ingold and Tickner [14], carried out experiments in a similar temperature range but at a much lower pressure. Helium gas at about 10 - 15 m.m. Hg. pressure containing 0·1% by volume of ethylene oxide was allowed to diffuse from the reactor, through a small hole into an ionisation chamber of a mass spectroscope where the mass and concentration of the radicals and molecules were measured directly. They reported that the ethylene oxide decomposition rate under these conditions is a first order rate process with an activation energy of 42 kcals per mole.

$$k_1 = 10^{9\cdot9} \quad 10^{-42/\theta} \ sec^{-1} \qquad II\ (14)$$

Again, the activation energy is low compared to the lower temperature experiments of Mueller and Walters [9,10]. In a discussion of this work, Polanyi [15] suggested that the presence of a non-uniform temperature distribution in the reactor could account for the discrepancy in the rate measurements. However, one of the most interesting aspects of Lossing's

work was that 0·6 moles of $\dot{C}H_3$ was produced per mole of ethylene oxide decomposed. This is the only investigation which has provided direct evidence of the presence of methyl radicals. No evidence was found for the presence of $:CH_2$, H, $H\cdot CHO$, $\dot{C}_2H_3O$ or $CH_3\cdot CHO$, presumably either these substances were present in minute quantities or had too short a life for detection. Thus it was concluded that methyl radicals played an important role in the high temperature decomposition mechanism of ethylene oxide.

It is concluded that the values for the rate constant of thermal decomposition of ethylene oxide vapour at temperatures in the range 900° - 1300° K are unreliable. The low temperature kinetic datum of Mueller and Walters [9,10] for the thermal decomposition of ethylene oxide is thought to be most reliable and is assumed to be valid for the high temperature conditions. The first order rate constant is given as

$$k = 1\cdot5 \times 10^{13} \; e^{\frac{-52,700}{RT}} \; sec^{-1} \qquad II\ (7)$$

As far as the decomposition mechanism is concerned, it is apparent that the thermal decomposition is a unimolecular process which proceeds via isomerisation to form an excited $(CH_3\cdot CHO)^{*}$ species. The excess energy in the excited molecule is given by the sum of the heat of isomerisation, 28 kcals/mole, and the activation energy, 52.7 kcal/mole. This excess energy which is about 3 kcal/mole greater than that of the c-c bond in $CH_3\cdot CHO$ which will cause the $(CH_3\cdot CHO)^{*}$ to decompose to give methyl and formyl radicals; some collision quenching will also occur to give acetaldehyde. Free radical mechanisms of the type given by equations II (5), II (6), II (8), II (9) and II (10) will then occur.

II B Explosive decomposition of pure ethylene oxide vapour.

In 1949, Burden and Burgoyne [16] carried out an investigation on the explosive decomposition of ethylene oxide in a closed tube at a temperature of 18° C and found all mixtures containing more than 3·6% ethylene oxide, as well as ethylene oxide itself, were combustible when ignited by a high temperature point source. At concentrations greater than 70% ethylene oxide in air, the colour of the flame changed from being luminous to that of pale blue which was invisible in daylight. They concluded that the explosive decomposition of pure ethylene oxide vapour plays an important role in rich mixture flames. In fact Burden and Burgoyne [16] were the first to demonstrate that the decomposition flame could propagate through pure ethylene oxide vapour. However, since downward propagation in a vertical tube was not found to be feasible it is apparent that the propagation of the decomposition flame is only marginally possible. They postulated the overall reactions for the explosive decomposition of ethylene oxide vapour as:-

$$C_2H_4O \longrightarrow CO + CH_4 \quad \Delta H = -32{\cdot}0 \text{ kcal/mole} \qquad \text{II (15)}$$

$$C_2H_4O \longrightarrow CO + \tfrac{1}{2} C_2H_4 + H_2 \quad \Delta H = -8{\cdot}0 \text{ kcal/mole} \qquad \text{II (16)}$$

$$C_2H_4O \longrightarrow CO + \tfrac{1}{2} C_2H_6 + \tfrac{1}{2} H_2 \quad \Delta H = -24{\cdot}0 \text{ kcal/mole} \qquad \text{II (17)}$$

From the analysis of the products of decomposition at 18° C and atmospheric pressure, it was calculated that 50·2% of the ethylene oxide was decomposed according to reaction II (15); and 23·3% by reaction II (16); and the remaining ethylene oxide remained undecomposed. Reaction II (17) occurred to a small extent.

Gerstein, Mcdonald and Schalla [17] made the first measurements of the burning velocity of an ethylene oxide decomposition flame propagating upwards through a tube under atmospheric pressure and temperature. They assumed reaction II (15) to be the sole reaction and estimated a flame temperature of 1460 - 1600° K. By assuming that Mueller and Walters' [9,10] rate constant for the low temperature decomposition, equation II (7), applied at high temperatures, they were able to calculate the burning velocity of the ethylene oxide decomposition flame according to the flame propagation theories of Semenov [18], Boys and Corner,[19] Adams,[20] and Hirchfelder and Curtiss.[21] The results are shown in Table I.

TABLE I. Comparison of the measured and the calculated burning velocities.

Method	Burning Velocity C/S
Experimental	12.5
Semenov [18]	8.0
Boys and Corner [19]	7.0
Adams [20]	12.0
Hirchfelder and Curtiss [21]	9.6

It can be seen that the measured burning velocity agrees fairly well with the theoretical calculated values. However, in the discussion that followed Gerstein's[17] paper, Burgoyne[17] commented that according to his work [16], ethylene and hydrogen were present in substantial amount in the final products of decomposition. By comparing the heats of reactions of equations II (15), II (16), II (17), it may be deduced that the formation of these compounds lead to a much smaller exothermic overall process and should give a calculated flame temperature of 1220° K. The lower flame temperature reduces the calculated burning velocities and therefore increases the descrepancy between the experimental determined burning velocities and the calculated values given in Table I.

Later in 1952, Friedman and Burke [22][23] succeeded in stabilising an ethylene oxide decomposition flame on a flat-flame burner of the Powling and Egerton [37] type. The burning velocities obtained were less than those of Gerstein et al [17] by a factor of four. This discrepancy led Friedman and Burke [22] to make a detailed analysis of the products in the decomposition flame. Their result for the flames decomposing at atmospheric pressure is shown in Table 2. These results correspond to 54% of ethylene oxide decomposing according to equation II (15) and 46% according to equation II (16). On the basis of these results they calculated that for ethylene oxide initially at 25° C the adiabatic flame temperature should be 1217° K. This was in good agreement with their measured value. Hence the flame temperature of 1465° K assumed

by Gerstein et al [17] in their calculation of the theoretical burning velocity was too high. Since the calculated burning velocity [17] is strongly dependent on the flame temperature, a reduction in the flame temperature from 1500° K to 1250° K would reduce the theoretical burning velocity from 15·0 c/s to 2·4 c/s. Thus, if the flame temperature is taken as 1217° K, Friedman and Burke's [22][23] measured value of 2·7 c/s would only be slightly higher than the calculated one. Friedman and Burke concluded that the method employed by Gerstein et al [17] was unreliable since convective currents influence the velocity of the slow burning flame as it progressed through the tube to an unknown extent. Also inaccurate measurements of the flame area of flames travelling up a tube may lead to errors in the estimation for the burning velocity. It is concluded, therefore that Friedman and Burke's [22][23] result is likely to be the more reliable.

The effect of temperature and pressure on the burning velocity of ethylene oxide has also been studied by Friedman and Burke [22][23] in the temperature range 70° - 130° C. and at pressures up to one and a half atmospheres. As is shown in Chapter III neither effect was found to be in accord with the results expected for a first order rate process. Instead of $S_u \propto p^{-\frac{1}{2}}$, it was found that $S_u \propto p^{-\frac{1}{4}}$. Furthermore, on the basis of the Zeldovich-Frank-Kamenetsky's equation [18] the effect of pre-heating the gas gives an activation energy of 14 Kcals per mole which is much smaller than the value of 52·7 kcals per mole used by Gerstein [17] to predict the magnitude of the burning velocity. It was suggested that although

the burning rate is governed by the first order reaction given by the low temperature decomposition, the subsequent flame reactions are governed by the composition of the decomposition products and therefore by the flame temperature. Increasing the pressure favours the more exothermic reaction II (15) which tends to increase the burning velocity with the result that the decrease in the burning velocity with pressure is less than that demanded by the first order rate law. Similarly, the effect of pre-heat is to promote endothermic reactions and so raise the flame temperature by a smaller amount than that calculated from the heat capacities of the burnt and unburnt gases. In this way, Friedman and Burke [22][23] were able to provide a qualitative explanation of all their experimental data. It is noteworthy that Burgoyne, Bett, Muir [24] in their work on the explosive decomposition of ethylene oxide vapour under pressure found more methane and less ethylene in the decomposition products than were found in the low pressure experiments of Friedman and Burke [22][23]. A summary of the products of decomposition under various conditions is given in Table 2.

TABLE 2. Product of Decomposition at various conditions.

Constituents	Flat Flame[23]	Flame propagation[16]	Explosive Decomposition[24]		Rocket Motor[25]
	volume %.	volume %.	volume %.		volume %.
H_2	19.6	12.7	16.4	16.1	9.5
CO	44.3	46.6	48.7	47.1	48.5
O_2	0	-	-	0.2	-
CH_4	25.9	32.2	32.2	35.2	39.9
C_3H_6	-	-	1.3	1.0	2.1
CO_2	-	1.0	0.2	0.3	-
C_2H_4	10.2	7.5	1.2	-	-
P_I (PSIA)	14.7	14.7	45	135	750 ± 50

II C Hazards and safe handling:-

II C (1) Spontaneous ignition of ethylene oxide and oxygen mixtures:

In 1949, Burden and Burgoyne [16] investigated the ignition and flame reactions of ethylene oxide and showed that oool flames could be initiated in ethylene oxide - oxygen mixtures at atmospheric pressure at temperatures between 270° - 380° C. This temperature range roughly corresponds to that for the formation of cool flames with higher hydrocarbon air mixtures. Small quantities of aoetaldehyde when added to the ethylene oxide vapour were found to lower the minimum temperature for the initiation of cool flames. It is concluded that ethylene oxide - oxygen,

or ethylene oxide - air mixtures are capable of igniting at low temperatures and that two stage combustion may occur.

II C (2). Limits of Flammability for Ethylene Oxide-Air-CO_2 Systems.

Early studies of the physiological properties of ethylene oxide in air showed that its pesticidal effect is promoted by the presence of CO_2 which increases the respiration rate of the insect. For this reason, it was the custom to introduce 10% CO_2 into the commercial ethylene oxide for use as a fumigant. It is not surprising therefore that early consideration was led to the use of CO_2 for suppressing the flammability of ethylene oxide in air. In 1930, Jones and Kennedy [27] found the limits of flammability of ethylene oxide in air with and without CO_2, using the U.S. Bureau of Mines apparatus.[36] Their result agreed well with the subsequent work of Jones [28] and Peters and Ganters [29]. From Jones' result, which is shown in Figure 1, it may be seen that in the absence of CO_2, the limits of flammability of ethylene oxide vapour in air are 3·0% and 80% by volume of ethylene oxide. The effect of CO_2 is to reduce the flammability limits until the mixture contains more than 42% of CO_2 at concentrations above which all possible mixtures of ethylene oxide and air becomes non flammable. The peculiar 'bulge' on ethylene oxide rich side of Figure 1 has been explained by Burden and Burgoyne on the basis that the flame becomes more closely associated with the explosive decomposition of ethylene oxide vapour. However, the peculiar 'bulge' obtained by Jones and Kennedy [27] and Jones [28] using a flame

EFFECT OF CO_2 ON THE FLAMMABILITY LIMITS OF ETHYLENE OXIDE-AIR MIXTURES

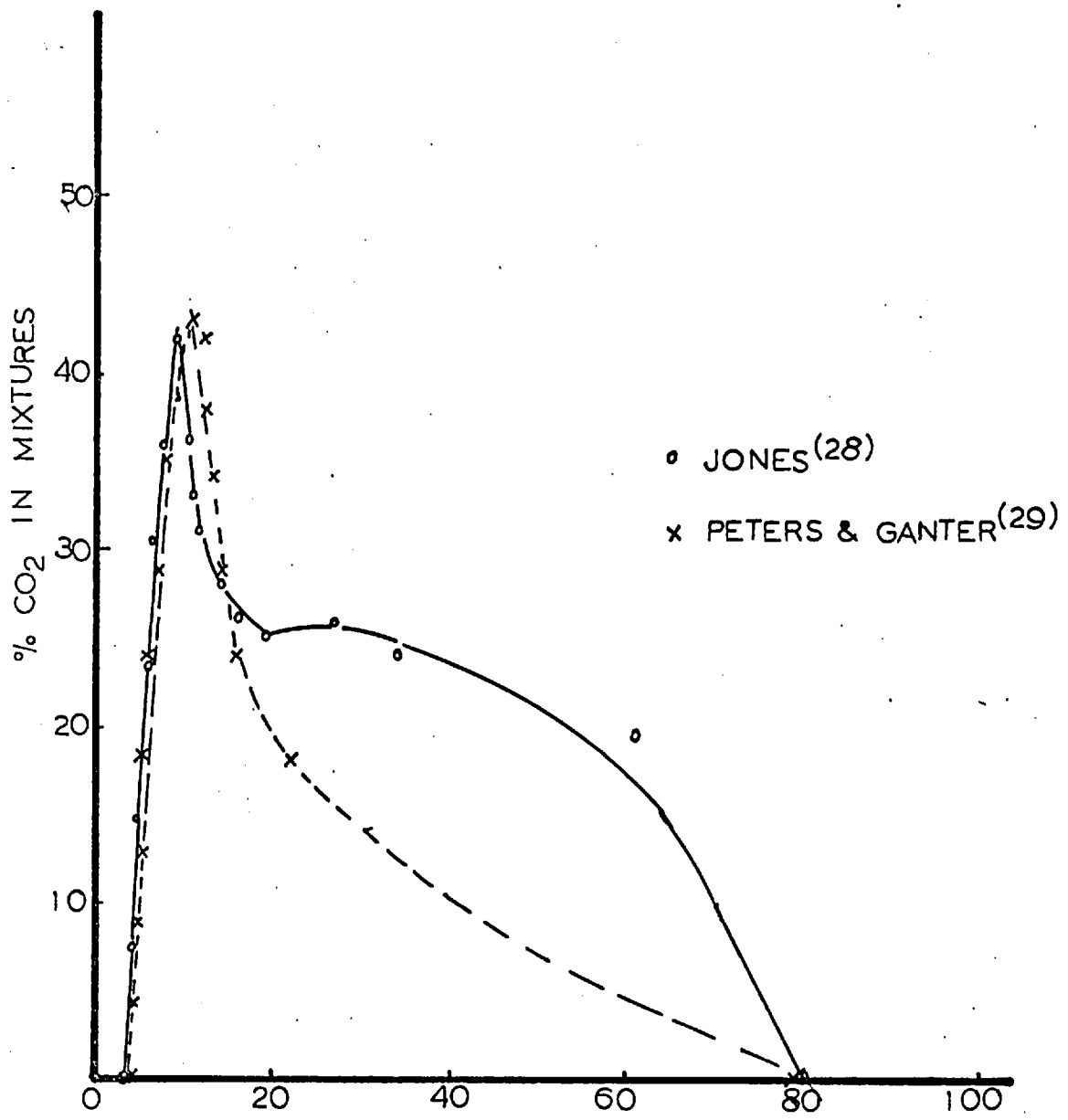

FIGURE 1

for igniting the ethylene oxide mixtures was not obtained by Peters and Ganter [29] who used an electric spark as the ignition source.

Burden and Burgoyne [16] in their closed tube experiments using a hot platinum wire as a source of ignition found that all mixtures containing more than 3·6% ethylene oxide would propagate flame upwards. The effect of reducing pressure on the flammability compositions for these flames at a temperature of 18°C has also been studied by these authors and their result is shown in Figure 2. The lower limit for the flammability of ethylene oxide and air mixture is shown to be little affected by reduced pressure. The decomposition flame of pure ethylene oxide would not propagate at pressures below 633 m.m. Hg, but upper composition limits for ethylene oxide/air flames fell rapidly with diminishing pressure. The determination of the pressure limits was repeated by Burden and Burgoyne [16] for downward propagation in a vertical tube. In these circumstances, these authors found that the blue and the decomposition flames would not propagate.

It is noteworthy that Jones and Kennedy [27] and Jones [28] found an upper flammability limit of 80% ethylene oxide in air. The apparati employed by Jones [28] and Burden and Burgoyne [16] were similar except that Jones employed a flame and Burden and Burgoyne a hot platinum wire to ignite their mixtures. It seems likely that the different ignition sources may account for the discrepancy in the results.

EFFECT OF PRESSURE (REDUCED) ON THE FLAMMABILITY RANGES OF ETHYLENE OXIDE IN AIR

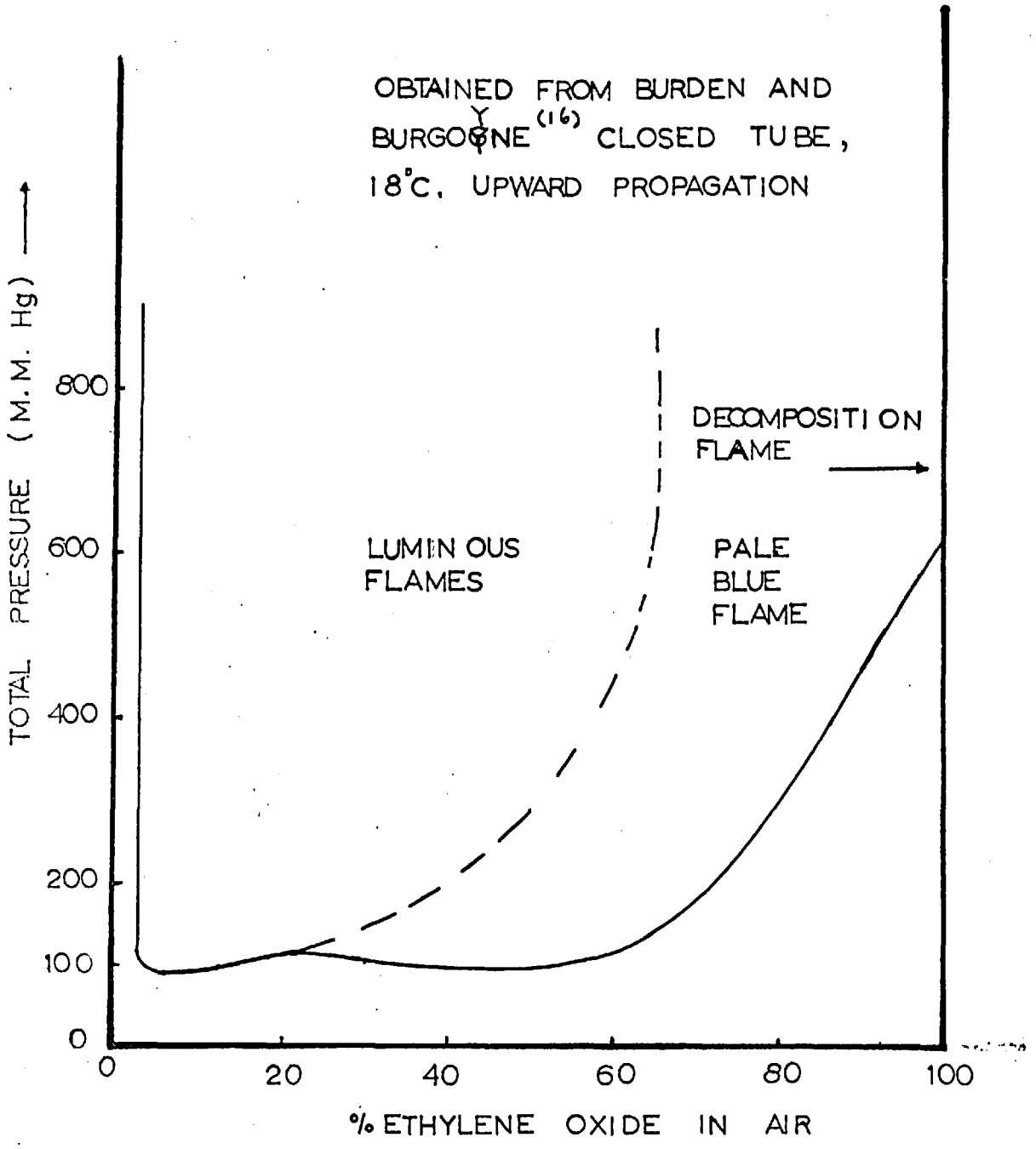

FIGURE 2

II C (3) Ethylene oxide - inert diluents.

Hess and Tilton [26] were the first to determine the limits for the propagation of the decomposition flame in the presence of inert diluents. The experiments were carried out in a closed pressure vessel at temperatures between 30 - 45° C and pressures in the range 30 - 70 psig. A hot platinum wire was employed either as the direct source of ignition or as an ignitor for mercury fulminate. The amount of inert diluent required to suppress the explosive decomposition of ethylene oxide vapour was found to be independent of the initial temperature and pressure. Their results for the flammability limits for mixtures of ethylene oxide and various inert diluents are given in Table 3.

TABLE 3. Flammability limit for ethylene oxide/diluents.

Initial Pressure = 30 psig; T_I = 30-40° C.

Diluent	Lower Limit of Explosibility. % C_2H_4O
H_2	75
N_2	75
CO_2	82
CH_4	85
C_2H_6	93
C_3H_8	95
C_4H_{10}	97

In 1960, Burgoyne, Bett and Muir [24] extended the work to a temperature of 125° C and partial pressures up to 155 psiA using a fusion wire as the ignition source. They also found that the amount of inert diluent required to suppress the explosive decomposition of ethylene oxide was only slightly influenced by temperatures in the range 89° - 184·5° C, but was markedly affected by pressure. For example, by increasing the initial partial pressure of the ethylene oxide vapour from 25 psiA to 135 psiA, the amount of nitrogen required to suppress the decomposition explosion increased from 40 to 65%. The authors attributed this to a change in the mechanism of the reaction such that the exothermicity of the overall reaction increased at higher pressures. The results obtained by Burgoyne et al [24] when extrapolated to the initial conditions of 60° C and a partial pressure of 33 psiA, show that 42% nitrogen is required to suppress the decomposition as compared with the value of 25% found by Hess and Tilton. [26] The large discrepancy in these results has been attributed [63] to the difference in the energy dissipated by the ignition sources used in the two investigations. In view of the practical importance of providing reliable data, one of the objects of this work was to determine the limits for the propagation of the decomposition flame in the presence of inert diluents over a wide temperature range so as to provide a link between the work of Hess and Tilton [26] and that of Burgoyne et al. [24]

II C (4) Development of the maximum explosion pressure:

The maximum pressure developed in a closed vessel as a result of the explosive decomposition of ethylene oxide vapour depends on the shape and size of the vessel. Hess and Tilton [26] studied the effect of the ratio internal surface area to the internal volume of the vessel on the maximum explosion pressure developed at an initial pressure of 5 psig and at a temperature in the range 30° - 40° C. However, they had difficulty in measuring the explosion pressure and tried various devices such as graduated rupture diaphragms, hydraulically activated gauges, a steam engine indicator and an unbonded Stratham strain gauge. They concluded that the ethylene oxide explosion propagated extremely rapidly and that the subsequent pressure rise was too fast for safety valves and rupture diaphragms to provide adequate relief in case of an explosion. Burgoyne [24] et al measured the pressure records during and after the explosions by means of a capacitance type of pressure transducer. The rate of pressure rise, as well as the ratio of the maximum pressure, P_E, to the initial pressure P_I, was found to increase as the initial pressure was increased. At an initial temperature of 125° C, and initial pressures in the range 45-55 psiA, they observed a maximum rate of pressure rise of only 1300 psi/S. In view of this, it is surprising that Hess and Tilton [26] should have found bursting discs and safety valves inadequate for explosion relief. The effect of surface area and internal volume of the vessel was

found to affect the rate of pressure rise as well as the maximum pressure attained during the explosion. As the volume to the internal surface area ratio of the vessel was increased, the maximum explosion pressure developed was found [26][24] to increase linearly. However, from thermochemical data for the reactants and the products, it was deduced that at an initial temperature of 100° C the ratio of the maximum explosion pressure to the initial pressure could not exceed ten even for a vessel of infinite volume/surface area ratio.

CHAPTER III

THEORY.

III A (1) Flame propagation theory:-

Because of the great difficulty of studying the detailed mechanism and kinetics of the successive and inter-related steps in the reaction zone of an ethylene oxide decomposition flame, an attempt was made to obtain some information about the overall kinetics of variables, such as temperature and pressure, on the burning velocity of the flame. A number of theories of flame propagation have been put forward and these have been reviewed by M.W. Evans [48]. For the purpose of this investigation, use was made of the theory of Zeldovich, Frank-Kamenetsky and Semenov, [18] because it has been shown that this theory is applicable to the decomposition flames of hydrazine [49] and ethyl nitrate [50].

The theory of flame propagation as developed by Zeldovich, Frank-Kamenetsky and Semenov assumes that the flame is controlled by a single overall reaction of the type

$$n\,A = B + C + \cdots \qquad \text{III (1)}$$

for which the reaction order may be zero, first or second order with respect to A. Intermediate reactions are not considered. Further assumptions made in the theory are:-

(1) Pressure is assumed constant.

(2) The specific heat, c_p , and the thermal conductivity λ are constant.

(3) The thermal diffusivity $\frac{\lambda}{c_p \rho}$ is equal to the molecular diffusivity, D.

(4) It is assumed that there is a temperature T_{ig} above which all the reaction occurs at the flame temperature T_f and below which no reaction is assumed to occur.

The equations of continuity, energy, state and mass can then be written as follows:-

$$D\rho \frac{d^2(\frac{\alpha}{\alpha})}{dx^2} - M \frac{d(\frac{\alpha}{\alpha})}{dx} - \omega = 0 \qquad \text{(continuity)} \qquad \text{III (2)}$$

$$\frac{\lambda}{c_p} \frac{d^2T}{dx^2} - M \frac{dT}{dx} + \frac{\omega Q'}{c_p} = 0 \qquad \text{(energy)} \qquad \text{III (3)}$$

$$\frac{\rho}{\rho_i} = \frac{T_i}{T} \qquad \text{(state)} \qquad \text{III (4)}$$

$$\rho S = \rho_1 S_1 = M \qquad \text{(conservation of mass)} \qquad \text{III (5)}$$

Assumption (3) allows the continuity and energy equations to be expressed in a similar form by employing dimensionless temperature, and concentration parameters, θ and α respectively. Thus

$$\theta = \frac{c_p (T_f - T_i)}{Q'} \qquad \text{III (6)}$$

$$\alpha = \frac{\alpha_0}{\rho_i} - \frac{\alpha}{\rho} \qquad \text{III (7)}$$

Equations III (2) and III (3) can then be written as

$$D\rho \frac{d^2\alpha}{dx^2} - M \frac{d\alpha}{dx} + \omega = 0 \qquad \text{III (8)}$$

$$\frac{\lambda}{c_p} \frac{d^2\theta}{dx^2} - M \frac{d\theta}{dx} + \omega = 0 \qquad \text{III (9)}$$

Since it is assumed that $\frac{\lambda}{c_p} = D\rho$, equations III (8) and III (9) as well as boundary conditions are identical, then $\alpha = \theta$ and the problem is reduced to solving only one differential equation. Equation III (9) is solved for S_u, by integrating over the pre-heat and the reaction zone separately and establishing the equation of continuity by equating $\frac{d\theta}{dx}$ at $x = x_3$ for the two zones, i.e. $x = x_3$ at $T = T_i$. For reactions obeying the simple Arrhenius rate expression of order 'n',

$$\omega = A\, \alpha^n\, e^{-E/RT_f} \qquad \text{III (10)}$$

then the theory of Zeldovich, Frank-Kamenetsky and Semenov yields the following equations for the burning velocity in the case of zero, first and second order reactions:

zero order $$S_u^2 = \frac{2\lambda_f A}{\bar{c}_{pf} \rho_i^2 c_0} (T_f - T_i) \cdot \frac{RT_f^2}{E} \cdot e^{-E/RT_f} \qquad \text{III (11)}$$

1st order $$S_u^2 = \frac{2\lambda_f c_{pf} A}{\rho_i \bar{c}_{pf}^2 (T_f - T_i)^2} \left(\frac{T_i}{T_f}\right) \left(\frac{n_i}{n_f}\right) \left(\frac{RT_f^2}{E}\right)^2 e^{-E/RT_f} \qquad \text{III (12)}$$

2nd order $$S_u^2 = \frac{2\lambda_f c_{pf}^2 Q_0 A}{\rho_i \bar{c}_{pf}^3 (T_f - T_i)^3} \left(\frac{T_i}{T_f}\right)^2 \left(\frac{n_i}{n_f}\right)^2 \left(\frac{RT_f^2}{E}\right)^3 e^{-E/RT_f} \qquad \text{III (13)}$$

III A (2) Reaction Order:-

By comparing the concentration terms in equations III (11), III (12), III (13), it is evident that the effect of pressure on the burning velocity is a function of reaction order. For a constant initial temperature of T_i , the specific heat c_p , the flame temperature T_f , and the thermal conductivity λ_f can be considered to be independent of pressure

Also, the ratio $\frac{n_i}{n_f}$ is only slightly affected by pressure compared with a_o and ρ_i which are functions of pressure such that $a_o \propto P$ and $\rho_i \propto P$. By grouping the pressure independent terms together in equations III (11), III (12), III (13), it may be shown that:-

for zero order $S_u^2 \propto a_o^{-1} \rho_i^{-1}$ i.e. $S_u \propto P^{-1}$ III (14)

for first order $S_u^2 \propto \rho_i^{-1}$ i.e. $S_u \propto P^{-\frac{1}{2}}$ III (15)

for second order $S_u^2 \propto a_o \rho_i^{-1}$ i.e. $S_u \propto P^{0}$ III (16)

Inspection of equations III (14), III (15), III (16), shows that the burning velocity may be written as

$$S_u \propto P^{\frac{n-2}{2}} \qquad \text{III (17)}$$

III A (3) Activation Energy:-

The activation energy for the overall reaction can also be estimated from equations III (11), III (12), and III (13) by rearranging these equations in terms of the flame temperature and the activation energy. Before this can be done, however, it is necessary to determine the temperature dependence of the terms in these equations as follows:-

(1) The thermal conductivity, λ_f, of the gaseous product is assumed to be proportional to the flame temperature and can be expressed as $\lambda_f = \lambda'_f \frac{T}{273}$ where λ'_f is the thermal conductivity at $0^\circ C$.

(2) The initial density of the reactant is inversely proportional to the initial temperature, and is written as $\rho_i = \rho_{io} \frac{273}{T_i}$ where ρ_{io} is the density at $0^\circ C$.

(3) The values of A, C_p, $\frac{n_i}{n_f}$, and E are all assumed to be independent of temperature.

Therefore, for a first order reaction, equation III (12) can be rewritten as

$$S_u^2 = \left(\frac{2\lambda'_f}{273^2} \frac{A}{\rho_{10}} \frac{C_{pf}}{\bar{c}_p^2} \frac{n_i}{h_f} \frac{R^2}{E^2} \right) \frac{T_i^2 T_f^4}{(T_f - T_i)^2} \epsilon^{-E/RT_f} \qquad \text{III(18}$$

let the temperature independent term be:-

$$B = \left\{ \frac{2\lambda'_f}{(273)^2} \cdot \frac{C_{pf}}{\rho_{10}} \cdot \frac{A}{\bar{c}_p^2} \quad \frac{n_i}{h_f} \cdot \frac{R^2}{E^2} \right\} \qquad \text{III(19}$$

therefore,

$$2 \log S_u = \log B + 2 \log T_i + 4 \log T_f - 2 \log (T_f - T_i) \frac{-E}{2{\cdot}303\, RT_f} \qquad \text{III(20}$$

$$\text{let } f(T) = 2 \log T_i + 4 \log T_f - 2 \log (T_f - T_i) - 2 \log S_u$$

$$\text{then } f(T) = \frac{E}{2{\cdot}303\, RT_f} - \log B - \qquad \text{III(21}$$

A knowledge of the effect of initial temperature on the burning velocity and the flame temperature enables the function $f(T)$ to be plotted against $\frac{1}{T_f}$; the activation energy of the overall reaction can be calculated from the slope of the straight line relationship. Alternatively, the change in the burning velocity and flame temperature on adding inert diluents can also be used to estimate the activation energy of the overall reaction. In this case, a plot of the function, $(f(T) + \log B)$, against $\frac{1}{T_f}$ yields the activation energy.

From a survey and subsequent analysis of the steady state flame propagation theory of Zeldovich, Frank-Kamenetsky and Semenov, a scheme was developed for evaluating the overall flame reaction kinetics. The method

was applied to determine the order and the activation energy for the overall reaction involved and to reduce from these results the rate controlling mechanism in the explosive decomposition of ethylene oxide vapour.

III (B) Flammability Limits:-

There is as yet no satisfactory theory to estimate the lower or the upper limits of flammability which depends only on the fundamental properties of the mixture, and it is therefore impossible to compare observed limits of flammability with those predicted by theory. However, for many practical purposes, it is necessary to determine the trends of flammability limits with temperature and pressure, and for this reason, it is of interest to consider these effects on the basis of the thermal theory (52).

Flame propagation is only possible if the heat emitted in the flame front is sufficient to heat the layer of fresh gas joining it to some 'ignition' temperature. The temperature in the flame front that corresponds to this quantity of heat can be expressed as

$$T_f = \left[T_I + \frac{\Delta H_0}{\bar{C}_{p\,\text{prod}} \bar{C}_{pN}} \right] \eta \qquad \text{III (22)}$$

where ΔH_0 = heat of reaction of 1 mole of stoichiometric fuel/air mixture.

$\bar{C}_p$ = mean specific heat of the products per mole of stoichiometric mixture burnt CAL/M/° C.

η = the coefficient allowed for a temperature reduction as a result for heat loss.

α is the molar ratio of the excess inert gas and stoichiometric mixture.

$\bar{C}_{pN}$ - mean specific heat of the excess inert gas. cals/M/°C

If it is assumed that the limits correspond to a certain minimum final flame temperature T_{fL}, below which the burning gas will not heat the layer of fresh mixture joining it to the ignition temperature and the flame propagation ceases, then

$$T_{fL} = \left[T_I + \frac{\Delta H_D}{\bar{C}_p + \alpha_1 \bar{C}_{pN}} \right] \eta \qquad \text{III (23)}$$

Similarly, if T_{fL} is independent of the initial temperature, then

$$T_{fL} = \left[T_2 + \frac{\Delta H_D}{\bar{C}_p + \alpha_2 \bar{C}_{pN}} \right] \eta \qquad \text{III (24)}$$

Combining equations III (23) and III (24),

$$\alpha_2 = \left[\frac{1}{\frac{1}{C + \alpha_1} - \frac{\bar{C}_{pN}}{\Delta H_D}(T_2 - T_1)} - C \right] \qquad \text{III (25)}$$

where $$C = \frac{\bar{C}_p}{\bar{C}_{pN}} \qquad \text{III (26)}$$

Equation III (25) has been used by Peshkin [52] to estimate the effect of initial temperature on the lower limit of flammability for carbon monoxide-air, ethylene-air, methane-air and pentane-air mixtures and the results shown to be in accord with experimental observations. This equation has also been employed by Egerton and Powling [53] and Zabetakis et al [55] for estimating limit processes. Unfortunately, no simple relation can be obtained for the effect of pressure on the limits of flammability because the minimum final flame temperature has been shown by Zabetakis et al [55] to decrease with increasing pressure. The effect being more marked at

lower pressures. Inspection of equation III (24) shows that at a constant initial temperature a larger quantity of inert diluent will be required to suppress the flammable gas mixture at a higher initial pressure.

CHAPTER IV

EXPERIMENTAL.

IV A Introduction:-

The primary object of this work was to investigate the hazards involved in the handling of ethylene oxide vapour. To this end, it was proposed to make measurements of the pressures developed as a result of the explosive decomposition of ethylene oxide and also the amounts of inert diluents and chemically active species required to suppress the decomposition.

The determination of limits of flammability for a gas mixture can be made using the type of apparatus developed by U.S. Bureau of Mines (36). It consists essentially of a vertical tube of internal diameter, 5 cms., and 150 cms. long. Provisions are made to introduce the fuel and inert diluents into the tube. The gas mixture after being thoroughly mixed is ignited at the end of the tube. If flame fails to propagate all the way up the tube, then the mixture is said to be non-flammable. The use of this sort of apparatus is confined mainly to conditions of atmospheric temperature and pressure.

An alternative method for determining limit conditions for flame propagation made use of Egerton and Powling's (37) flat flame burner. Inert diluents can be introduced into the gas stream until the flame cannot be stabilised. The burner can be pre-heated to any desired temperature and gas mixtures can be regulated to any pressure. However, the flow of flammable mixtures at high temperatures and pressure renders

the process hazardous.

In view of the hazards involved in the handling of ethylene oxide under pressure it was decided to use a constant volume vessel for this investigation. With a vessel, it is relatively easy to change the initial temperature and pressure of the gas; furthermore by inserting liners into the vessel, it is possible to alter the shape and size of the chamber so as to study these effects on the maximum explosion pressures developed. However, the closed vessel has its limitations in that once an explosion has started, both the burnt and unburnt gases are compressed and consequently the products of decomposition do not correspond to the initial conditions. Also the burning velocities of slow burning fuels cannot be measured accurately in a closed vessel.

IV B The Vessel:-

The explosion vessel which was previously used by Burgoyne et al [24] is shown in Figure 3. The vessel is cylindrical in shape with an internal diameter of 4.5" and an internal volume of 148·9 in^3. It is constructed of stainless steel type EN 58B. No copper, silver and other acetylide forming metals were used in its construction so as to prevent the possibility of forming acetylides, which, if detonated, could have initiated the explosive decomposition of ethylene oxide vapour. The vessel was designed to withstand dynamic pressures up to 1500 psig. The end cover, A, is attached to the screwed flange, B, by eight tensile steel nuts and bolts

EXPERIMENTAL PRESSURE VESSEL

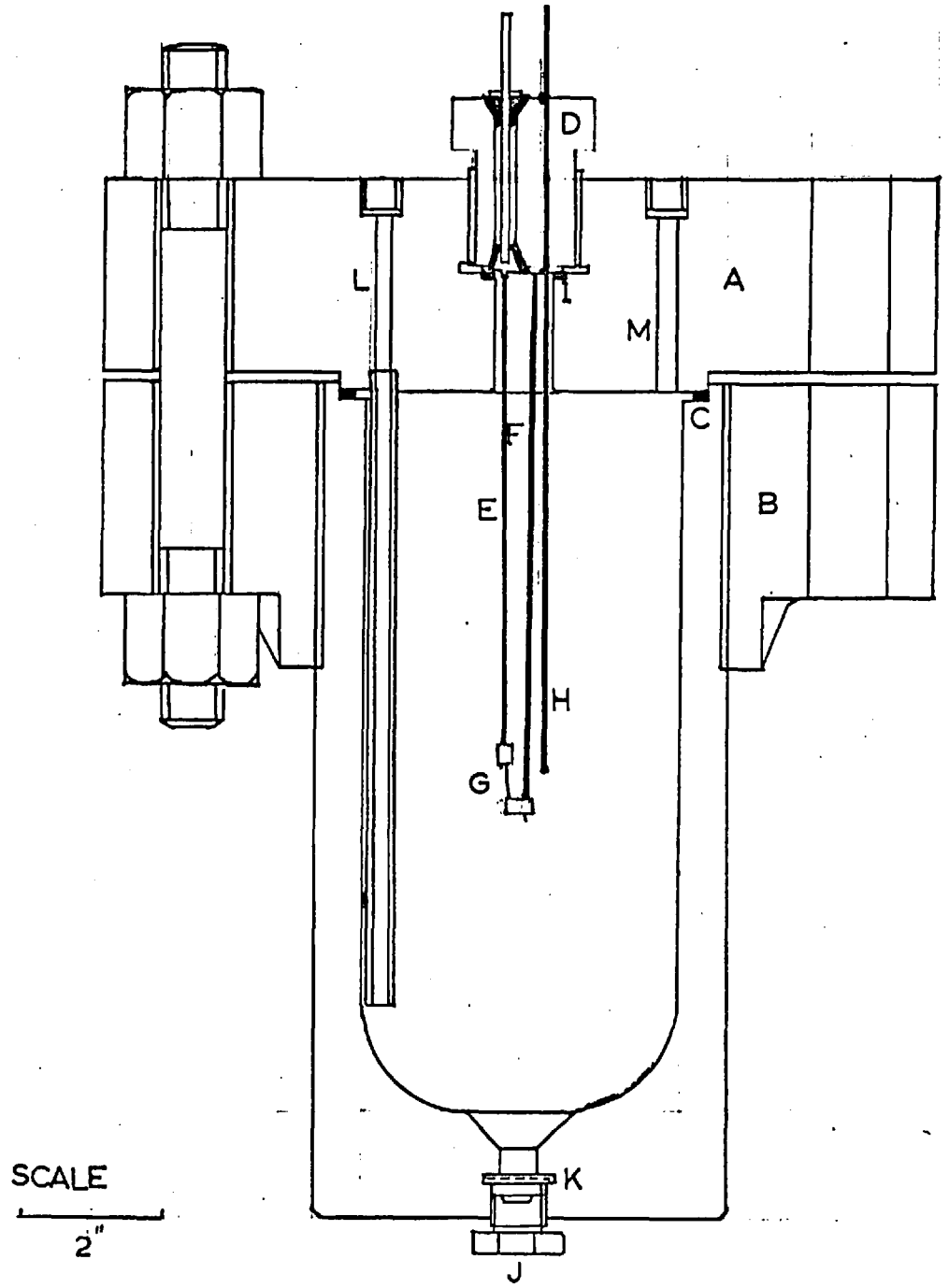

FIGURE 3

A semi confined gasket, C, machined from fully annealed nickel, forms the seal between the cover and the end of the vessel. The firing plug, D, is provided with two electrodes; one of which is electrically insulated from the plug by two cone shaped Fluon bushes, while the other, F, serves as an earth return. The ignition source, G, consists either of a straight nichrome wire or a coil and is clamped between the electrodes located at the centre of the vessel. A stainless steel sheathed thermocouple, H, is welded into the firing plug so that the tip is located near the ignition source. A flat P.T.F.E. joint ring, I, is employed as a pressure seal between the firing plug and the vessel. Provision is made to evacuate and fill the vessel through two pipe inlets, M and L, the latter being provided with a pipe extension inside the vessel to promote mixing when an inert diluent is added to the ethylene oxide vapour. The pipe is removed when liners are inserted. Dynamic pressure measurements were made by a pressure transducer, J, which was protected from the hot impinging flame by a wire gauze. The dimensions of the vessel and liners are shown in Figure 4, and the ratios of the internal volume to the surface area of the vessel are given in Table 4.

TABLE 4. Dimensions of vessel and liners.

	Vessel	Liner I	Liner II
Internal volume in^3 (cm^3)	148·9 (2440)	79·7 (1310)	8·0 (131)
Ratio V/A in^3/in^2 (cm^3/cm^2)	0·935" (2·38)	0·73 (1·93)	0·258 (0·605)
Ratio L/D	2.25	2.25	6·76

VESSEL LINERS

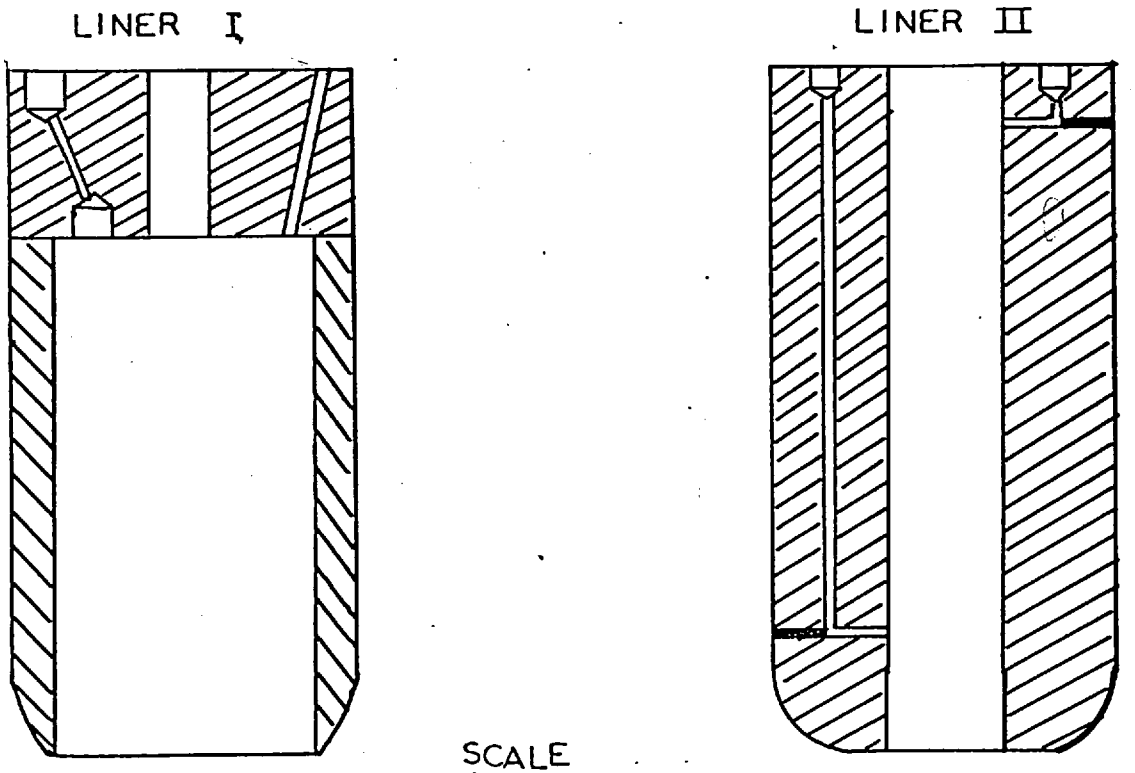

FIGURE 4

IV C. Dynamic Pressure Measurements.

The chief requirements for the pressure transducer were that it should be capable of operating at a temperature of 150° C continuously, have a linear pressure-output characteristic at pressures up to 1500 psig, have a rapid response time and be capable of measuring static pressures. Two types of pressure transducers were employed in this work. One was a capacitance type and the other a piezo electric type.

IV C (1) Capacitance type pressure transducer.

The capacitance pressure transducer type G246, was supplied by the Southern Instruments Ltd. Four different transducers were used to cover the pressure ranges 0 to 28 psig, 0 to 220 psig, 0 to 600 psig and 0 to 1500 psig. The temperature stability of the transducer was reported to be about 1% full scale output for temperature change of 20° C. The pressure transducer and its lead formed an integral part of an oscillator circuit; the radio frequency signal resulting from a change in capacitance of the gauge was fed to a frequency modulated pre-amplifier, Southern Instrument type MR 513, the output voltage of which could be displayed on a cathode ray oscilloscope screen, Southern Instrument type M 977. The output voltage was directly proportional to the change in capacitance of the transducer and hence directly proportional to the pressure change. A calibrated control dial which supplied a variable D.C. voltage was used to balance the output of the transducer. By applying a series of known pressure

to the transducer and noting the reading on the control dial necessary to reduce the signal to zero, it was possible to produce a calibration curve in which the dial readings were plotted against the corresponding pressures. The graph could then be used to obtain the readings necessary to provide the calibration signal for any pressure within the range of the transducer.

IV C (2) Piezoelectric type pressure transducer.

The piezo electric pressure transducer type PZ 14 employed in this work was made by the Swiss Locomotive and Machine Works (SLM) and was capable of operating at a maximum pressure of 2000 psig. Its response, according to the manufacturers did not change by more than 1% for a 20° C temperature change. When pressure was applied to the transducer a charge was generated across the faces of the piezo electric crystal. This charge was transferred through a low loss electrical cable to a calibrated condenser which then supplied the grid voltage to an electrometer valve in an SLM type PV 17 amplifier. The electrometer valve had an extremely high input impedance, so that the charge in the transducer did not decrease by more than 1% within 20 seconds. The output from the electrometer valve was amplified by a D.C. amplifier, Cossor type 1440, to enable it to be displayed on the cathode ray oscilloscope. A reference dial which enabled calibration charges to be fed into the electrometer valve was incorporated in the SLM preamplifier and used to balance the output signal from the pressure transducer. A static pressure calibration curve could be obtained for this apparatus in the similar way to that for the capacitance type. A general layout of the equipment is shown in Figure 5.

GENERAL LAYOUT OF
ELECTRICAL COMPONENTS

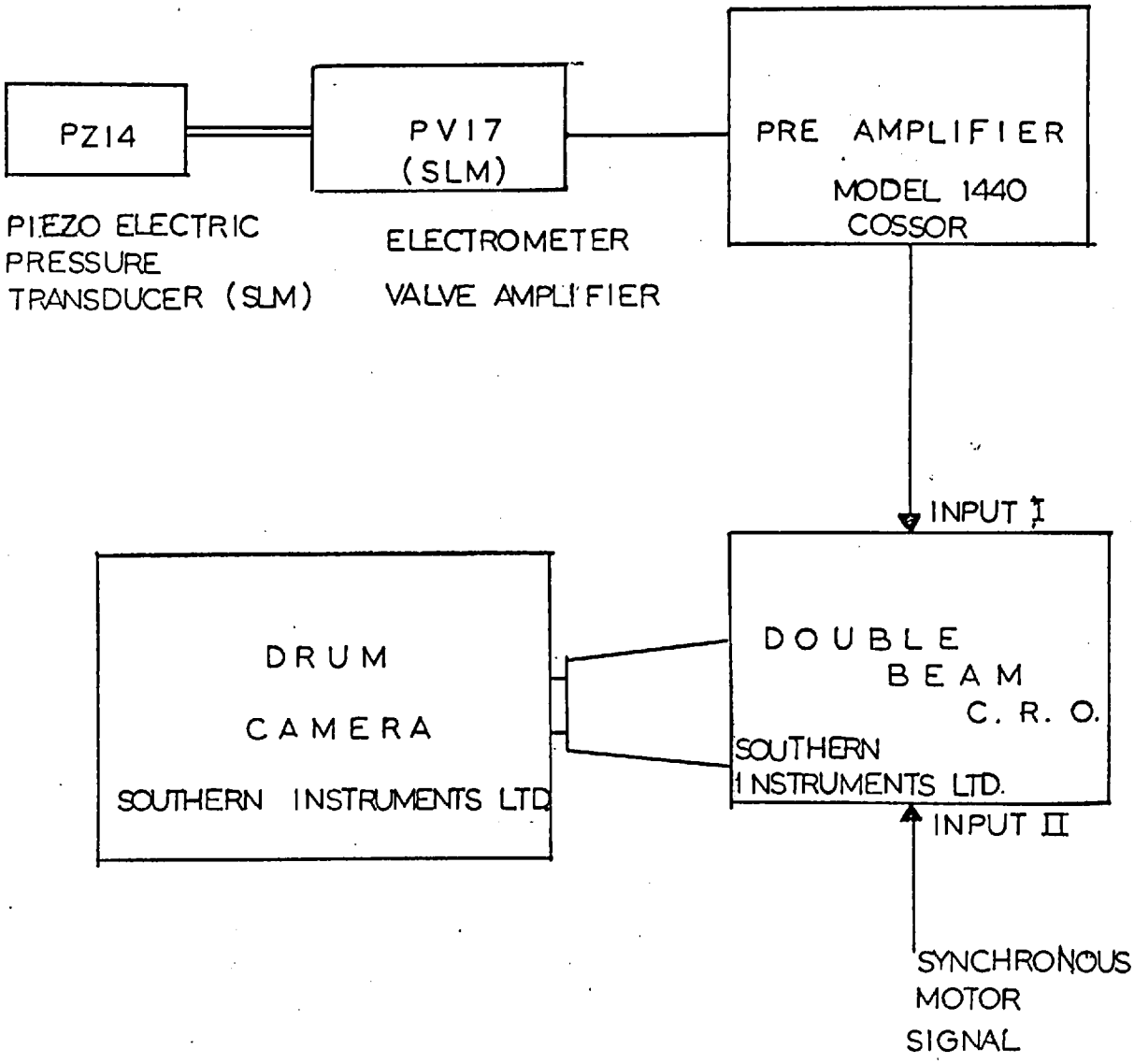

FIGURE 5

IV C (3) Performance of the pressure transducers:-

To prevent the hot flame from damaging the pressure transducer, a stainless steel wire gauze, 30 mesh, was fixed in front of the transducer to act as a flame arrestor. The efficiency of the flame arrestor was tested by constructing a 'dummy' transducer with copper-constantan thermocouples 0·028" diameter, inserted in the positions shown in Figure 6A. It was found that after igniting ethylene oxide vapour in the vessel the maximum change in temperature indicated by the various thermocouples was $\Delta T_o = 0^oC$, $\Delta T_i = 20^oC$, $\Delta T_2 > 100^oC$. Since ΔT_i was no greater than 20^oC, it was concluded that the gauze was sufficient to prevent the flame from damaging the transducer. However, the effect of a temperature difference of 20^oC across the diaphragm on the response of the transducer had to be investigated. It was found that when the flame from a match was held near the diaphragm of the SIM pressure transducer for 5 seconds, a negative deflection corresponding to 15% full scale deflection was observed on the oscilloscope screen. However, when a finger, 37^oC, was gently placed on the diaphragm of the transducer (18^oC), no observable deflection was noticed on the cathode ray oscilloscope screen. It is therefore concluded that the measured temperature difference, ΔT_i, of 20^oC across the diaphragm would not affect the response of the pressure transducer.

The pressure transducers were calibrated statically against a Bourdon tube gauge which in turn was calibrated against a dead-weight tester. All these transducers gave straight line pressure-output

characteristics under static conditions. The SLM piezo electric type of pressure transducers has been tested dynamically by the Royal Aircraft Establishment [32] using shock tube techniques and found to have a linear characteristic to within ± 1%. In view of this, it was assumed that the piezo electric transducer responded correctly under dynamic conditions and it was subsequently employed to test the dynamic loading characteristics of the capitance type transducers. The two different types of pressure transducer were simultaneously exposed to a pressure pulse using the arrangement shown in Figure 6B and the pressure recorded by the various gauges are shown in Figure 7. It was found that the capacitance pressure transducer having a range 0 - 1500 psig indicated explosion pressures 25% lower than those recorded by the piezo electric gauge. Burgoyne et al [24], in their work, on the explosive decomposition of ethylene oxide vapour did in fact use this particular pressure transducer and therefore their explosion pressure measurements may have been in error. In view of the results of these experiments, the piezo electric type of pressure transducer was used in this investigation.

IVC (4) Time Base:-

Electrical signals of 0·3s. duration were applied to the second beam of the cathode ray oscilloscope by means of a timer which consisted of a synchronous motor (10/3 RPS) driving a P.T.F.E. drum. A brass strip mounted on the drum made contacts with copper brushes so as to supply a

EFFECT OF FLAME ON TRANSDUCER

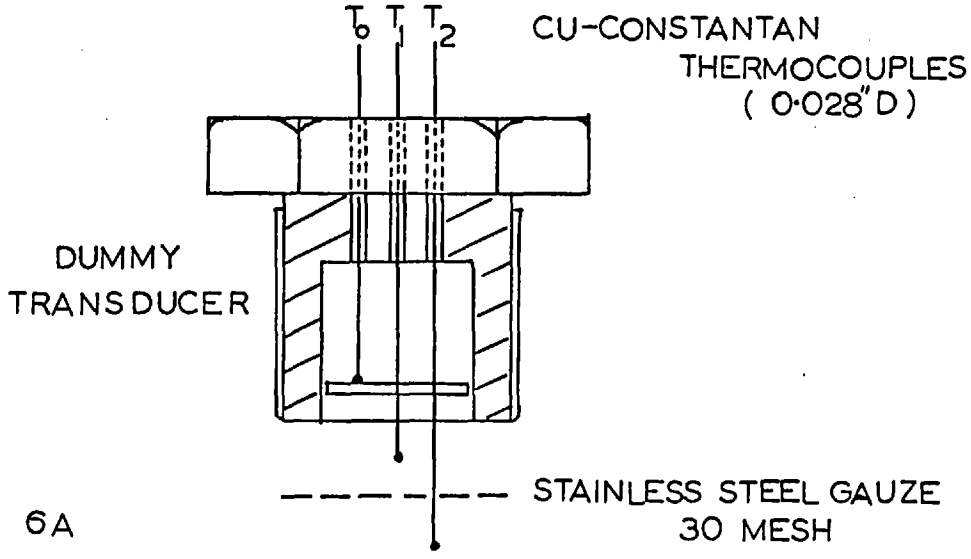

FIGURE 6A

COMPARISON OF DYNAMIC PRESSURE LOADING
BETWEEN A PIEZO AND A CAPACITANCE TRANSDUCER

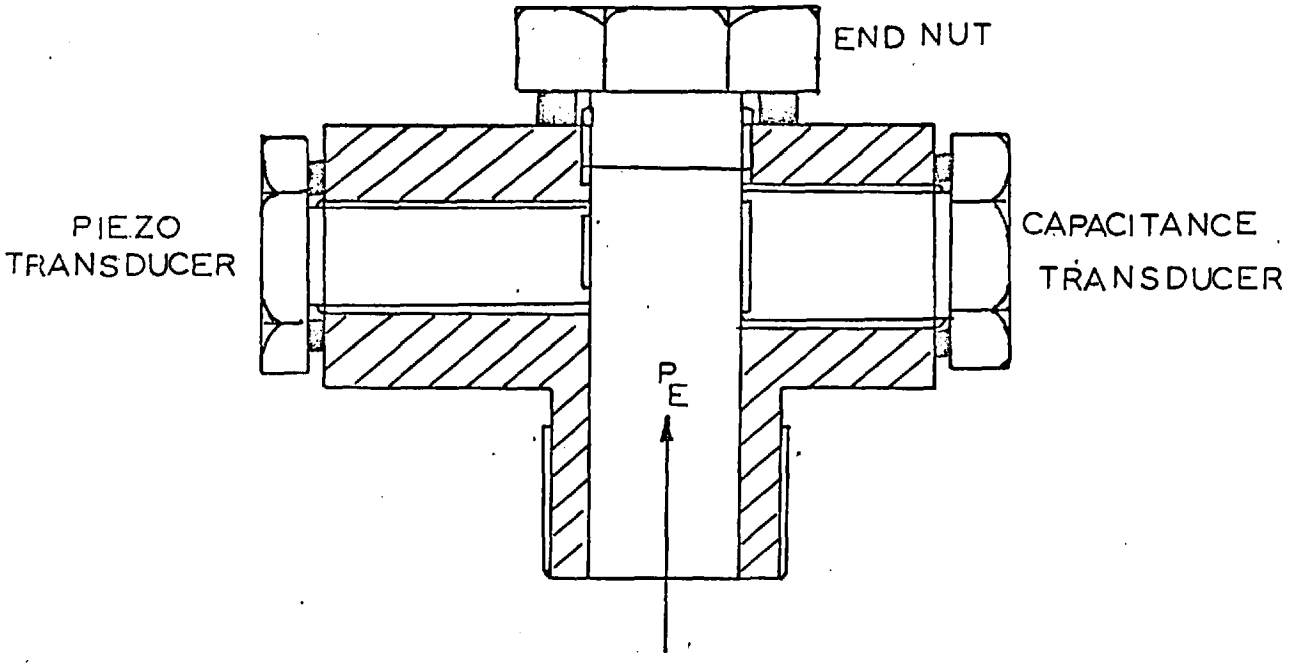

FIGURE 6 B

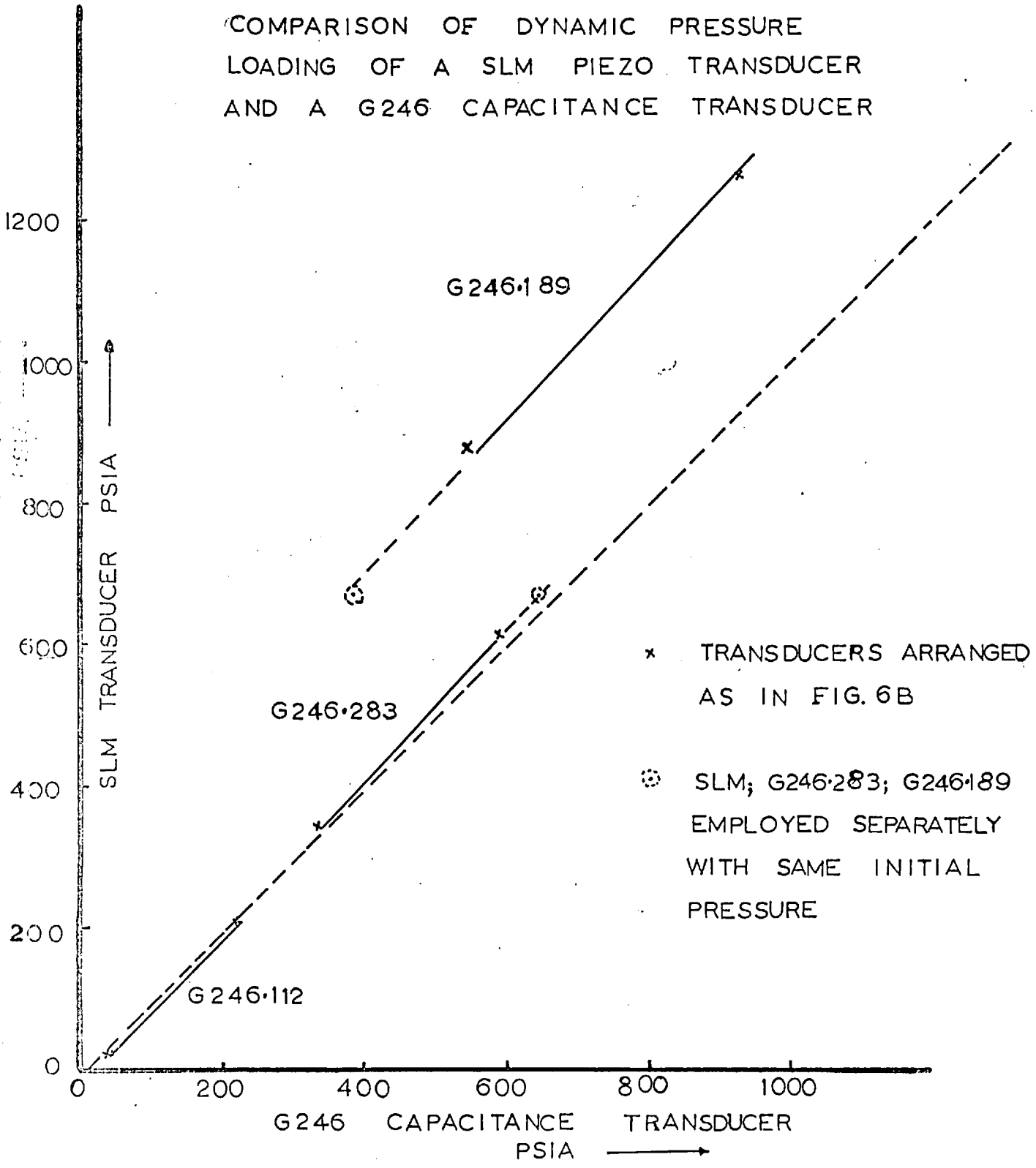
COMPARISON OF DYNAMIC PRESSURE
LOADING OF A SLM PIEZO TRANSDUCER
AND A G246 CAPACITANCE TRANSDUCER
1200
1000
800
600
400
200
0
SLM TRANSDUCER PSIA
G246·189
G246·283
G246·112
× TRANSDUCERS ARRANGED AS IN FIG. 6B
⊙ SLM; G246·283; G246·189 EMPLOYED SEPARATELY WITH SAME INITIAL PRESSURE
0
200
400
600
800
1000
G246 CAPACITANCE TRANSDUCER PSIA

FIGURE 7

2 volt d.c signal to the oscilloscope once every 0·3 seconds. A photograph of the synchronous motor is shown by PLATE I.

IV D The ignition system:-

The ignition of an explosive mixture can be achieved in a number of ways, such as by a hot coil, a condenser spark or a flame. For closed vessel experiments, ignition is generally accomplished by either a spark or a hot coil. Because the supply of energy to an explosive mixture by a heated coil is slow, convective currents are set up, and the method is not recommended for the determination of flammability limits. In the case of spark ignition, concentrated energy is supplied very rapidly; whether a steady flame can develop from the shock discharge mainly depends on the physical and chemical properties of the gas mixture and on the heat losses to the electrodes.

Gerstein et al [17] made several attempts to ignite ethylene oxide vapour at atmospheric pressure and temperature using a single spark between needle electrodes at a potential greater than 10,000 volts. Although 11·0 joules were estimated to have been dissipated in the spark, ignition was possible only with successive sparks. The difficulty of igniting ethylene oxide vapour which was also reported by Courtney [35] is consistent with its low burning velocity, high activation energy and large quenching distance. In view of this difficulty, exploding wire was employed as the ignition source in this investigation. The advantage of an

SYNCHRONOUS MOTOR

PLATE I

exploding wire is that energy is rapidly supplied to the vapour in a single exploding process producing multiple point sources of ignition which are essential for the initiation of ethylene oxide decomposition flames.

A nichrome wire, 0·8" long (quenching distance [23] 0.55") was caused to explode by applying 240 volts a.c. across it. A 10 ampere fuse was used to protect the mains fuse as shown in Figure 8. The amount of nitrogen required to suppress an ethylene oxide explosion [24] was found to depend on the wire size for wires having diameters less than 34 SWG, whereas for wires having diameters larger than 34 SWG, it was independent of the size of the wire. For this reason exploding nichrome wires of 31 SWG were employed in this work.

It was demonstrated that an exploding wire provided multiple point ignitions by comparing the pressure-time record of an ethylene oxide explosion initiated by an exploding wire with one using a hot coil as an ignition source. Figure 9 shows that in the former case the pressure rise was more rapid than in the latter case. The delay period between the switching on of the electric circuit and the observable pressure rise following an ignition using a hot coil was approximately 1·2 seconds. This time was estimated to correspond with the time taken to raise the heating coil to a temperature not exceeding 700° C. In the case of an exploding wire, there was no delay and the pressure started to rise immediately the electrical circuit was closed. The hot coil ignition

IGNITION CIRCUITS

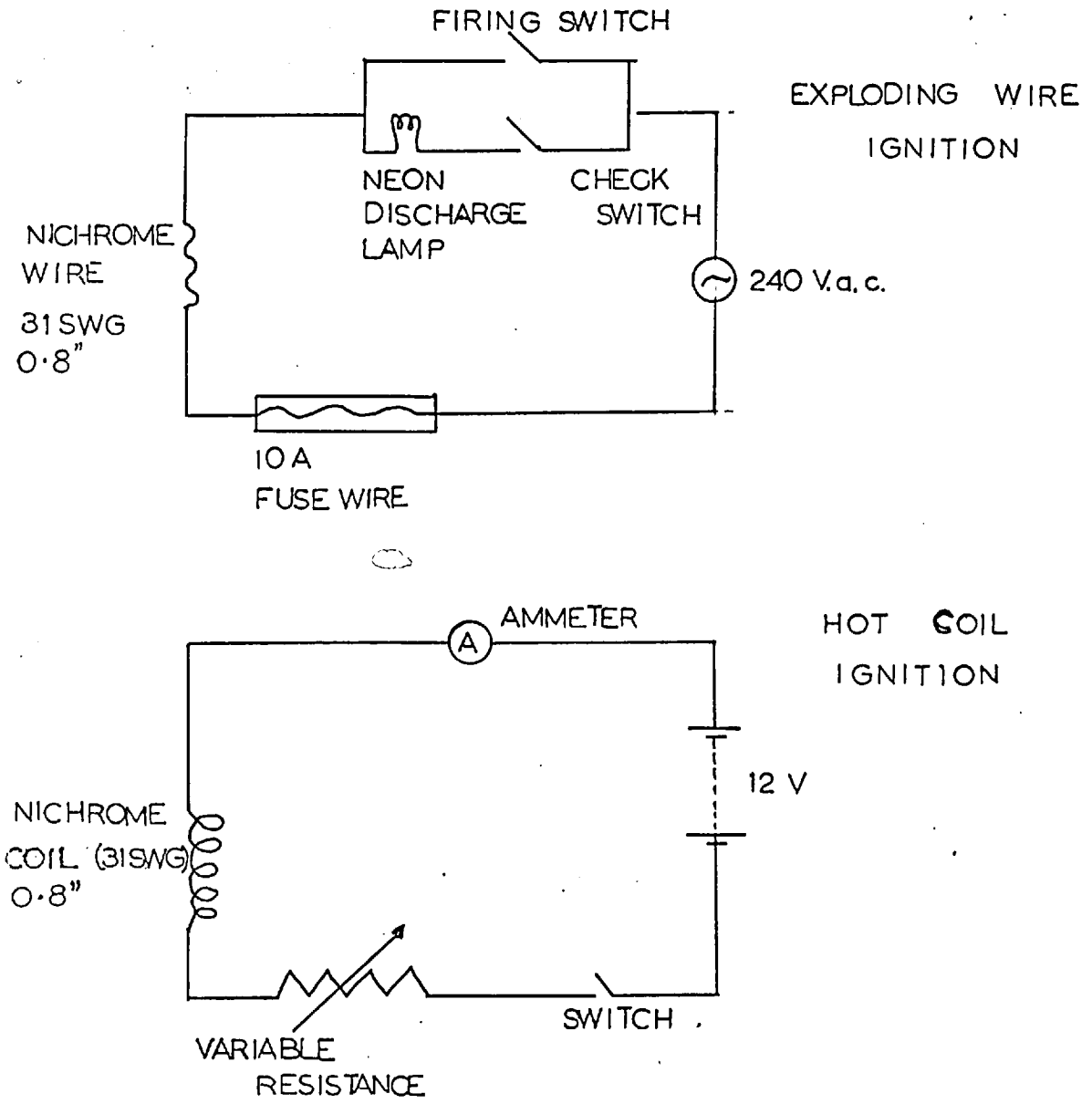

FIGURE 8

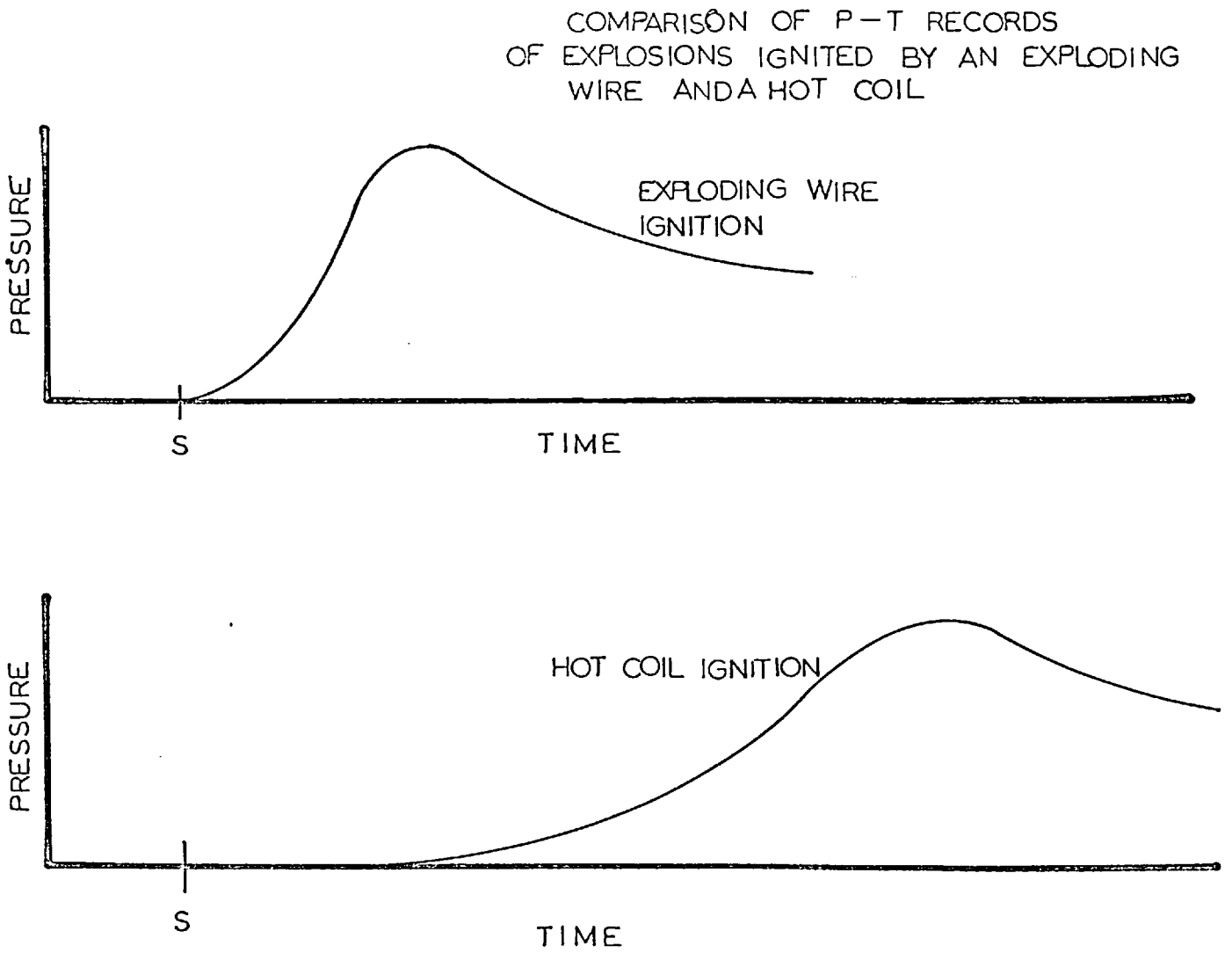
COMPARISON OF P–T RECORDS
OF EXPLOSIONS IGNITED BY AN EXPLODING
WIRE AND A HOT COIL
PRESSURE
EXPLODING WIRE
IGNITION
S
TIME
PRESSURE
HOT COIL IGNITION
S
TIME

FIGURE 9

system shown in Figure 8 was employed only when burning velocity determinations were required, whereas the exploding wire was used for the determination of limits and for those experiments in which study was made on the products of decomposition.

IV I Ancillary equipments:-

The vessel was supported at the centre of an enclosed electrically heated oven which could be adjusted and controlled at any temperature from 25° to 200° C. Provisions were made for the firing plug to be withdrawn and replaced in the vessel as required without having to remove the oven. Four thermocouples were fixed at various external parts of the vessel surface to allow the temperature distribution over the external surface of the vessel to be measured. It was found that when thermal equilibrium was established at, say, 100° C, the outside surfaces of the vessel were all within ± 2° C of the temperature measured by the thermocouple inside the vessel.

All pressure gauges, valves and pipes employed in this work were of stainless steel. Those valves and pipes leading to the pressure vessel were also heated to 100° C by means of electrically heated tapes. All pressure gauges were mounted on a steel panel designed to provide some protection in the event of the pressure vessel failing. Plate II and III shows photographs of the oven and the panel respectively.

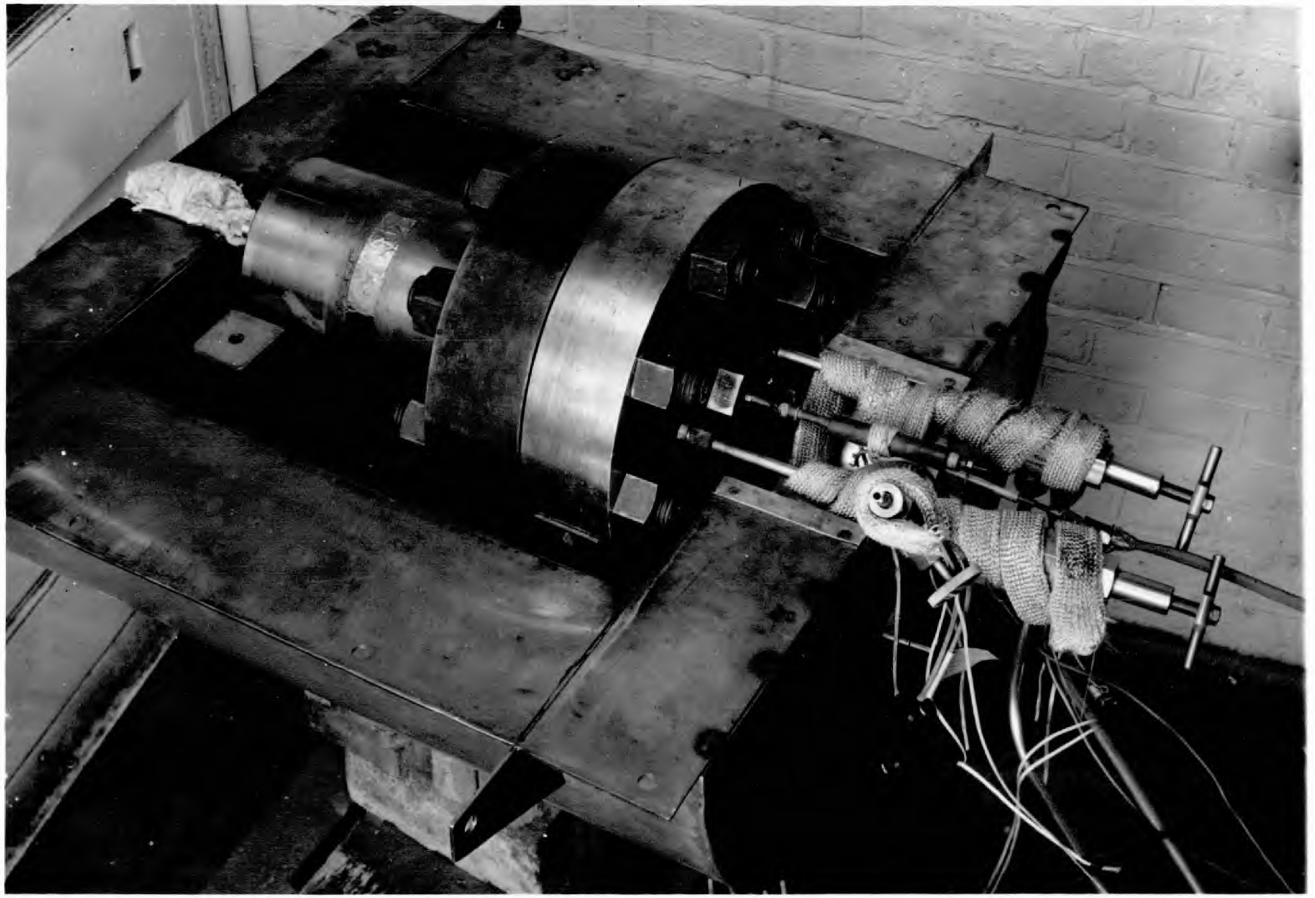

VESSEL & OVEN

PLATE II

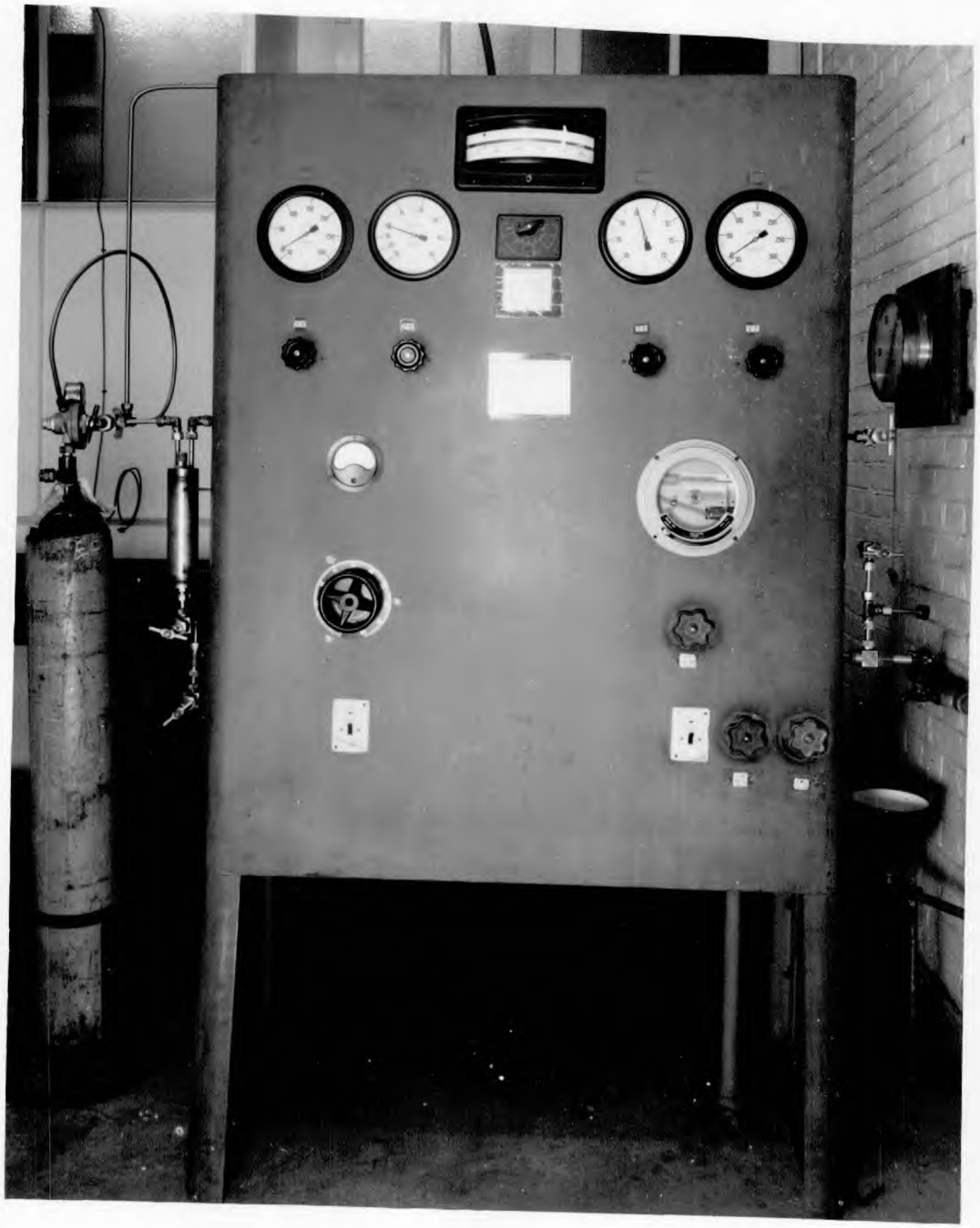

THE PANEL

PLATE III

Liquid ethylene oxide was stored under its own vapour in a feed bottle, (A), which could be refilled through a screwed cap. This vessel which had an internal volume of 23·5 cubic inches was designed to withstand a working pressure of 200 psig. It was protected by a bursting disc, B, designed to rupture at 250 psig.

Liquid additives such as water, methanal, and propylene oxide were introduced into the explosion vessel by means of a syringe which is shown in Figure 10. After the vessel had been evacuated, valves 13 and 14, see Figure 11, were closed, and valve 16 opened so as to allow the liquid in the syringe to be forced into the apparatus. Valve 16 was then closed and the liquid evaporated, its vapour pressure being recorded by the pressure transducer.

IV F Procedure:-

A flow diagram of the apparatus is shown in Figure 11. After the vessel had been heated to the desired temperature, say, 100° C, all valves except 7, 9, 11, 13 and 14 were closed and the vessel evacuated by a rotary pump, C, until the pressure recorded by the manometer 'D', with the valve 11 closed, was less than 1 m.m. Hg pressure. Commercially available oxygen-free nitrogen was then introduced into the vessel through valve 2 until the Bourden tube gauge, G1, recorded a pressure slightly above atmospheric, after which the vessel was re-evacuated. Valve 14 was

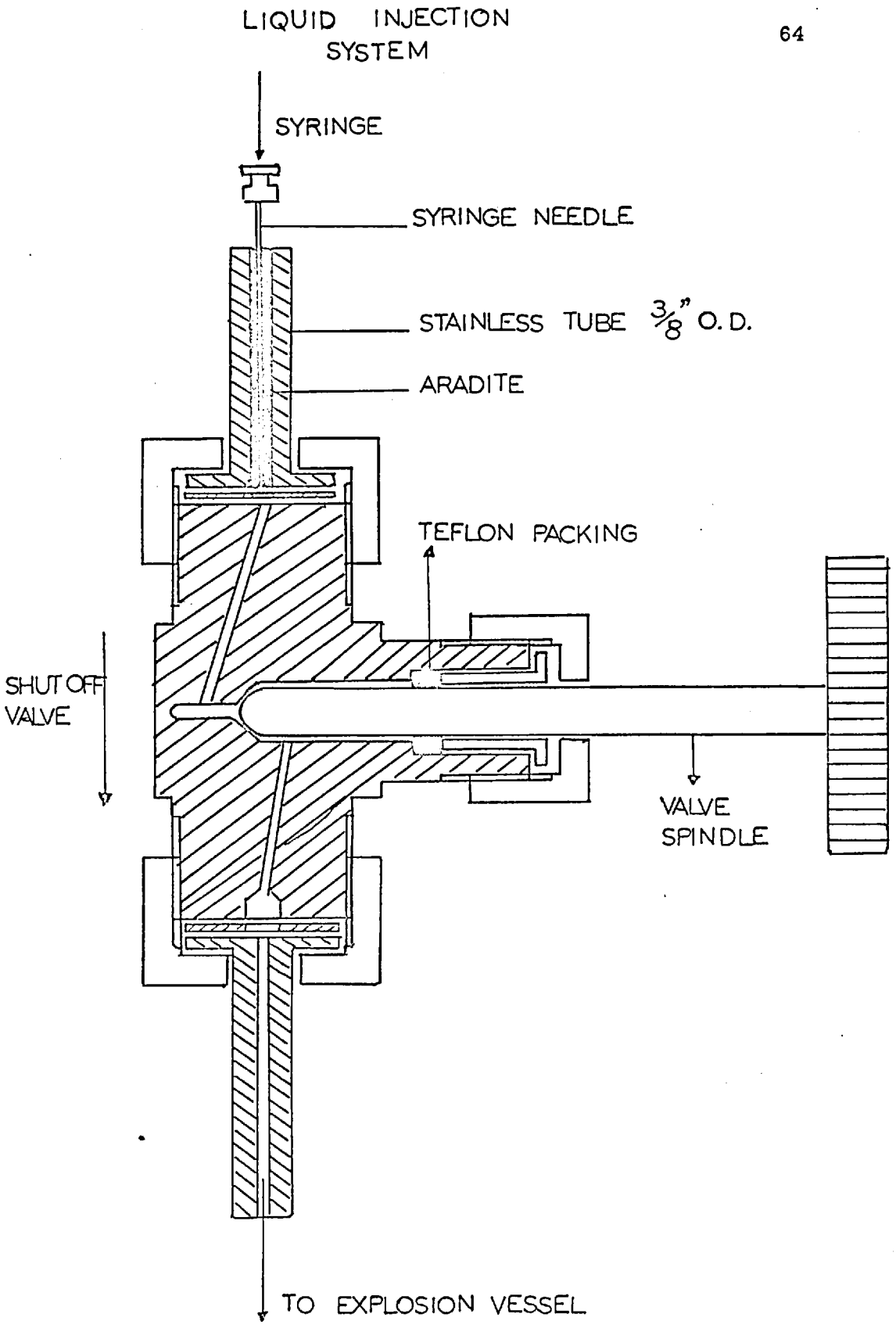
LIQUID INJECTION SYSTEM
SYRINGE
SYRINGE NEEDLE
STAINLESS TUBE 3/8" O.D.
ARADITE
TEFLON PACKING
SHUT OFF VALVE
VALVE SPINDLE
TO EXPLOSION VESSEL

FIGURE 10

FLOW DIAGRAM OF EQUIPMENTS

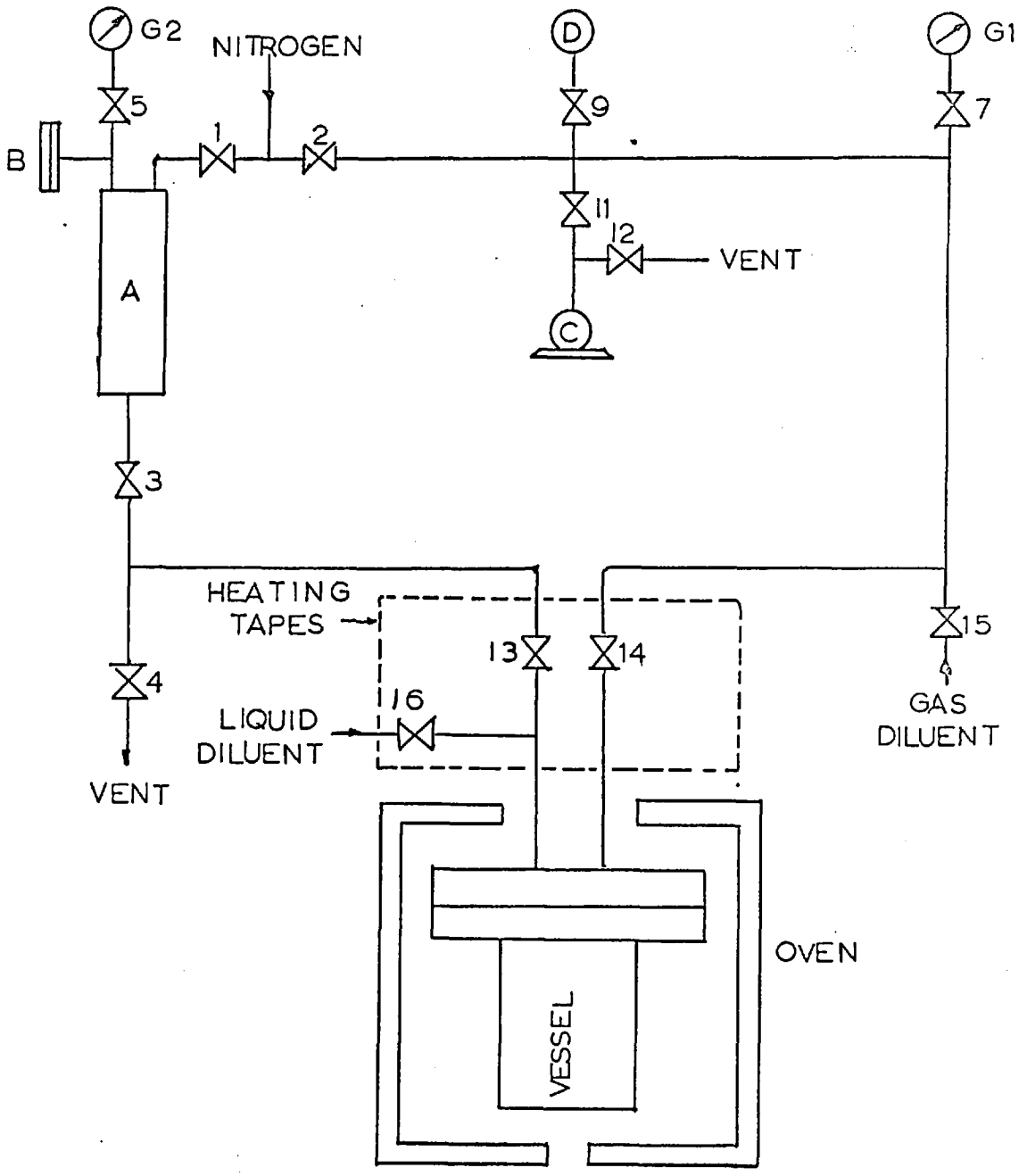

FIGURE 11

then closed and valve 3 opened to allow ethylene oxide to be drawn slowly into the explosion vessel where it vaporised quickly until the pressure inside the explosion vessel was equal to that in the feed bottle (G2). Nitrogen was then slowly admitted to the feed bottle via valve 1 to force more ethylene oxide into the explosion vessel until the required pressure was registered by gauge G2. When equilibrium had been established, valves 1, 3 and 13 were closed and the remaining ethylene oxide in the pipe was removed by a wet vacuum pump through valve 4. Inert diluents such as CO_2, or NH_3 were admitted through valve 15 (for N_2 through valve 2) until the pressure recorded by G1 was greater than the pressure inside the vessel. Valve 14 was then opened and further inert diluent added to the required total pressure. Valve 15 and 14 were then closed and the inert diluent in the pipe line was withdrawn through valve 16 by a wet vacuum pump. Liquid diluents such as water, methanol and propylene oxide were injected into the evacuated vessel before ethylene oxide was introduced. After allowing the mixture to mix for half an hour, the pipe lines joining valves 13 and 14 to the vessel were disconnected and the mixture in the vessel ignited. The pressure time trace was recorded by a drum camera. When the decomposition products had cooled to 100° C, the total final pressure was recorded by gauge G1. The products were then passed either directly, through heated pipes via valve 13 into a gas chromatography unit or collected in gas sampling bottles for subsequent analysis. The vessel was

periodically cleaned to remove carbon deposits.

IV G Gas Chromatography Analysis:-

(1) The quantitative analysis of the important products obtained from the explosive decomposition of ethylene oxide vapour was made with the aid of a standard Beckman G.C.2 gas chromatograph.Carier gas, such as hydrogen or nitrogen, was divided into two streams as shown in Figure 12. Each stream was passed through a similar capillary orifice which restricted the flow to the required rate. One stream flowed directly to the reference side of the detector cell and out through the exhaust line. The other flowed through a sample inlet system and then through a chromatographic column to the sensing side of the cell before leaving the instrument via the exhaust line. Samples were introduced by a vacuum system through a sampling valve which had fixed volume loops of 1 ml. and 10 ml. The detector cell which was of the thermal conductivity type could be operated at a temperature range 20 to 220^{o} C. The change in the temperature and hence the resistance of the filaments in the cell caused by the difference in thermal conductivity between the carrier gas and the sample, resulted in a voltage differential across the bridge which was recorded on a Honeywell recorder. The amount of each component was proportional to the area under the recorder curve which was measured by a digital integrator of Honeywell type. In order to analyse the decomposition products, two chromatographic columnswere used in series by means of a dual column valve.

FLOW DIAGRAM OF GAS CHROMATOGRAPH

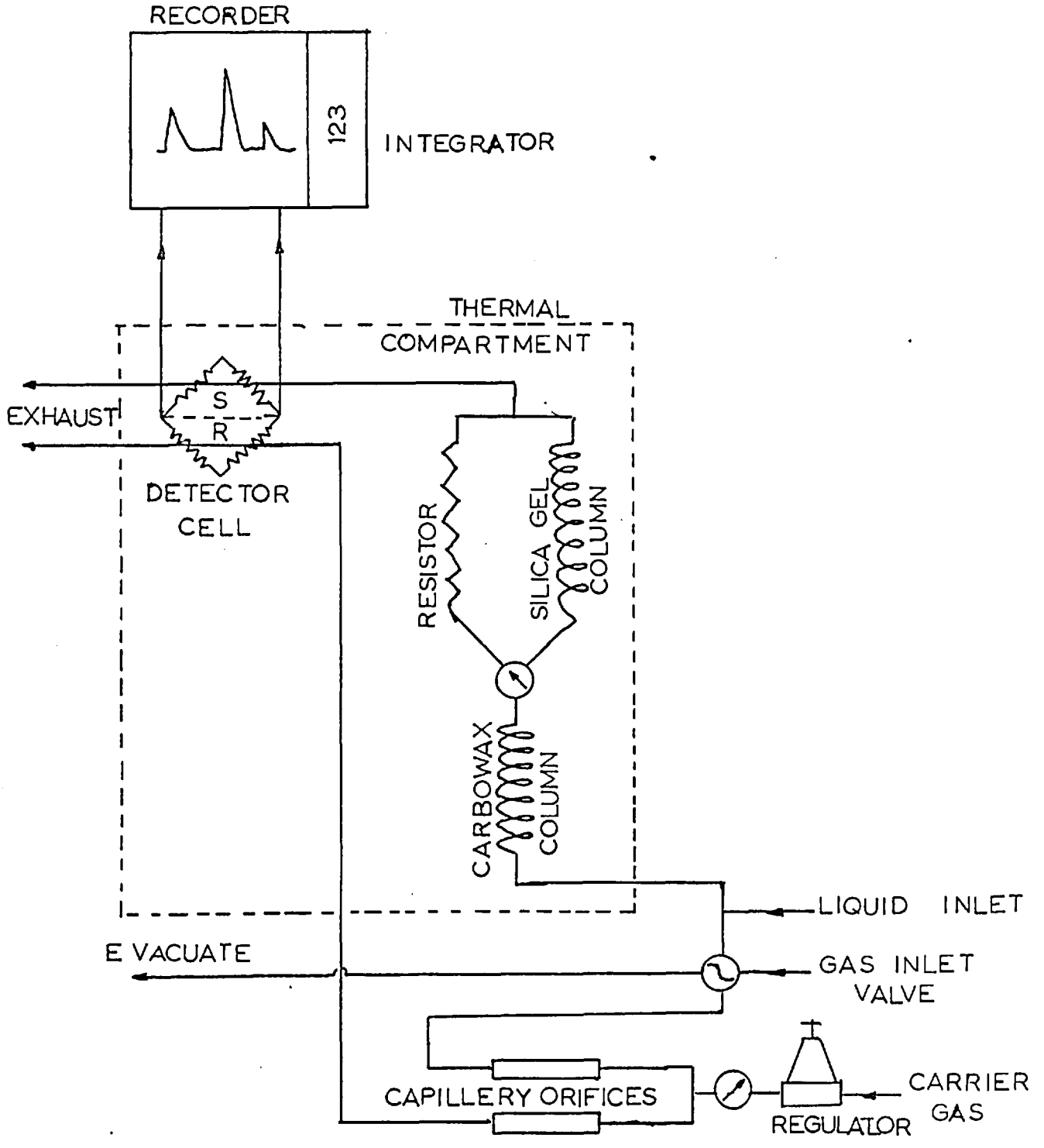

FIGURE 12

IV G (2) Columns used for separating various gases:-

An eight foot silica gel column, Davidson 28 - 200 mesh, was employed for the separation of H_2, CO, CH_4, C_2H_6, CO_2 and C_2H_4. at 70° C. A sample of 1 ml. was injected for the analysis of CO and CH_4, hydrogen being used as the carrier gas at an inlet pressure of 20 psig. Because C_2H_6, CO_2, C_2H_4 were present in small quantities and that they have long retention times, 10 mls. of sample were employed and the pressure of the hydrogen carrier gas was increased to 40 psig. Hydrogen was analysed using nitrogen as the carrier gas.

CH_3OH, C_2H_4O, C_3H_6O, H_2O and C_6H_6 were all separated by a six foot column of Carbowax 400 supported on 42 - 60 mesh teflon.

A molecular sieve (5A) column was used to detect the presence of O

Ammonia and amines were separated by a 12' column containing 20% cetyl alcohol on alkaline washed embacel (60 - 100 mesh) at 40° C with hydrogen as the carrier gas.

IV G (3) Calibration:-

A standard gas sample containing H_2, CO, CH_4, C_2H_6, CO_2 and C_2H_4 was supplied by the Infrared Co. Ltd. This standard sample was made by accurately measuring the partial pressures of each of the pure components Higher boiling liquids such as methanol, amines and propylene oxide were calibrated by direct injection into the carrier gas stream using a micro syringe. A plot of the concentration against the area under the recorder curve gave straight lines for each component.

IV G (4)Sensitivity and accuracy:-

The sensitivity of the gas chromatograph for analysing trace components such as ethylene, ethane and carbon dioxide depended mainly on the sample size and the conditions under which the instrument was operating. With a normal recommended bridge current of 250 mA, a 10 ml sample and hydrogen as the carrier gas, the minimum detectable percentage of each component was as follows:-

Components	Vol. %
Ethylene (SH_4)	0.100
Carbon dioxide (CO_2)	0.05
Ethane (SH_6)	0.05
Ethylene Oxide (SH_4O)	0.005
Propylene Oxide (C_3H_6O)	0.005
Ammonia (NH_3)	0.015
Methylamine ($CH_3.NH_2$)	0.015
Ethylamine (SH_5NH_2)	0.015
Methanol (CH_3OH)	0.03

With a maximum bridge current of 400mA, the sensivity increased approximately four fold.

The accuracy of the gas analysis was estimated by repeatedly analysing the standard gas sample for about ten times. The maximum difference between each analysis was found to be $\pm$ 1%.

IV G (5) Chemical Analysis:-

The Carbowax 400 column was unable to separate acetaldehyde, formaldehyde and ethylene oxide. Hence chemical analysis was employed to detect and determine the aldehyde content in the products of decomposition as well as in the initial ethylene oxide vapour. Aldehydes were removed from the gaseous decomposition products by means of a trap maintained at $-71^{\circ}C$ by a mixture of cardice and methylated spirit. Traces of acetaldehyde ($> 1\ \gamma$) could be detected [34] when added to a mixture containing equal volumes of 20% morpholine and 5% sodium nitro prusside solution by the blue coloration produced. Formaldehyde, if present ($> 0{\cdot}14\ \gamma$) was detected with Chromotropic acid [34] in a strong sulphuric acid by the appearance of a violet pink coloration. The total aldehyde content was determined by titrating the excess sodium bisulphite [40] in the mixture with iodine using starch as an indicator.

CHAPTER V.

EXPERIMENTAL RESULTS FOR THE EXPLOSIVE DECOMPOSITION OF PURE ETHYLENE OXIDE VAPOUR.

V A Products of decomposition.

The explosive decomposition of pure ethylene oxide vapour has been studied over a temperature range 20 to 100° C and at initial pressures up to 135 psiA. Typical gas analyses for the products of decomposition are given in Table 6.

TABLE 6.

Analysis of products of decomposition of pure Ethylene Oxide Vapour at 100° C

Products	Volume (%)		
	P_I = 4.66 psiA	P_I = 14.7 psiA	P_I = 74.7 psiA
C_2H_4O	2·62	0·90	0·44
CH_4	20·95	27·80	28·10
CO	44·10	46·15	43·40
H_2	23·15	22·20	27·52
C_2H_6	1·08	0·50	0·11
CO_2	——	0·10	0·20
C_2H_4	8·0	1·91	0·11
C_6H_6	——	0·44	0·12

Solid carbon was also observed at the end of each explosion. It was found that the amount of ethylene oxide remaining undecomposed at the end of the explosion increased greatly as the temperature of the vessel was reduced from 100°C to 20°C as shown in Figure 13. Therefore, in order to study the effect of experimental conditions such as temperature, pressure and vessel shape on the decomposition mechanism, the products are expressed as moles of product per mole of ethylene oxide decomposed. On this basis the effect of temperature and pressure on the decomposition products is shown in Figures 14 and 15 respectively. Increasing the vessel temperature from 20°C to 100°C was found to have little effect on the products of decomposition except that the formation of methane was slightly reduced. On the other hand, pressure was found to have a definite effect on the products of decomposition in that methane formation was favoured at higher pressures and ethylene at lower pressures.

The effect of the surface area to the internal volume ratio, (S/V), of the vessel on the products of decomposition of the ethylene oxide vapour is illustrated in Figure 16. The results show that as the S/V ratio is increased increasing amounts of ethylene and ethane are formed with a corresponding reduction in the amount of methane and hydrogen. However, the formation of carbon monoxide is unaltered by changes in S/V ratio of the vessel.

EFFECT OF INITIAL TEMPERATURE ON

THE % ETHYLENE OXIDE VAPOUR UNDECOMPOSED

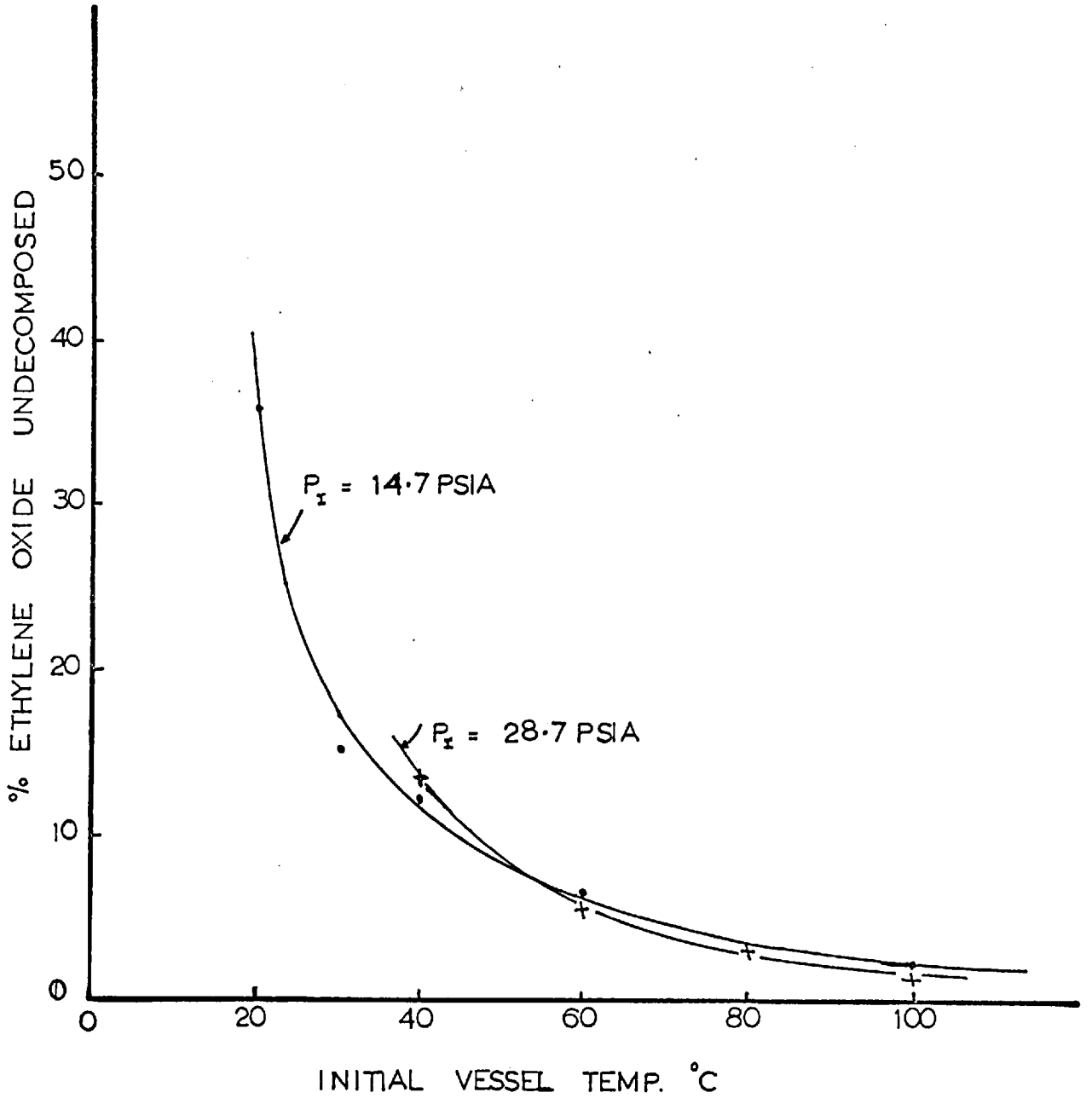

FIGURE 13

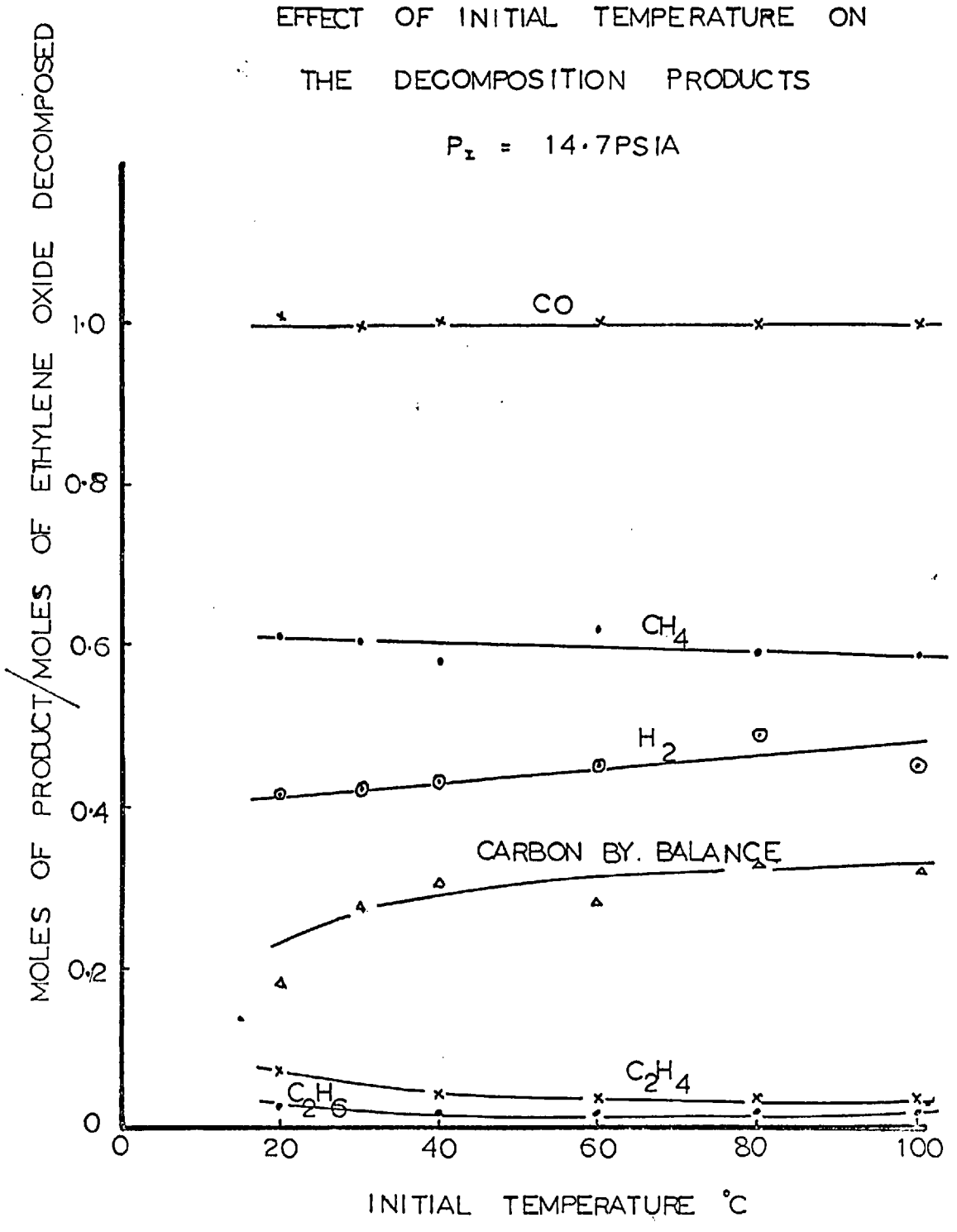
EFFECT OF INITIAL TEMPERATURE ON
THE DECOMPOSITION PRODUCTS
P_I = 14·7PSIA
MOLES OF PRODUCT/MOLES OF ETHYLENE OXIDE DECOMPOSED
1·0
0·8
0·6
0·4
0·2
0
CO
CH_4
H_2
CARBON BY. BALANCE
C_2H_4
C_2H_6
0
20
40
60
80
100
INITIAL TEMPERATURE °C

FIGURE 14

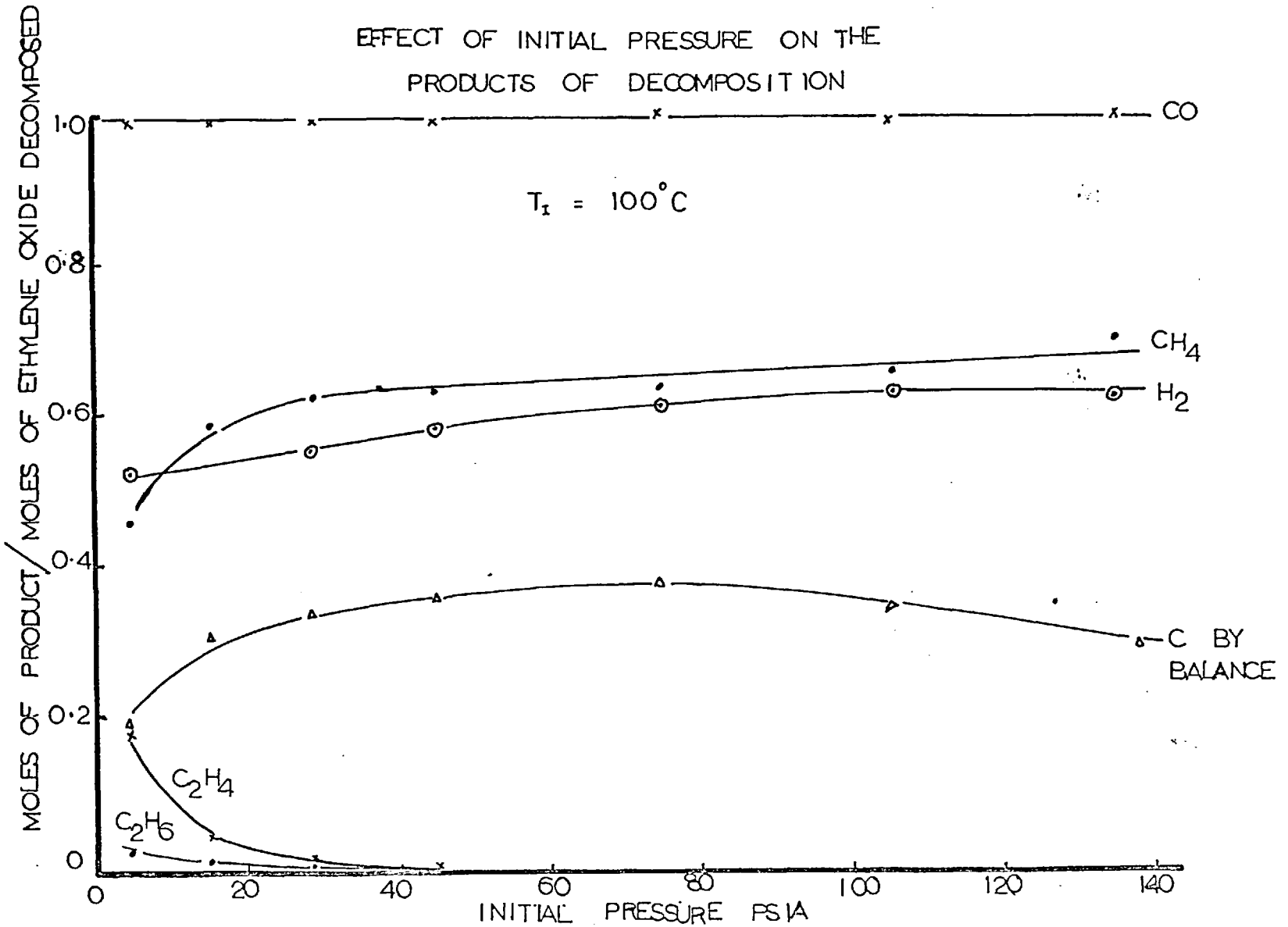
EFFECT OF INITIAL PRESSURE ON THE
PRODUCTS OF DECOMPOSITION
T_I = 100°C
MOLES OF PRODUCT / MOLES OF ETHYLENE OXIDE DECOMPOSED
1·0
0·8
0·6
0·4
0·2
0
CO
CH_4
H_2
C BY BALANCE
C_2H_4
C_2H_6
0
20
40
60
80
100
120
140
INITIAL PRESSURE PSIA

FIGURE 15

P_I = 25 PSIA
T_I = 100°C

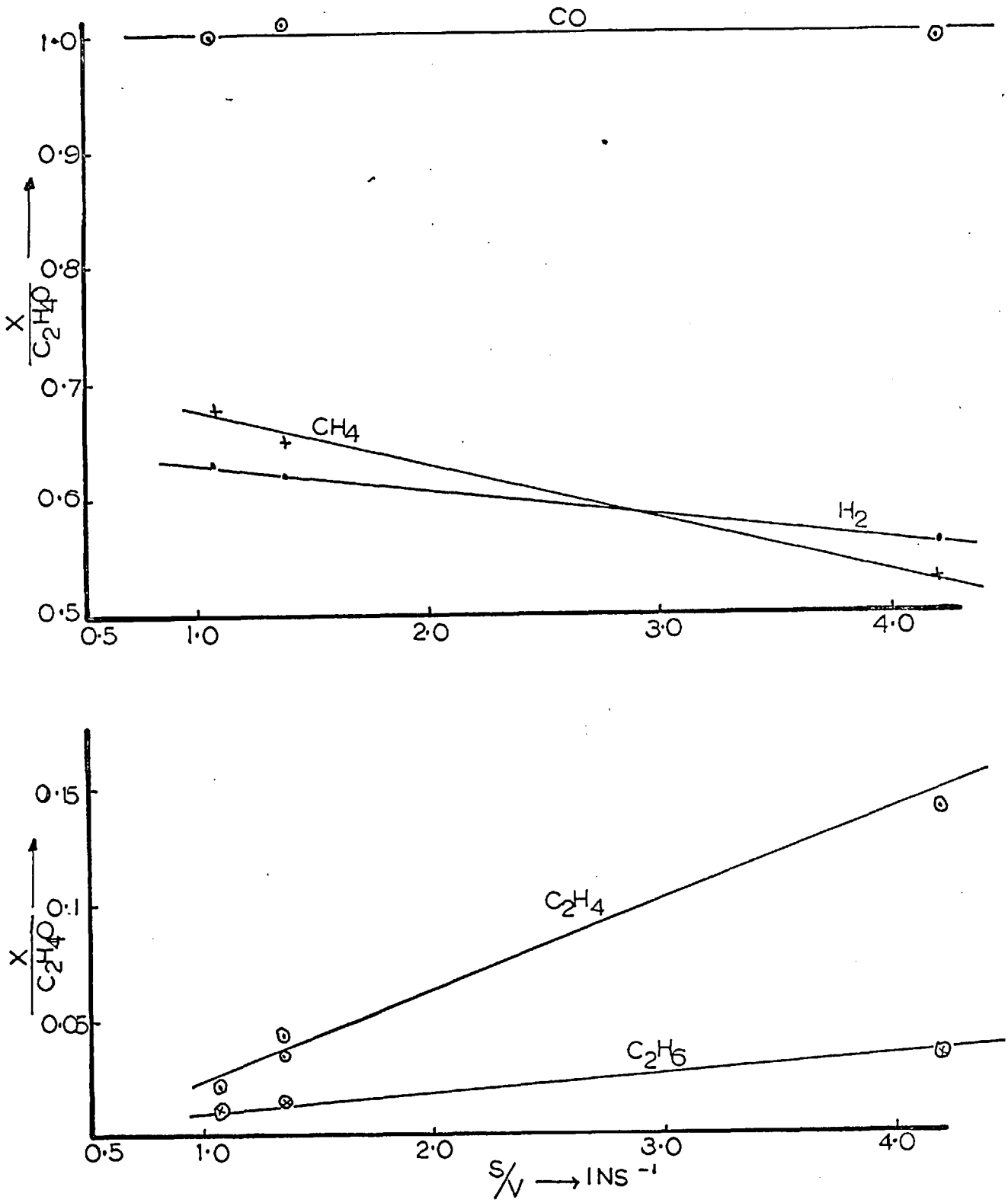

FIGURE 16

V B Ratio of the maximum explosion pressure to the initial pressure P_E/P_I.

The effect of the initial gas temperature on the ratio of the maximum explosion pressure to the initial pressure, P_E/P_I, was studied at an initial pressure of 14·7 psiA in the temperature range 20 - 100°C. Figure 17 shows that the ratio increases from 5·6 to 7·6 as the initial temperature is increased from 20 to 60°C and then decreases as the temperature is increased above 60°C.

The effect of initial pressure on the ratio of P_E/P_I has been studied at an initial temperature of 100°C and pressures in the range 4·16 to 135 psiA. Figure 18 shows that for initial pressures below 14·7 psiA, the ratio P_E/P_I decreases rapidly; it was found that flame propagation was not possible for initial pressures less than 4·17 psiA. However, as the initial pressure is increased from 14·7 psiA to 135 psiA, the ratio P_E/P_I was found to increase steadily from 6·85 to 9·4. A series of experiments were performed using a hot coil as ignition source and the values of P_E/P_I obtained, shown in Figure 18, were lower than those when exploding wires were employed. Figure 18 also shows that the ratio of the final pressure to the initial pressure P_F/P_I increases from 2·04 to 2·62 as the initial pressure is increased from 4·17 to 135 psiA.

The effect of the volume/surface area ratio of the vessel on P_E/P_I was also studied. The decomposition explosions were carried out a

EFFECT OF INITIAL TEMPERATURE P_E/P_I ON P_E/P_I

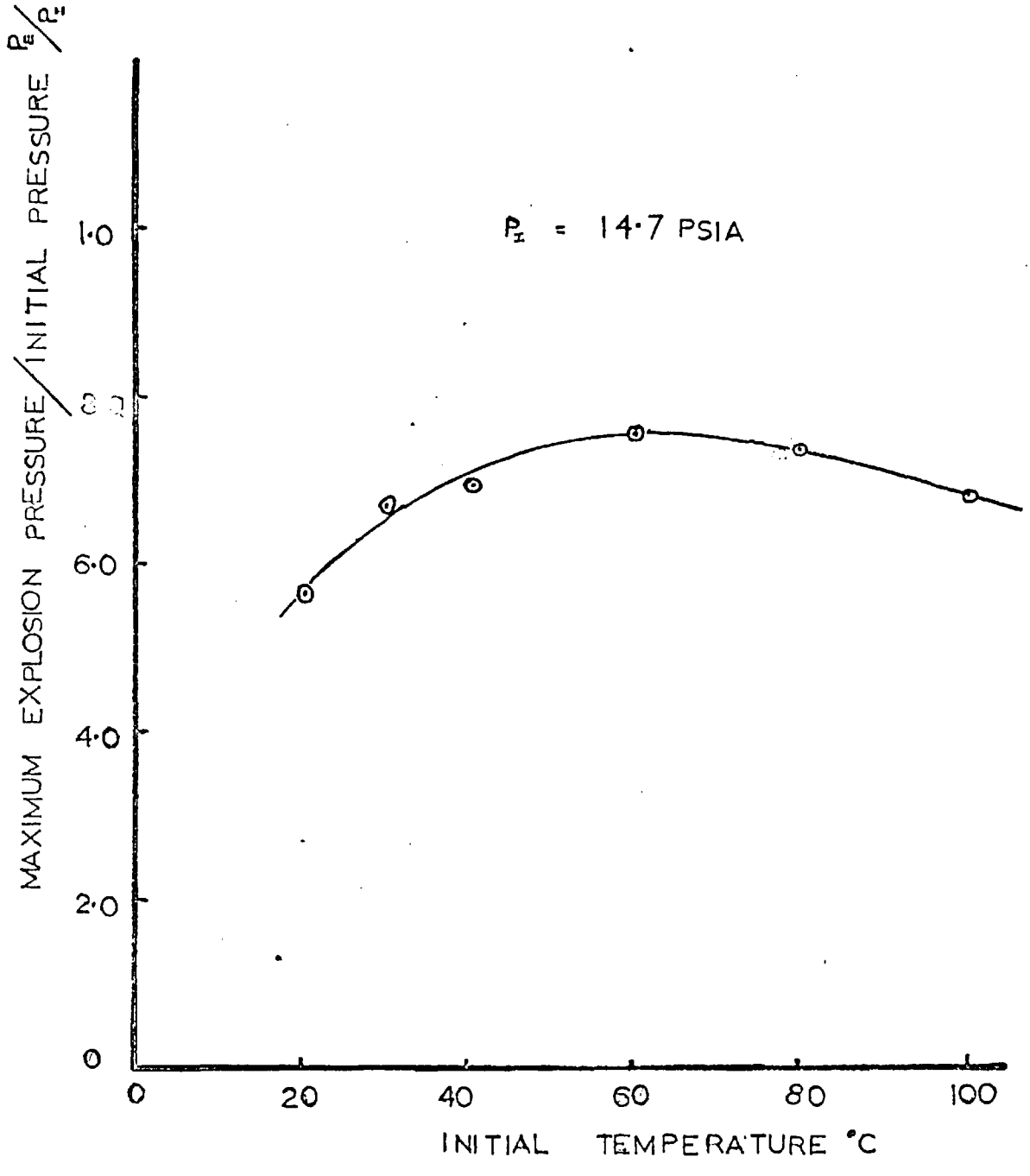

FIGURE 17

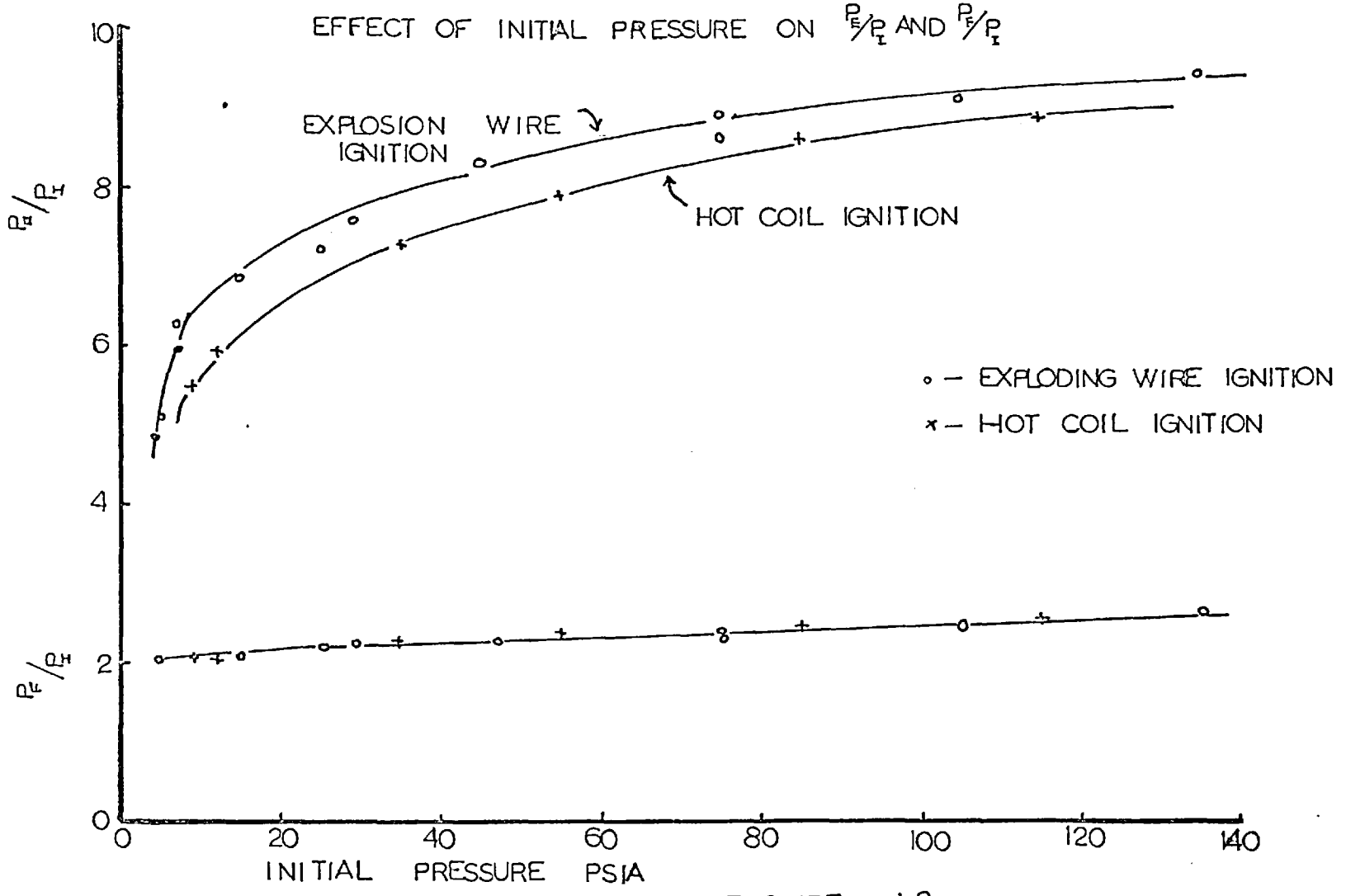
EFFECT OF INITIAL PRESSURE ON P_E/P_I AND P_F/P_I
EXPLOSION WIRE IGNITION
HOT COIL IGNITION
P_E/P_H
P_F/P_H
o — EXPLODING WIRE IGNITION
x — HOT COIL IGNITION
0
2
4
6
8
10
0
20
40
60
80
100
120
140
INITIAL PRESSURE PSIA

FIGURE 18

temperatures in the range 25 - 100°C and at initial pressures up to 45 psiA. The results are shown in Figure 19 from which it is seen that in all cases increasing the V/S ratio of the vessel increases the P_E/P_I ratio. The relationship between V/S and P_E/P_I is approximately linear for the experimental conditions investigated.

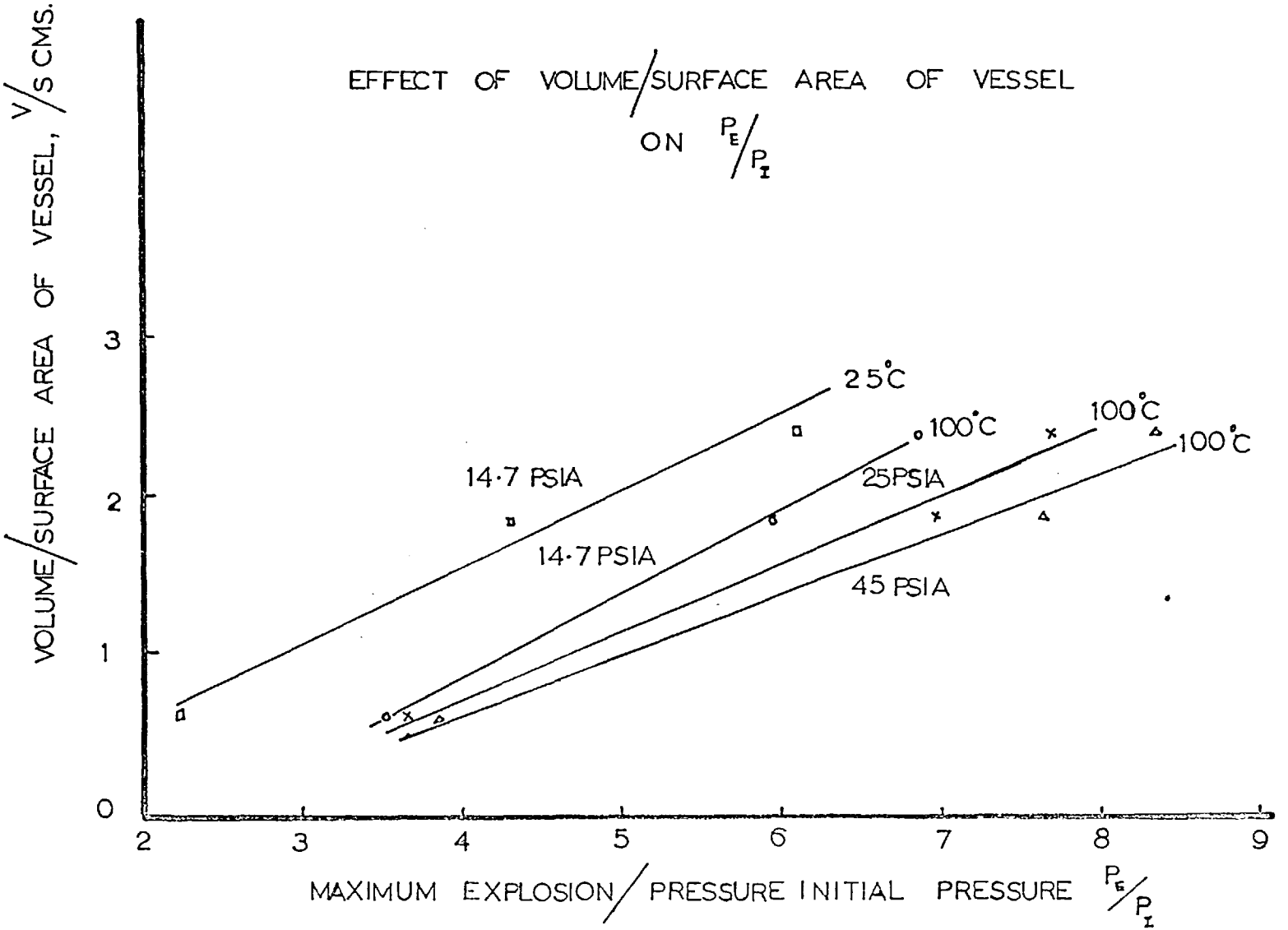
EFFECT OF VOLUME/SURFACE AREA OF VESSEL ON P_E/P_I
VOLUME/SURFACE AREA OF VESSEL, V/S CMS.
0
1
2
3
2
3
4
5
6
7
8
9
MAXIMUM EXPLOSION/ PRESSURE INITIAL PRESSURE P_E/P_I
25°C
14·7 PSIA
100°C
14·7 PSIA
100°C
25PSIA
100°C
45 PSIA

FIGURE 19

CHAPTER VI.

DISCUSSION OF RESULTS ON THE EXPLOSIVE DECOMPOSITION OF PURE ETHYLENE OXIDE VAPOUR.

VI A Interpretation of results from closed vessel experiments:

When an explosive gas mixture is ignited by a suitable source at the centre of a closed vessel, a spherical flame will propagate towards the wall of the vessel. As the flame progresses, the temperature of the unburnt gas will rise in accordance with the laws of adiabatic compression. Immediately after ignition, the gas in the region of the ignition source burns by expanding at practically constant initial pressure, P_I, but it is subsequently compressed to nearly its original volume by the combustion of the rest of the gas in the vessel. This work of compression will be larger than the work of expansion because the compression of the gas takes place at a pressure which steadily increases from P_I to the final pressure P_E, whereas the expansion occurs at the lowest pressure P_I. The last portion of the unburnt gas is compressed under a pressure which rises from P_I to P_E and then expands on burning at the pressure P_E to approximately its original volume. It is therefore apparent that the gas that burns last loses some of its energy while the gas which burns first gains energy in excess of the chemical energy released by combustion. This results in the establishment of a temperature gradient which rises from that portion of the gas burnt last to that burnt first.

Although this temperature difference may be a few hundred degrees, e.g. 800°K in H_2/O_2 explosions [1], it only increases the explosion pressure by about 0·5% [1] compared with the value which would have been obtained had the temperature been uniform. If it is assumed that a uniform temperature, T_E, exists, then for an ideal gas the following relation between P_E and T_E holds:-

$$\frac{P_E}{P_I} = \frac{T_E}{T_I} \frac{n_e}{n_i} \qquad \text{VI (1)}$$

The mean uniform maximum explosion temperature, T_E, can be estimated by applying energy balance equations before and after the explosion. For the purpose of calculation, the explosion is considered to occur in three steps. Firstly, ethylene oxide vapour decomposes to completion at T_I, liberating thermal energy equivalent to $\Sigma n_i (\Delta U_D) T_I$. Secondly, part of this energy is used to dissociate decomposition products at T_I, so that the concentrations correspond to the equilibrium temperate T_E and pressure P_E. Thirdly the rest of the energy is used to raise the equilibrium mixture to a temperature T_E. Equation VI (2) relates these changes in energy.

$$\Sigma n_i (\Delta U_D) T_I = \Sigma j^n{}_{dis} (\Delta U_{dis}) T_I + \Sigma j\, n_e (U T_e - U T_I) \qquad \text{VI (2)}$$

in which n_{dis} and ΔU_{dis} represent moles of product dissociated and the change in internal energy due to the dissociation respectively; each quantity being based on the decomposition of n_i mole of ethylene oxide.

Equation VI (2) assumes that no heat is lost during the explosion; if this were the case, then an ideal type of the pressure - time record such as A B C E shown in Figure 20 would result. In practice several factors influence the shape of the actual pressure - time record. As soon as combustion is initiated, some energy is lost by radiation and conduction to the walls of the vessel and to the ignition electrodes. Thus, at any moment up to the maximum pressure, the actual pressure observed will be lower than that represented by the ideal curve. The rate of heat loss will increase as the combustion proceeds until a condition is reached at which it is equal to the rate of heat liberated. This condition will correspond to the maximum observed explosion pressure, P_E. Combustion is, however, not necessarily complete at the maximum pressure because at the high temperature a state of equilibrium may be established between the reactant and the products. Also, the cooling effect of the walls of the explosion vessel may cause a thin surface layer of the reactant to remain unburnt. In some cases, chemical reaction, with subsequent liberation of heat will continue for a short period after the attainment of the maximum explosion pressure. The effect of this will be to reduce the normal rate of cooling and the slope of the curve DE will be less than that of the ideal curve CE. At some later period, the two cooling curves will meet and thereafter remain superimposed until cooling is completed. It is therefore apparent

COMPARISON OF AN IDEAL AND OBSERVED PRESSURE - TIME RECORD

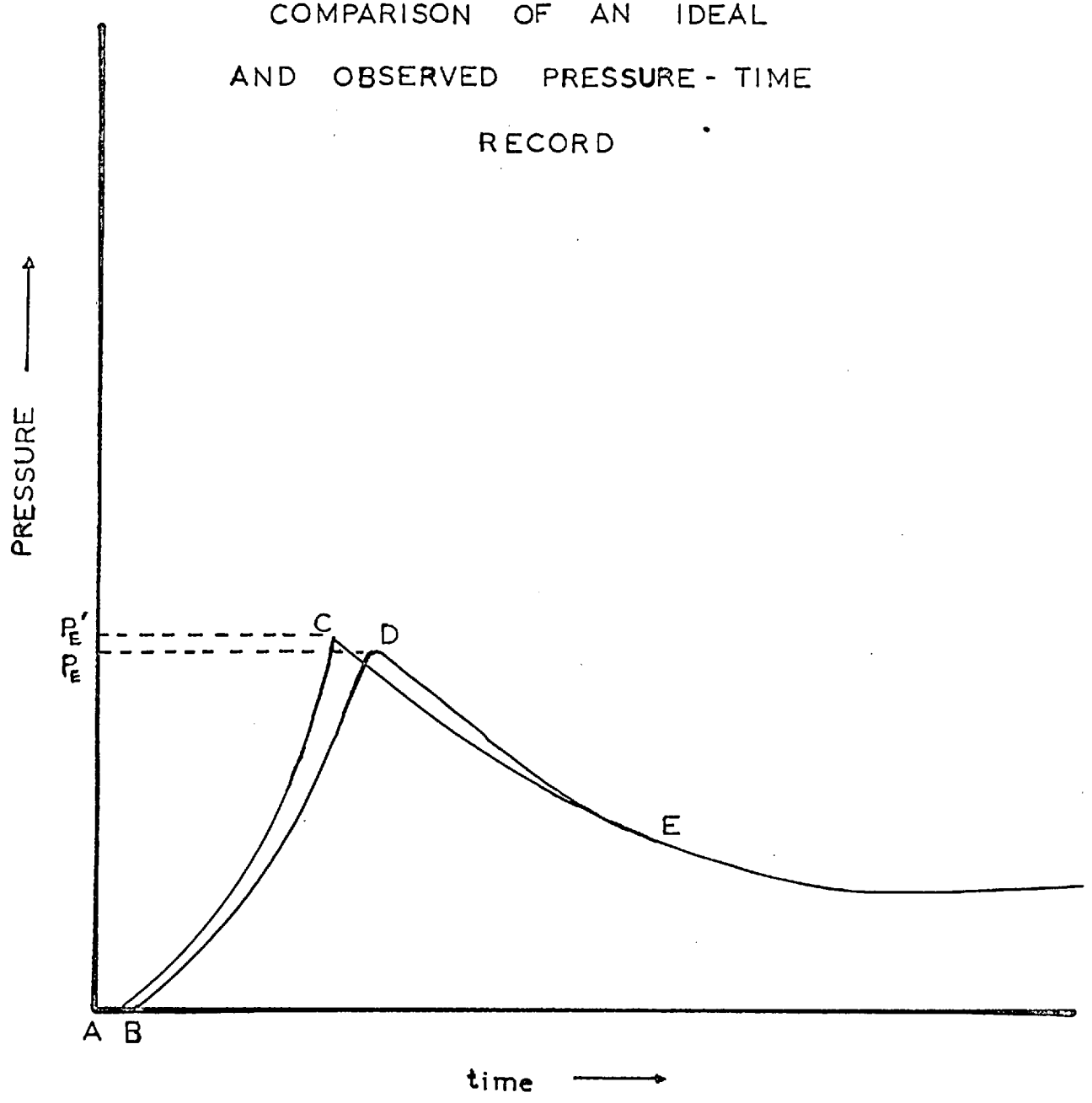

FIGURE 20

that the main factors influencing the final shape of the observed pressure time curve are the heat loss rate during the explosion; the amount of dissociation of the products at P_E, and the amount of the reactant remaining unburnt. Each of these effects was studied during the course of this investigation.

VI B. Products of decomposition.

The final products after complete decomposition of ethylene oxide vapour in a closed vessel are not, of course, the same as the products formed during the initial stages. The major part of the ethylene oxide is decomposed close to the wall after being adiabatically compressed prior to the expansion and subsequent compression of the hot gases produced in the earlier phase of the decomposition. Under these conditions, much higher explosion temperatures are reached compared with the constant pressure flame temperature with the result that secondary decomposition of the products such as CH_4, C_2H_6 and C_2H_4 is likely to occur. It may be seen from Table 6 that a smaller amount of C_2H_4 remains in a closed vessel than is formed in a constant pressure burner for conditions in which the initial pressure of the ethylene oxide in the vessel is the same as that of the flat flame burner.

TABLE 6

Comparison of products of decomposition in a constant volume vessel with a constant pressure burner.

Products	This Work	Flat Flame (23)
	P_I = 14·7 psiA, T_I = 100°C	P = 14·7 psiA, T_I = 70°C
	Volume %	
C_2H_4O	0·90	——
CH_4	27·80	25·9
CO	46·15	44·3
H_2	22·20	19·6
C_2H_6	0·50	——
CO_2	0·10	——
C_2H_4	1·91	10·2
C_6H_6	0·44	——

Apart from C_2H_4, pyrolysis of CH_4, and C_2H_6 may also occur and therefore an estimate was made of the extent to which each of these can be pyrolysed under explosion conditions. The thermal decomposition rate constants (39) for CH_4, C_2H_6, C_2H_4 are shown in Figure 21. From these data an estimate was made of the extent of secondary decomposition that may occur during and after the explosion by applying the first order rate equation,

$$\frac{Q}{Q_0} = e^{-kt} \qquad \text{VI (3)}$$

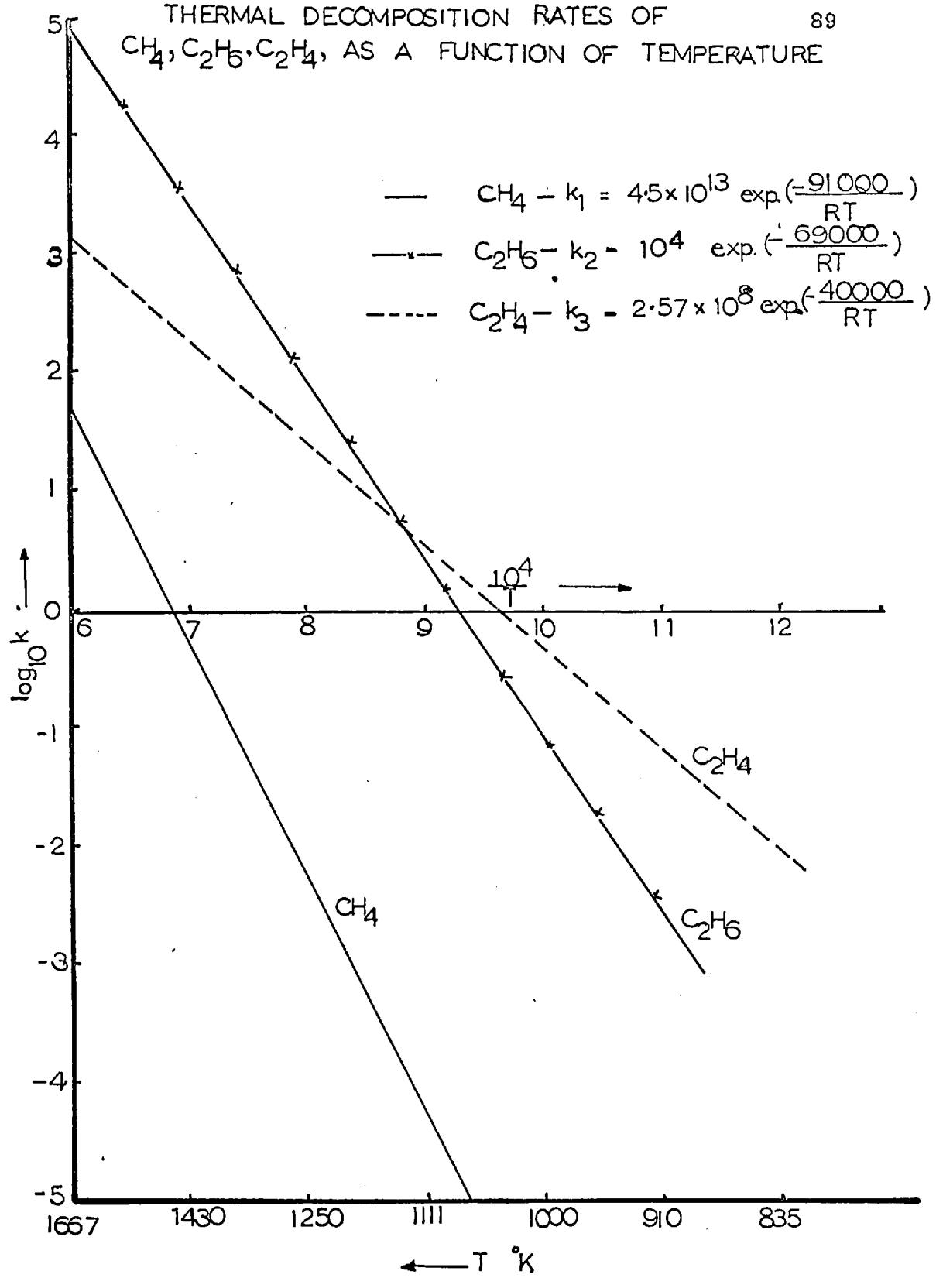
THERMAL DECOMPOSITION RATES OF
CH_4, C_2H_6, C_2H_4, AS A FUNCTION OF TEMPERATURE
$CH_4 - k_1 = 4.5 \times 10^{13} \exp.(-\frac{91000}{RT})$
$C_2H_6 - k_2 = 10^4 \exp.(-\frac{69000}{RT})$
$C_2H_4 - k_3 = 2.57 \times 10^8 \exp.(-\frac{40000}{RT})$
$\log_{10} k$
10^4
C_2H_4
CH_4
C_2H_6
T °K
1667
1430
1250
1111
1000
910
835

FIGURE 21

where a/a_o is the fraction of any component remaining undecomposed. If it is assumed that the major part of the pyrolysis of CH_4, C_2H_6 and CH_4 occurs at the mean maximum explosion temperature, T_E, the fractions of these hydrocarbons not pyrolysed at various time intervals are as given in Table 7.

TABLE 7

Pyrolysis of CH_4, C_2H_6, C_2H_4 under explosion conditions.

P_I = 14·7 psiA, T_E = 1220°K, t_t = 0·3175s

Components	a/a_o			
	0·1s	0·2s	0·3s	0·4s
CH_4	1	0·9995	0·9993	0·9991
C_2H_6	$1·66 \times 10^{-2}$	$3·4 \times 10^{-4}$	$6·3 \times 10^{-6}$	$1·23 \times 10^{-7}$
C_2H_4	0·197	0·039	$7·6 \times 10^{-3}$	$1·5 \times 10^{-3}$

It may be seen from this table that CH_4, unlike C_2H_6 and C_2H_4, is very stable under ethylene oxide explosion conditions and the comparatively large quantities of carbon together with the C_2H_6 and C_2H_4 in the decomposition products are unlikely to have been produced by the pyrolysis of CH_4. The small quantities of C_2H_6 and C_2H_4 present at the end of the explosion, together with the fact that ethane decomposes (39)(40) readily

to give C_2H_4, CH_4 and hydrogen, indicates that the pyrolysis of ethane plays an important role in determining the final products of an ethylene oxide decomposition explosion. It is suggested, therefore, that although ethane is one of the primary products formed in the decomposition of ethylene oxide most of it decomposes during the explosion to give ethylene which then decomposes to give carbon, methane and hydrogen. The proposed overall reactions for the decomposition of ethane are as follows:-

$$C_2H_6 \longrightarrow C_2H_4 + H_2 \qquad \text{VI (4)}$$

$$C_2H_4 \begin{cases} \longrightarrow C + CH_4 \\ \longrightarrow 2C + 2H_2 \end{cases} \qquad \text{VI (5)}$$

Evidence in support of this suggestion is given in Figure 15 from which it may be seen that an increase in the initial pressure from 4.66 psiA to 30 psiA results in a decrease in C_2H_4 and C_2H_6 concentration together with a corresponding increase in the amount of CH_4, carbon and hydrogen according to equation, VI (5). At pressuresabove 30 psiA, the increases in methane formation is probably due to an increase in the reactivity of the methyl radicals present. The overall reaction mechanisms for the explosive decomposition of ethylene oxide vapour can be summarised as follows:-

$$C_2H_4O \longrightarrow CO + CH_4 \qquad \text{VI (6)}$$

$$C_2H_4O \longrightarrow CO + C + 2H_2 \qquad \text{VI (7)}$$

$$C_2H_4O \longrightarrow CO + \tfrac{1}{2}C_2H_4 + H_2 \qquad \text{VI (8)}$$

$$C_2H_4O \longrightarrow CO + \tfrac{1}{2}C_2H_6 + \tfrac{1}{2}H_2 \qquad \text{VI (9)}$$

Traces of CO_2, H_2O and C_6H_6 have also been detected in the products of the explosive decomposition of ethylene oxide vapour. The presence of C_6H_6 probably arises from the mechanism of carbon formation, while the presence of CO_2 and H_2O is due to side equilibrium reactions of the type

$$CO + 3H_2 \rightleftharpoons CH_4 + H_2O \qquad \text{VI (10)}$$

$$CO + H_2O \rightleftharpoons CO_2 + H_2 \qquad \text{VI (11)}$$

The effect of the surface area to the internal volume ratio, S/V, on the products of decomposition of ethylene oxide vapour is illustrated in Figure 16. These results confirm that pyrolysis of C_2H_4 and C_2H_6 occurs during the explosive decomposition of ethylene oxide vapour according to equations VI (4), (5). For vessels having a large S/V ratio, the heat loss during the explosion results in a lower maximum explosion pressure and causes less C_2H_4 and C_2H_6 to be pyrolysed. For vessels with small S/V ratio the reverse is true.

VI C Heat transfer in closed-vessel explosions.

(1) The heat loss rate and the maximum explosion pressure:-

A quantitative study of the heat losses by radiation, convection and conduction in a gaseous explosion is most difficult. As far as convection is concerned it is generally conceded that the rate of heat flow from the hot gases per unit area of the wall surface of the explosion vessel is dependent mainly on the temperature difference, the gas pressure and the degree of turbulence. Also, the rate of heat loss by convection

will decrease as the size of the vessel is increased and in fact will be dependent, in the main, on the ratio of the surface area to the internal volume of the vessel. Radiation is no less complicated. Although it is known from Stefan's law that the rate of heat loss for black body radiation is proportional to the fourth power of the absolute temperature difference, radiation emission from gaseous combustion products largely occurs in well defined frequency bands and the variation in the rate of heat loss with temperature is uncertain.

In order to estimate the heat losses, it is assumed that the part of the pressure-time curve succeeding the maximum explosion pressure is a true cooling curve and that its slope represents the rate of pressure fall, $(-\frac{dP}{dt})$, due to the overall heat losses. From this cooling curve, the maximum rate of pressure fall, $(-\frac{dP}{dt})_{max.}$ will correspond to conditions at the maximum explosion pressure, P_E. The major part of the heat loss during the cooling process will be by convection and therefore can be represented as

$$+\frac{Q}{S} = h\,(T - T_I) \qquad \text{cal/s/cm}^2 \qquad \text{VI (12)}$$

where h, is the heat transfer coefficient, cal/s/cm^2/^{o}K

Q, is the heat loss rate, cal/s

S, is the surface area of vessel, cm^2

and T, is the gas temperature ^{o}K.

Now, the heat loss rate, Q, can also be expressed as

$$Q = n_e \bar{C}_v \frac{dT}{dt} \qquad \text{VI (13)}$$

where $\bar{c}v$ is the mean molar specific heat of the gas mixture.

By combining equations VI (12) and VI (13), then

$$- \frac{n_e \bar{C}_v}{S} \frac{dT}{dt} = h (T - T_x) \qquad \text{VI (14)}$$

Expressing pressure in units of atmospheres,

$$- \frac{dP^*}{dt} = \frac{h S}{n_e \bar{C}_v} (P^* - P_F^*) \qquad \text{VI (15)}$$

Integrating equation VI (15)

$$\log \left\{ \frac{P_E^* - P_F^*}{P^* - P_F^*} \right\} = \frac{h \quad S}{ne \ \bar{c}v \ 2.303} \cdot t. \qquad \text{VI (16)}$$

A plot of $\log \left\{ \frac{P_E^* - P_F^*}{P^* - P_F^*} \right\}$ against 't' is shown in Figure 22 to give straight lines whose slope, B, can be used to evaluate the overall heat transfer coefficient, h, for each explosion. The overall heat transfer coefficients are correlated with the maximum explosion pressures as shown in Figure 23. Over the straight line part of the graph, the following expressions are obtained:-

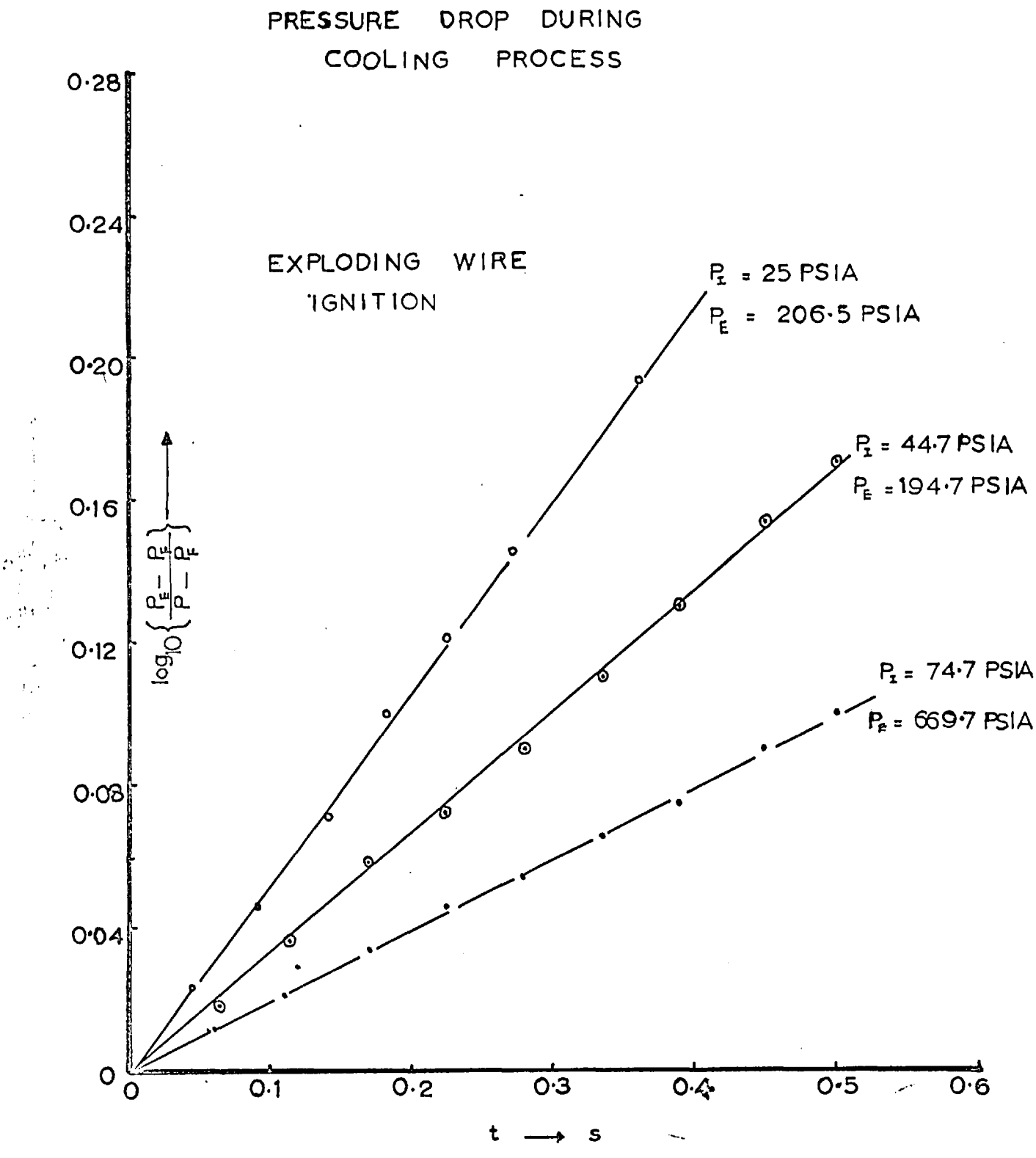
PRESSURE DROP DURING
COOLING PROCESS
EXPLODING WIRE
IGNITION
P_I = 25 PSIA
P_E = 206·5 PSIA
P_I = 44·7 PSIA
P_E = 194·7 PSIA
P_I = 74·7 PSIA
P_E = 669·7 PSIA
$\log_{10}\left\{\frac{P_E - P_I}{P - P_I}\right\}$
0·28
0·24
0·20
0·16
0·12
0·08
0·04
0
0·1
0·2
0·3
0·4
0·5
0·6
t ⟶ s

FIGURE 22

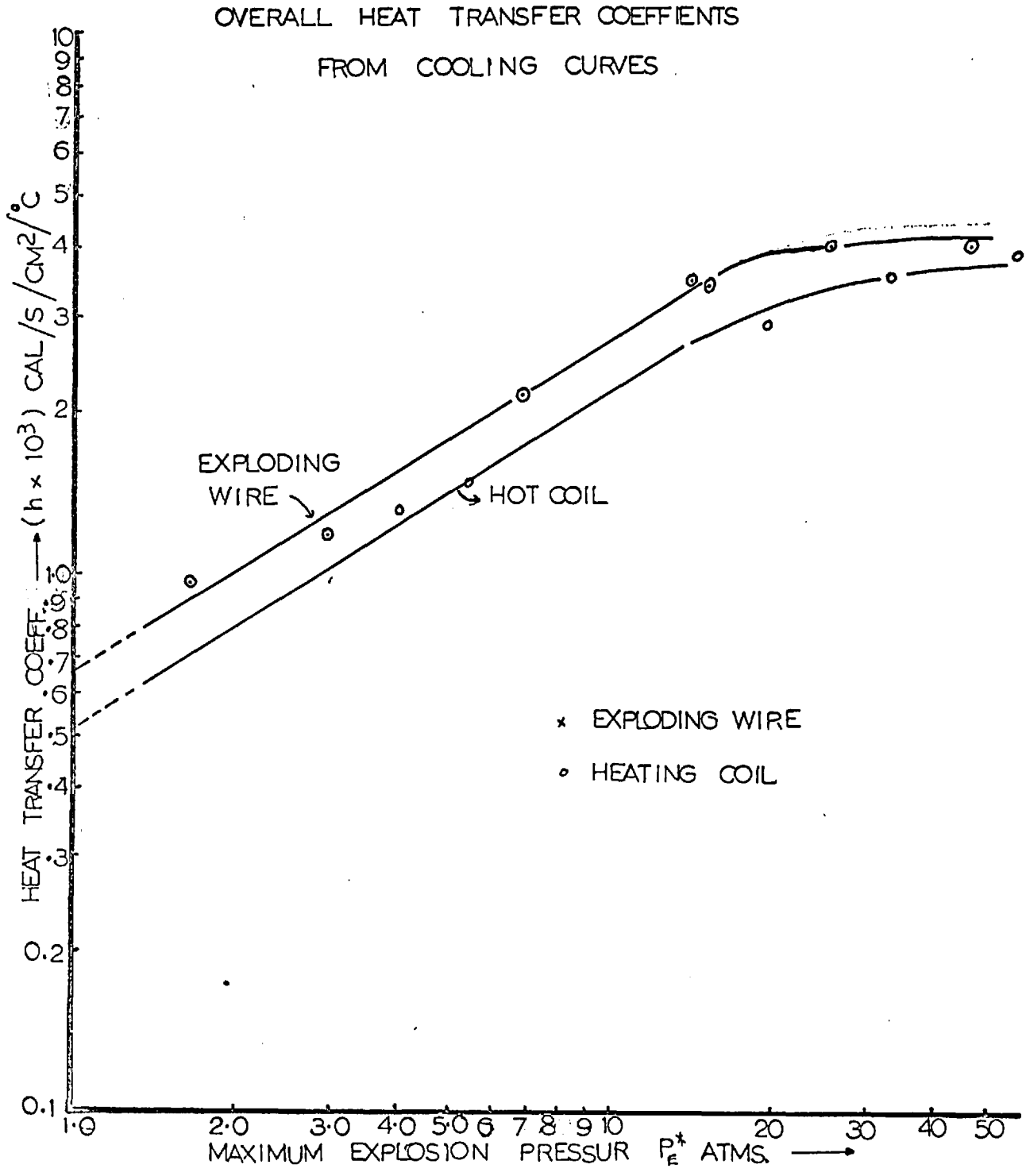
OVERALL HEAT TRANSFER COEFFIENTS
FROM COOLING CURVES
HEAT TRANSFER COEFF. → (h × 10³) CAL/S/CM²/°C
EXPLODING WIRE
HOT COIL
× EXPLODING WIRE
○ HEATING COIL
MAXIMUM EXPLOSION PRESSUR P*E ATMS. →

FIGURE 23

$$h = 0{\cdot}66 \times 10^{-3} \left(P_E^*\right)^{0{\cdot}6} \quad \text{for exploding wire ignition} \qquad \text{VI (17)}$$

$$h = 0{\cdot}52 \times 10^{-3} \left(P_E^*\right)^{0{\cdot}6} \quad \text{for hot coil ignition} \qquad \text{VI (18)}$$

The maximum rate of cooling, $-\left(\frac{dP^*}{dt}\right)_{max.}$ can then be calculated from equation VI (15). A summary of the results is given in Table A2, in Appendix 2.

The rate of heat loss during the explosion period will vary from zero at the instant of ignition to a maximum at the end of the explosion. If it is assumed that the rate of heat loss during the explosion period is proportional to the area of a spherical flame of radius, r_b, then the equivalent rate of pressure decrease due to the heat loss is given by

$$-\frac{dP}{dt} \propto r_b^2 \qquad \text{VI (19)}$$

The radius of the spherical flame, r_b, can be estimated from the pressure-time curve together with equation IX (6). Figure 16 shows that the area of the flame increases in proportion with the time of the explosion during the greater part of the explosion period. Hence

$$r_b^2 \propto t \qquad \text{VI (20)}$$

Towards the end of the explosion period, contact of parts of the flame with the vessel wall quenches the flame and the flame area is reduced.

FLAME AREA Vs time

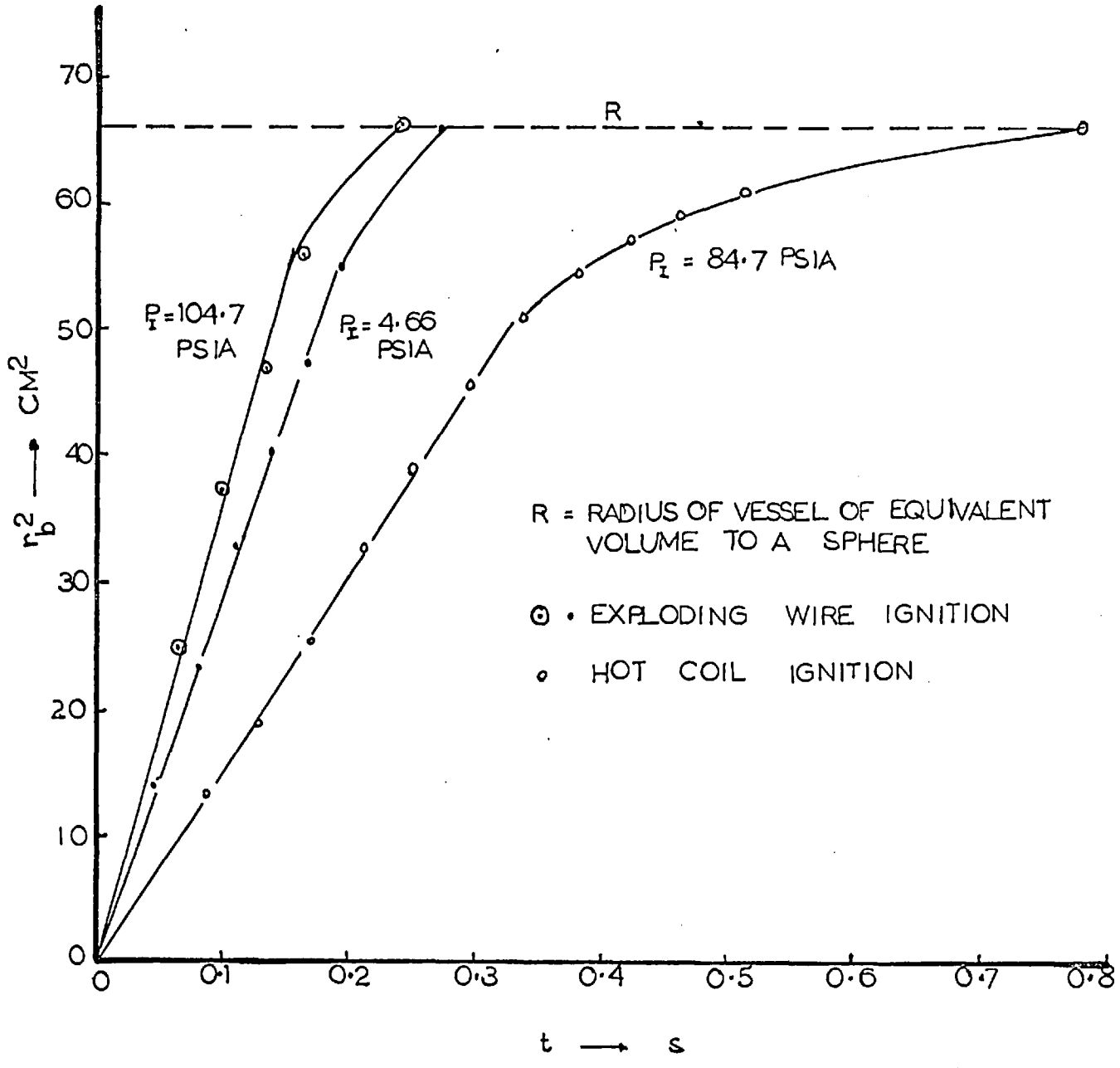

FIGURE 24

This is particularly so for explosions initiated by the hot coil. Combining equations VI (19) and (20), the following expression is obtained:-

$$-\frac{dP}{dt} \propto t \qquad \text{VI (21)}$$

Thus the rate of heat loss during the explosion period varies linearly from zero on ignition to a maximum at P_E, and the loss during the explosion is equivalent to a decrease in pressure $\Delta P'$ which is given by

$$\Delta P' = \frac{1}{2} \left(-\frac{dP}{dt} \right)_{max.} t_t \qquad \text{VI (22)}$$

Hence the maximum explosion pressure corrected for heat loss, P_E' is given by

$$P_E' = P_E + \Delta P' \qquad \text{VI (23)}$$

A summary of the results is contained in Table A3 in Appendix 2.

The maximum explosion pressures can also be calculated from the thermo-chemical properties of the reactant and the products of decomposition using equation VI (2). In order to make this calculation it is assumed that no dissociation of the products of decomposition occurs and that the number of moles at the end of the explosion, n_e, is equal to the number of moles, n_f, after the products of the decomposition have been cooled to the

initial temperature, T_I. Figure 25 shows the results for the measured values of the ratio of the maximum explosion pressure to the initial pressure, P_E/P_I, the results when corrected for heat losses, P'_E/P_I, and the calculated values, $(P_E/P_I)c$. It can be seen that when ethylene oxide at low pressure is ignited, e.g. P_I = 4·17 psiA, a large quantity of heat is lost during the explosion process and this accounts for the measured explosion pressure being 27% lower than the value corrected for heat loss. At higher pressures, e.g. P_I = 134·7 psiA, this difference is only 4·4%. The calculated maximum explosion pressures are, on the average, 3% higher than the experimental values corrected for heat losses. This discrepancy may be attributed to two factors; firstly, the error involved in the estimation of the rate of heat loss during the explosion, and secondly the assumption that $n_e = n_f$. The latter assumption is not strictly true because pyrolysis of some of the decomposition products may occur during the cooling process. Nevertheless the procedure adopted for the estimation of the rate of heat loss provides a simple but adequate approach to the solution of the complex problems associated with heat transfer in explosion processes.

VI C (2) Effect of volume/ surface area of the vessel on P_E/P_I.

The results for the effect of the volume to the surface area ratio on P_E/P_I are shown in Figure 16. A comparison of the results with other workers [24][26] is shown in Figure 26. For vessels of similar

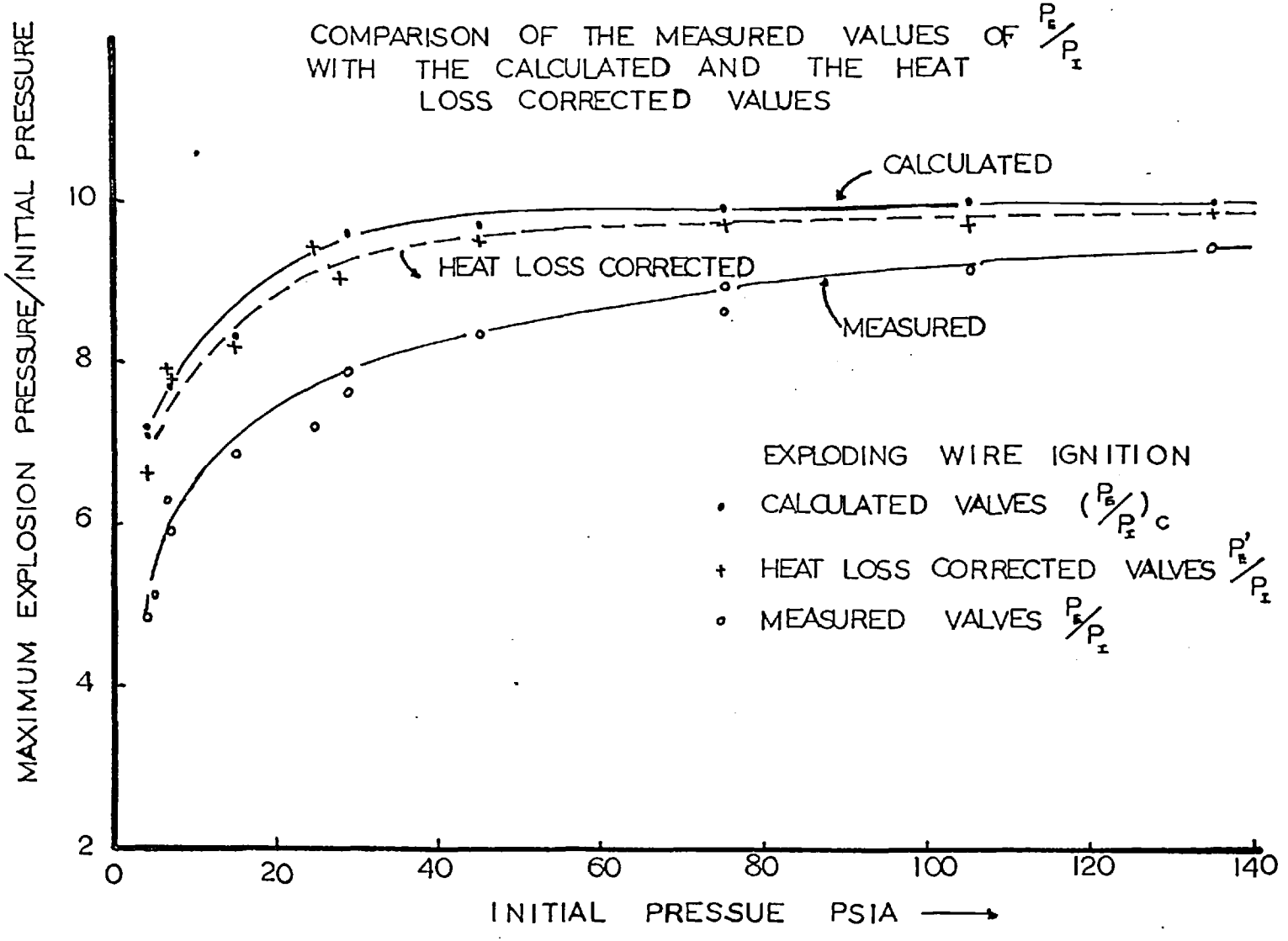
COMPARISON OF THE MEASURED VALUES OF P_E/P_I WITH THE CALCULATED AND THE HEAT LOSS CORRECTED VALUES
CALCULATED
HEAT LOSS CORRECTED
MEASURED
EXPLODING WIRE IGNITION
• CALCULATED VALVES $(P_E/P_I)_C$
+ HEAT LOSS CORRECTED VALVES P'_E/P_I
○ MEASURED VALVES P_E/P_I
MAXIMUM EXPLOSION PRESSURE/INITIAL PRESSURE
10
8
6
4
2
0
20
40
60
80
100
120
140
INITIAL PRESSUE PSIA ⟶

FIGURE 25

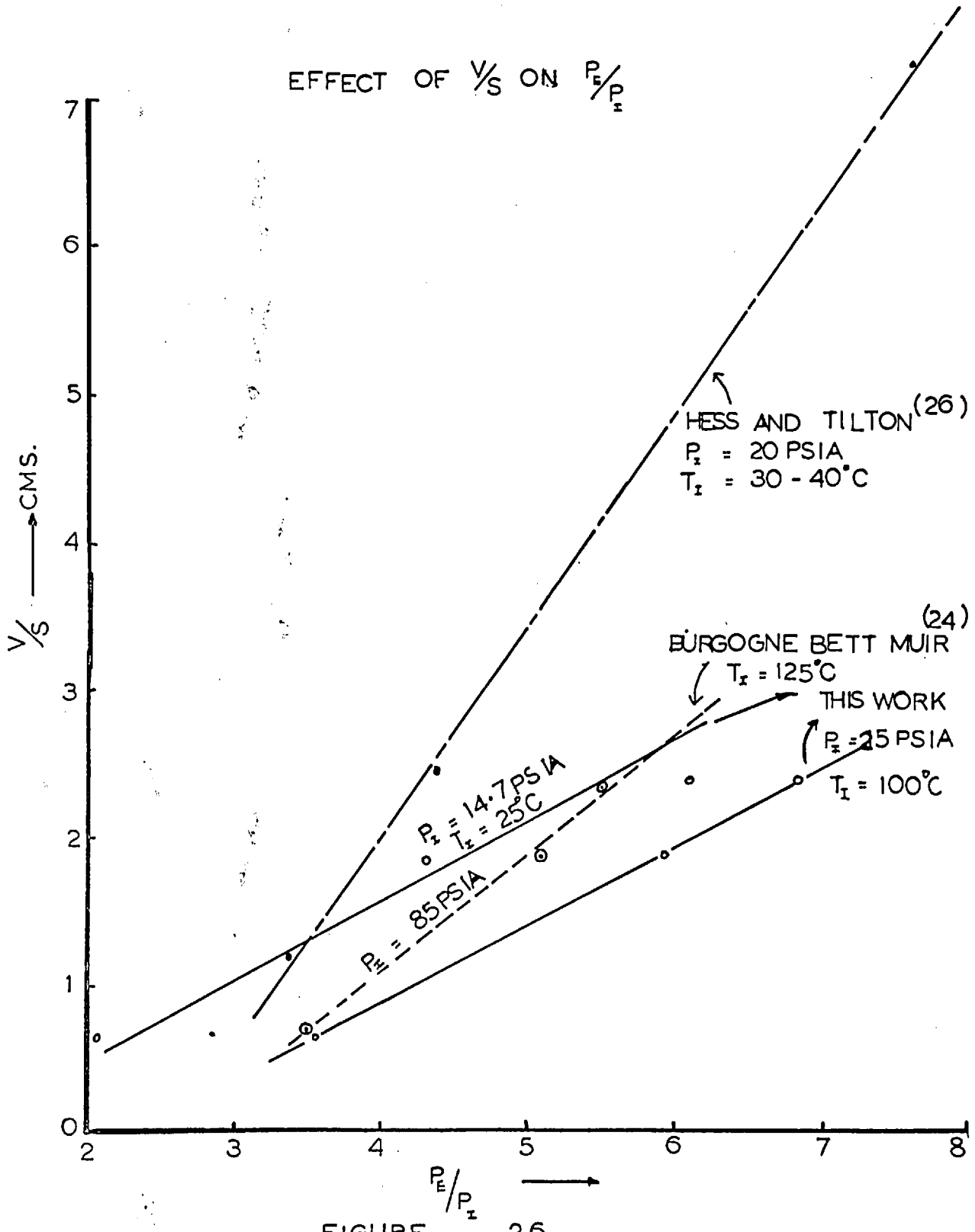
EFFECT OF V/S ON PE/PI
V/S ——→ CMS.
PE/PI ——→
HESS AND TILTON (26)
PI = 20 PSIA
TI = 30 - 40°C
BURGOGNE BETT MUIR (24)
TI = 125°C
THIS WORK
PI = 25 PSIA
TI = 100°C
PI = 14.7 PSIA
TI = 25°C
PI = 85 PSIA
0
1
2
3
4
5
6
7
8

FIGURE 26

ratios, it is seen that the results of both Hess and Tilton's [26] and Burgoyne et al [24] differ from those obtained in this work. The reason for the low values of P_E/P_I obtained by Burgoyne et al [24] has been shown to be due to the use of a faulty pressure transducer. It is difficult to comment on the low explosion pressure obtained by Hess and Tilton,[26] because the experimental conditions were not specified accurately. For example, although the authors mentioned that they had great difficulty in measuring their explosion pressures and that they had employed several pressure measuring devices, they did not specify which one they used to obtain their results. Also, their result on the effect of V/S on P_E/P_I referred to an initial temperature between 30 and 40°C. It is shown in Figure 17 that for an ethylene oxide explosion at an initial pressure of 14·7 psiA, a temperature increase from 30 to 40°C will increase the explosion pressure by 9%. Thus, even if it is assumed that Hess and Tilton worked at the maximum temperature of 40°C, their measured explosion pressure are still low compared to the results obtained in this work. One possible explanation for this discrepancy is that although their vessel may have the same volume to surface area ratio as that used in this investigation, geometrical factors such as the length to diameter ratio of the vessel and the difference in the orientation of the vessels may have increased the amount of ethylene oxide which remained undecomposed and hence lowered the explosion pressures.

A decrease in the maximum explosion pressure can be caused by a decrease in the volume to the surface area ratio of the vessel and also by an increase in the amount of ethylene oxide vapour which remains undecomposed at the end of the explosion. Therefore in order to study the effect of the ratio V/S of the vessel on the maximum explosion pressure, it is necessary to correct the measured explosion pressures to correspond to a situation in which all the ethylene oxide vapour is decomposed. The calculated corrections are summarised in Table A4 in Appendix 2c. If it is assumed that the cooling rates calculated in the preceding section are applicable to vessels of different V/S ratios, then from equations VI (15), (22), (23)

$$P'_{Eo} - P_{Eo} = \Delta P' = \tfrac{1}{2} t_t \frac{h\, RT_E}{P_E\, \bar{C}v} \cdot \frac{S}{V} (P_{Eo} - P_{Fo}) \qquad \text{VI (24)}$$

where P'_{Eo} represents the maximum explosion pressure which occurs when all the gas decomposes assuming that no heat loss occurs. As the V/S of the vessel changes, the total explosion time, t_t, and the heat transfer coefficient, h, will also change. In order to study the effect of V/S on P_E/P_I, it is necessary to study the behaviour of the function $\frac{1}{2} t_t \frac{h\, RT_E}{P_E\, \bar{C}_v} \cdot \frac{S}{V}$ Hence from equation VI (24), the following relation is obtained:-

$$\frac{P_{Eo}}{P_I} = \frac{\frac{1}{2} t_t \frac{h\, RT_E}{P_E\, \bar{C}_v} \cdot \frac{S}{V} \cdot \frac{P'_{Eo}}{P_I} + \frac{P_{Fo}}{P_I}}{1 + \left(\frac{1}{2} t_t \frac{h\, RT_E}{P_E\, \bar{C}_v} \frac{S}{V}\right)} \qquad \text{VI (25)}$$

Equation VI (25) may be expressed more simply as

$$\frac{P_{Eo}}{P_I} = \frac{X\frac{P'_{Eo}}{P_I} + \frac{P_{Fo}}{P_I}}{1 + X} \qquad \text{VI (25a)}$$

where

$$\frac{1}{X} = \frac{1}{2}\frac{h\,R\,T_E}{P_E\,C_v}\frac{S}{V} \qquad \text{VI (26)}$$

The results of specific experiments for which the values of $\frac{P'_{Eo}}{P_I}$ and $\frac{P_{Fo}}{P_I}$ are known, enabled the plot of $\frac{P_{Eo}}{P_I}$ against X shown in Figure 27 to be constructed for arbitrary values of X. The values of $\frac{P_{Eo}}{P_I}$ and X evaluated from experimental observations have been superimposed on Figure 27 from which it may be seen that the various points fall near the appropriate curve suggesting that equation VI (25) is in accord with experimental observations. This is substantiated by inspection of Figure 27 which shows that:-

(i) as the ratio V/S of the vessel is increased to an infinite value, the ratio P_{Eo}/P_I approaches P'_{Eo}/P_I asymtotically.

(ii) for vessels of small V/S ratio, excessive heat is lost and the value P_{Eo}/P_I tends towards the value P_{Fo}/P_I.

It is therefore concluded that there is no direct relationship between V/S and P_E/P_I, factors such as the total explosion time· the heat transfer coefficient and the amount of ethylene oxide remain

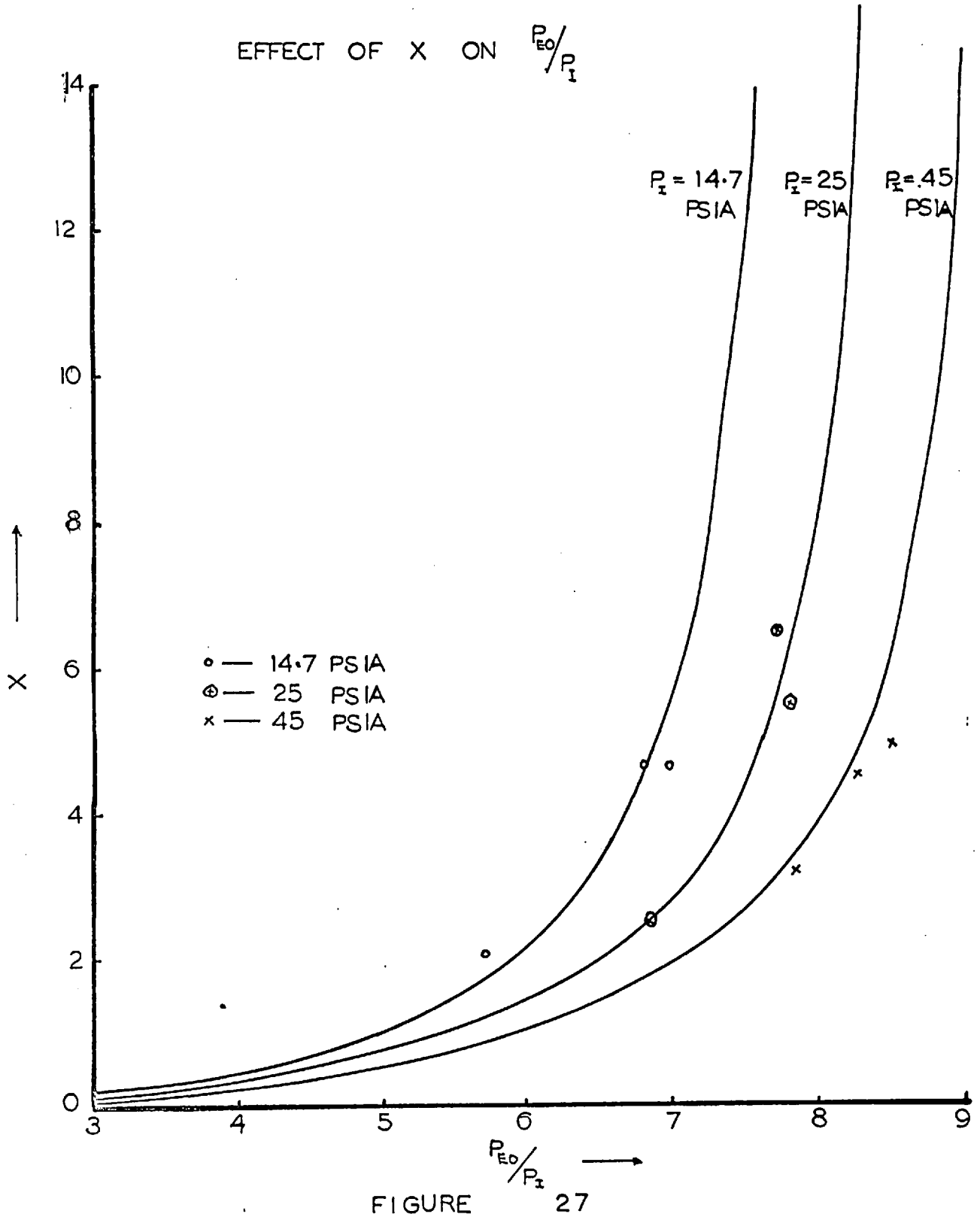
EFFECT OF X ON P_{EO}/P_I
P_I = 14.7 PSIA
P_I = 25 PSIA
P_I = 45 PSIA
o — 14.7 PSIA
⊗ — 25 PSIA
× — 45 PSIA
X
P_{EO}/P_I
0
2
4
6
8
10
12
14
3
4
5
6
7
8
9

FIGURE 27

undecomposed will always be closely associated with changes in the size and shape of the vessel. The relationship between all these factors being represented by equation VI (25). In view of this it is unadvisable to extrapolate the lines shown in Figure 19 into regions for which experimental results are not available.

VI C (3) Effect of initial gas temperature on P_E/P_I.

Figure 17 shows that P_E/P_I increases from 5·6 to 7·6 as the initial temperature is increased from 20 to 60°C and then decreases as the temperature is increased above 60°C. It is shown in Figure 13 that the increase in P_E/P_I is due to the decomposition of increasing amounts of ethylene oxide. At temperatures above 60°C nearly all the ethylene oxide vapour is decomposed and the drop in P_E/P_I arises as a consequence of the higher initial temperature.

VI D Wall quenching of the ethylene oxide decomposition flame.

VI D (1) Introduction:-

Whenever a gaseous explosion occurs in a closed vessel there is a small but finite quenched layer at the wall surface that remains unburnt. This unburnt layer, or quenched zone, is frequently known as the 'dead space'. The thickness of the 'dead space' is not constant, for besides being dependent on the explosion mixture, the vessel temperature and the

explosion pressure, it is also affected by such factors as the degree of turbulance and the shape and size of the vessel. During an explosion, the quenching of the flame by the vessel wall will not occur simultaneously at all points on the flame front, neither will it produce a dead space which is uniformly thick. In view of these factors, the percentage of the ethylene oxide vapour which remains undecomposed can be regarded only as an indication of the mean thickness of the 'dead space'.

VI D (2) The effect of various factors on the percentage of ethylene oxide remaining undecomposed.

Figure 13 shows that for vessel temperature above 80°C, the percentage of undecomposed ethylene oxide decreases only slightly with increasing temperature. However, for vessel temperatures below 80°C, the amount of ethylene oxide remaining undecomposed increases rapidly. The reason for this is that during the explosion, some of the ethylexe oxide vapour condenses on the vessel wall, where it remains undecomposed, until it is finally revapourised and mixes with the decomposition products. Condensation of ethylene oxide vapour will always occur if the explosion pressure exceeds the saturated vapour pressure of ethylene oxide at the vessel temperature. For the data presented in Figure 13, the maximum explosion pressure are such that no condensation occurs at vessel temperatures above 80°C, hence temperature has only a slight effect on the amount of ethylene oxide remaining undecomposed.

At a temperature of 100°C, the saturated vapour pressure of ethylene oxide vapour is 195 psiA. Therefore, at maximum explosion pressures in excess of 195 psiA, condensation of ethylene oxide is likely to occur at the wall of the vessel. It may be seen from Figure 28 that at pressures greater than 200 psiA, the percentage of undecomposed ethylene oxide decreases slowly to a constant value of 0·9%. If no condensation occurs and all the ethylene oxide vapour remaining undecomposed comes from the wall quenching process, then the amount of undecomposed ethylene oxide will depend on the maximum explosion pressure. This was found to be so; for explosion pressures below 200 psiA, the amount of undecomposed ethylene oxide vapour increases steeply until flame propagation fails. A plot of the percentage undecomposed ethylene oxide against $10^3/P_E$ is also shown in Figure 28, which gives a straight line through the origin for low explosion pressures. Hence it may be concluded that if there is no condensation, the percentage of undecomposed ethylene oxide is inversely proportional to the maximum explosion pressure developed during the explosion.

The ratio S/V of the vessel was altered in the usual manner by inserting appropriate liners into the vessel. Figure 29 shows that increasing amounts of ethylene oxide remained undecomposed for those vessels with large S/V ratios. Although this result conforms with the wall quenching process, it must be borne in mind that other factors such as the shape and diameter of the vessel will also influence the amount of undecomposed ethylene oxide.

EFFECT OF MAXIMUM EXPLOSION PRESSURE ON % ETHYLENE OXIDE UNDECOMPOSED

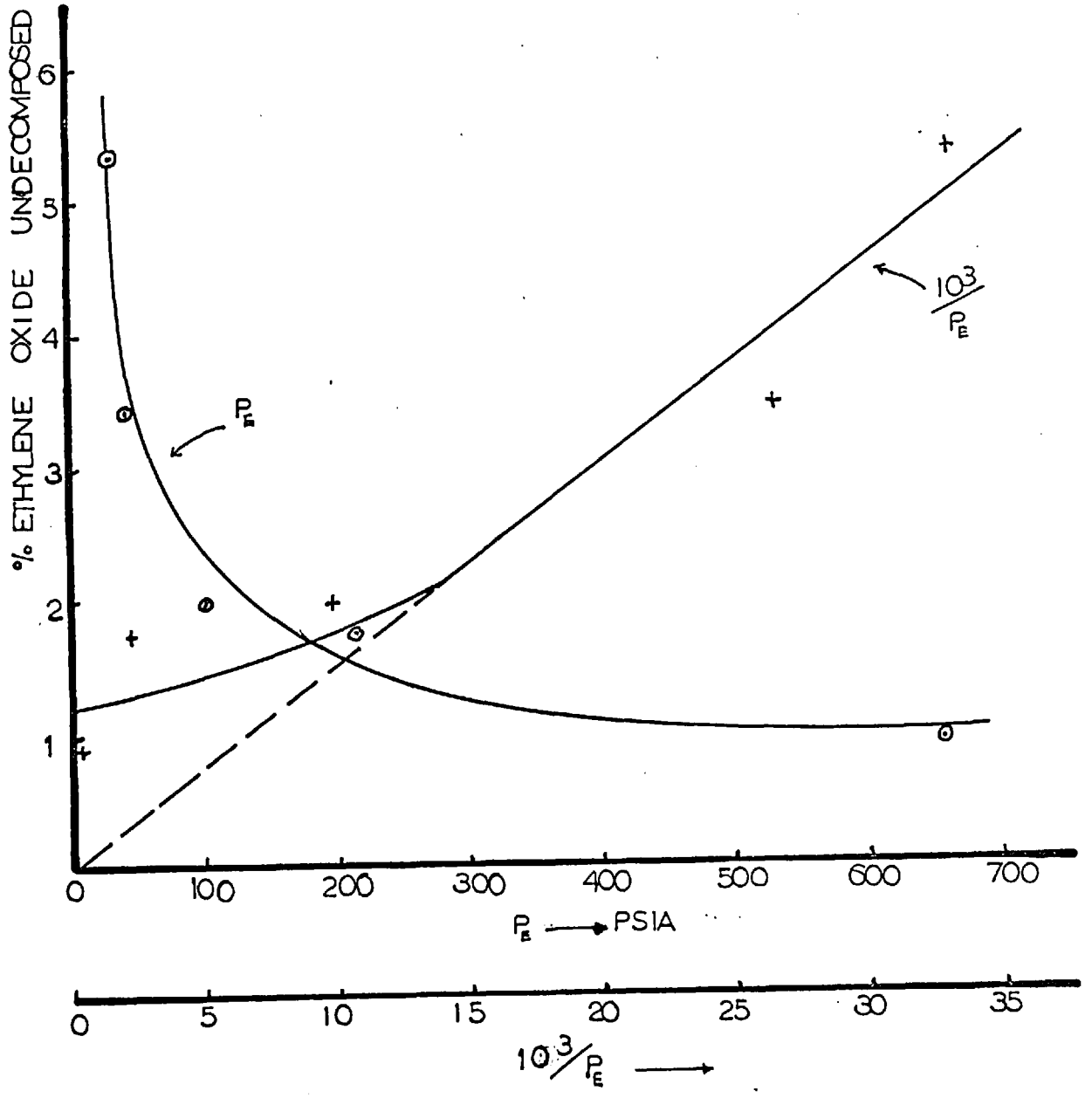

FIGURE 28

EFFECT OF SURFACE-VOLUME RATIO OF THE VESSEL ON % C_2H_4O REMAINED UNDECOMPOSED

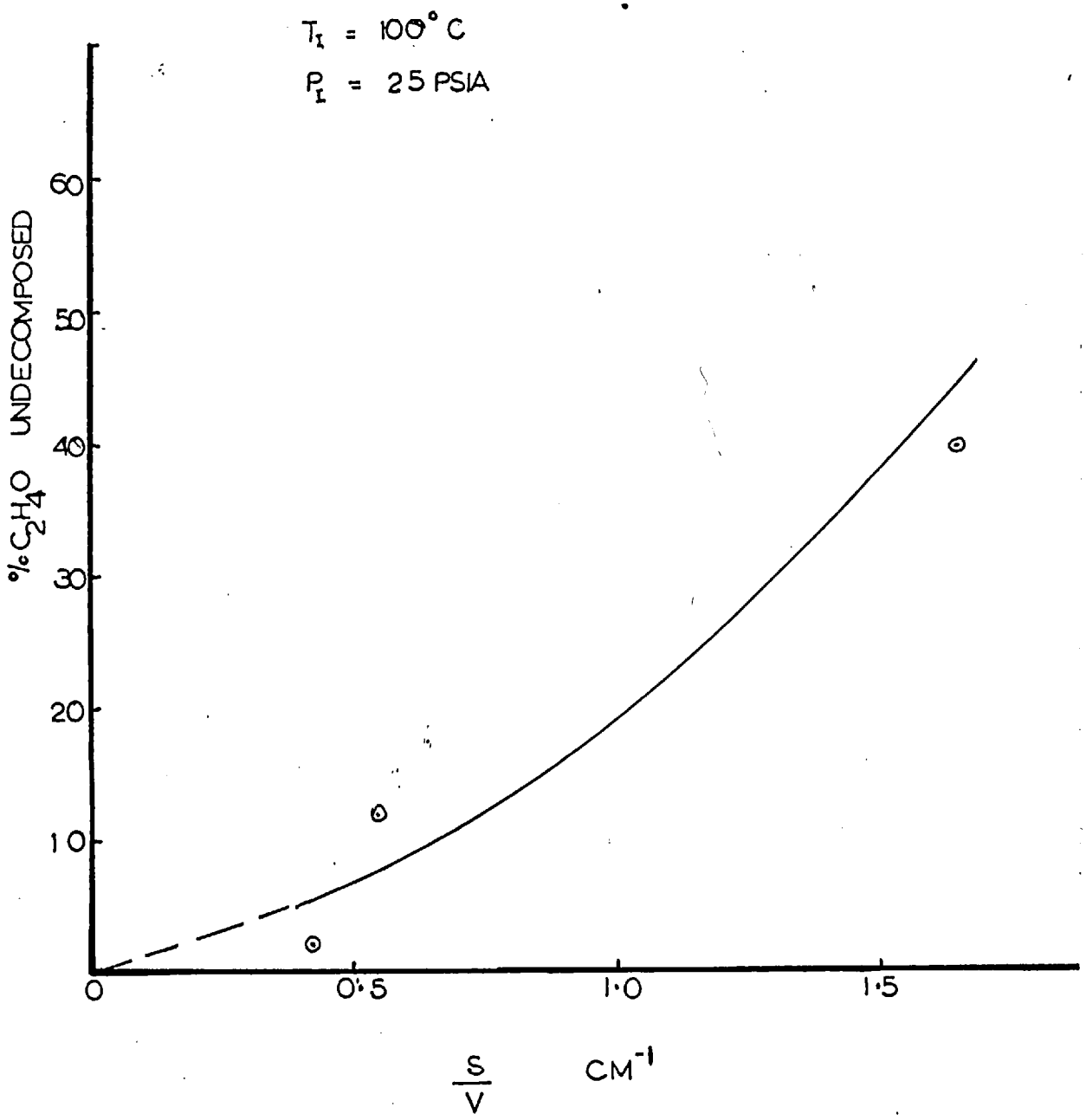

FIGURE 29

It has been shown [1] that with a laminar flame produced by hydrocarbon air systems, the quenching distance is dependent on the fuel to air ratio and is always a minimum at around its stochiometric composition. Thus in the case of the explosive decomposition of ethylene oxide vapour, the reaction rate should influence the amount of undecomposed vapour when its decomposition rate is progressively reduced by additions of inert diluents such as nitrogen and carbon dioxide. It was found that increasing amounts of ethylene oxide remained undecomposed as the percentage of the inert diluent is increased as shown in Figure 30. It is interesting to note that this figure closely resembles a typical quenching distance versus fuel-air ratio curve in that the minimum quenching distance corresponds to the case of pure ethylene oxide vapour.

VI D (3) Relation between the undecomposed ethylene oxide vapour, the thickness of the dead space and the quenching distance.

The effect of pressure on the quenching distance for an ethylene oxide decomposition flame has been studied by Courtney et al [35] using an apparatus in which high energy sparks were discharged between two circular flat plates. The results obtained may be represented by equation VI (27).

$$dq = \frac{10}{p^*} \text{ m.m. at } 175^\circ C \qquad \text{VI (27)}$$

where p^* is the pressure in atmospheres. It is apparent that the percentage of undecomposed ethylene oxide and the quenching distances both obey

EFFECT OF REACTION RATE ON THE % C_2H_4O UNDECOMPOSED

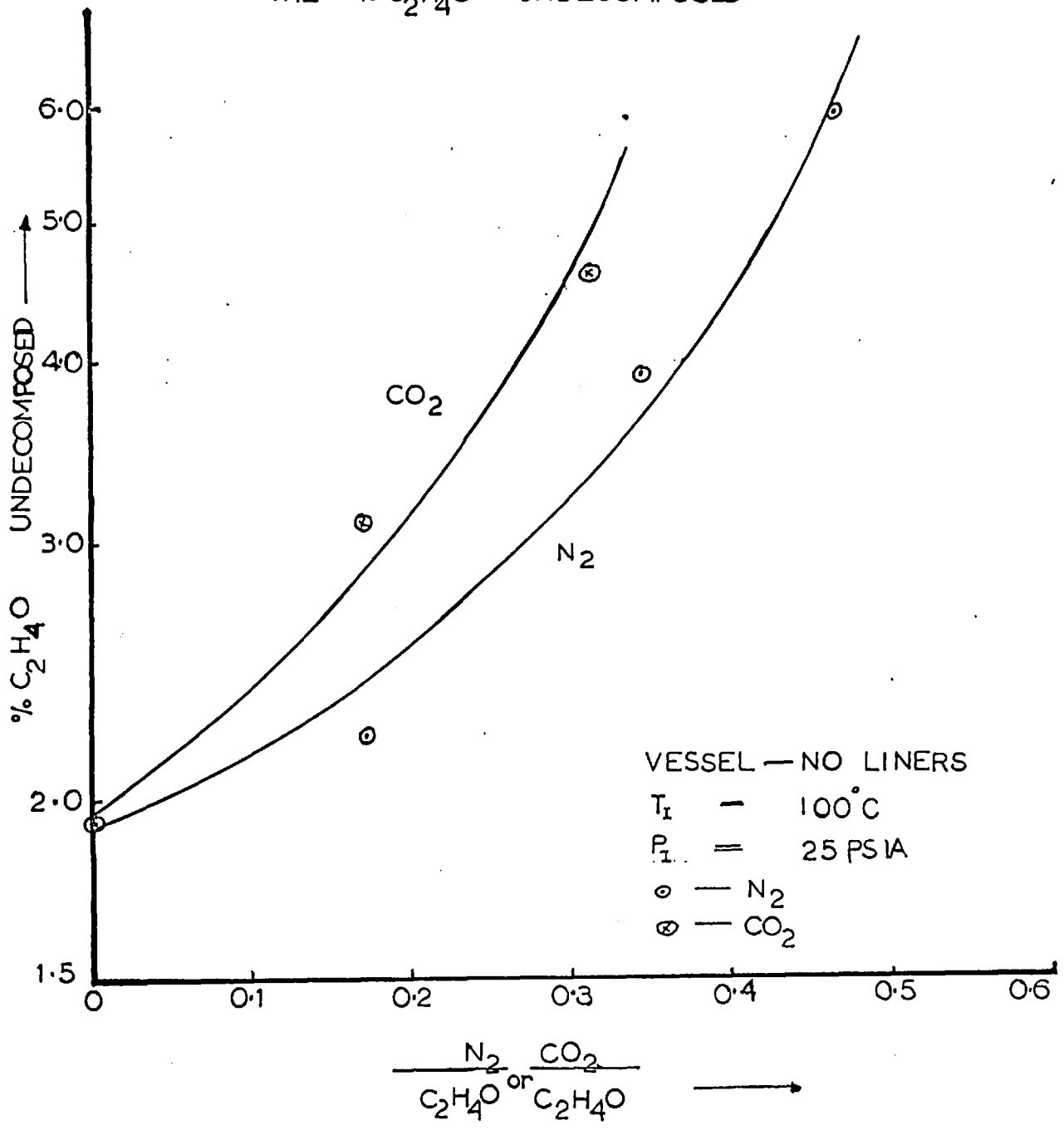

FIGURE 30

an inverse pressure law. It is therefore concluded that the percentage of undecomposed ethylene oxide vapour is proportional to the quenching distance.

Direct experimental evidence that this is true was provided by Gottenberg et al [41] in their study of flame quenching process in a combustion chamber. Besides measuring the amount of hydrocarbon unburnt at the end of the explosion process, they also inserted a variable width quenching slot in the combustion chamber to measure the quenching distance directly and found that the latter was approximately directly proportional to the percentage unburnt hydrocarbon. In view of this result it is of interest to see if there is relation between the mean thickness, δ, of the 'dead space' and the quenching distance, d_q, of the ethylene oxide decomposition flame. An approximate estimation of the thickness of the 'dead space' can be made by assuming that all the undecomposed ethylene oxide vapour comes from a quenched zone of uniform thickness, δ, which is at a temperature T_I, and that none of this quenched ethylene oxide vapour is decomposed after the attainment of the maximum explosion pressure, P_E. Then the ratio of the quenched volume, V_q, to the volume of the vessel is given as

$$\frac{V_q}{V} = \frac{\delta S}{V} \qquad \text{VI (28)}$$

By applying the ideal gas law to the quenched volume and the volume of the vessel, it may be shown that

$$V_q = n_q \frac{RT_I}{P_E} \qquad \text{VI (29)}$$

$$\text{and} \quad V = n_I \frac{RT_I}{P_I} \qquad \text{VI (30)}$$

Combining VI (28), (29), (30), the thickness of the quenched zone is given by

$$\delta = \frac{n_q}{n_i} \cdot \frac{P_I}{P_E} \cdot \frac{V}{S} \text{ cms} \qquad \text{VI (31)}$$

From Figure 31 it may be seen that at pressures above 13 atms. the thickness of the quenched zone does not change much with increasing pressure because of the condensation which occurs. However, for pressures below 13 atms., the thickness of the quenched zone increases rapidly. If a straight line is drawn through the three low pressure points of Figure 31, a slope of 0·5 is obtained indicating

$$\delta \propto \frac{1}{P_E} \qquad \text{VI (32)}$$

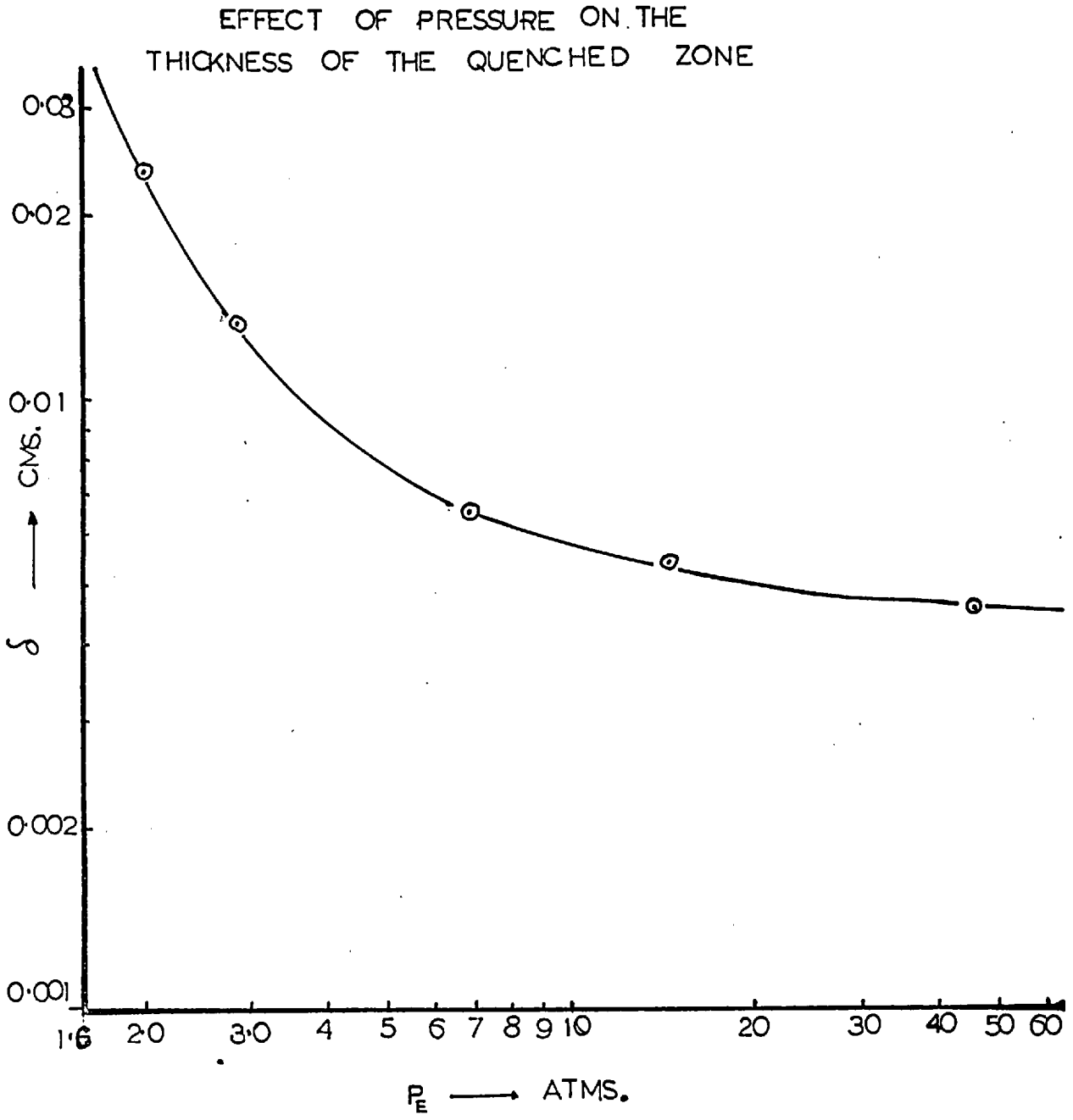
EFFECT OF PRESSURE ON THE
THICKNESS OF THE QUENCHED ZONE
0·03
0·02
0·01
0·002
0·001
δ ⟶ CMS.
1·6
2·0
3·0
4
5
6
7
8
9
10
20
30
40
50
60
P_E ⟶ ATMS.

FIGURE 31

However, much more work needs to be done to confirm this. On extrapolating the quenching distance result of Courtney et al [35] to conditions of 4 atms., a quenching distance of 0·25 cms is obtained at 175°C; whereas the thickness of the quenched zone is only 0·009 cms. at 100°C. The much smaller value for the thickness of the quenched zone is probably due to the highly turbulent nature of the decomposition explosion as compared to the method [35] by which the quenching distance for the decomposition flame was determined. Another factor that may reduce the calculated value for the thickness of the quenched zone is that some of the ethylene oxide vapour in the quenched zone may be decomposed during the cooling process following the explosion.

Daniel [42] has shown by means of photographs of flame radiation in a single cylinder internal combustion engine using a propane-air mixture as fuel, that a quenched zone exists at the wall of the combustion chamber at the time when the flame front passes the wall surface. In addition, he has presented data which indicates that there is reasonable agreement between the width of the quenched zone and the flame quenching distance calculated on the basis of Friedman and Johnston's [43] work for comparable operating conditions. This result is rather surprising, for in the case of Daniel's apparatus [42], the explosion process will produce turbulence in the quenched zone, whereas Friedman and Johnston [43] determined the quenching with the gas mixtures flowing under essentially laminar conditions.

It may be concluded that all the undecomposed ethylene oxide vapour must have come from the wall quenching process and therefore will be related to the quenching distance of the decomposition flame. Although the results of this work, indicate that the percentage of ethylene oxide undecomposed at the end of the decomposition explosion is proportional to the quenching distance of the decomposition flame, further work is needed to confirm this.

VI E Conclusions

The explosive decomposition of pure ethylene oxide vapour has been studied under various conditions, such as the initial vessel temperature, initial pressure and size and shape of the explosion vessel. The products of the explosive decomposition were analysed and it was confirmed that the formation of methane was favoured at high pressures and that of ethylene at low pressures. It was concluded that the carbon deposited during the explosion came from the pyrolysis of ethane and ethylene. It was also found that a small, but finite amount of ethylene oxide vapour remained undecomposed at the end of the explosion. Experimental evidence indicated that the undecomposed vapour occurs mainly as a result of the wall quenching process. In addition, under the experimental conditions studied, the percentage of the undecomposed ethylene oxide was found to be proportional to the quenching distance of an ethylene oxide decomposition flame.

The maximum explosion pressure attained during an ethylene oxide decomposition explosion was found to depend on the initial temperature, pressure and volume to surface area ratio of the vessel. Heat loss factors were found to be the main cause for the lowering of the maximum explosion pressure. However, for an initial vessel temperature of 100°C, it was calculated that the ratio of the maximum explosion pressure to the initial pressure could never exceed ten irrespective of the initial pressure of the ethylene oxide vapour, or the shape and size of the vessel.

CHAPTER VII

ADDITION OF INERT GASES.

VII A Method of determining the Limit Concentration for Flame Propagation:

Inert gases such as nitrogen, steam and carbon dioxide have been employed to suppress the explosive decomposition of the pure ethylene oxide vapour. The method employed in this work for determining the limit concentration for flame propagation was to measure explosion pressure developed by a series of mixtures when ignited by an exploding wire. Figure (32) shows typical results obtained for the effect of mixture composition on the ratio of the maximum explosion pressure to the total initial pressure. It may be observed that the ratio of the maximum explosion pressure to the total initial pressure decreases slowly and approximately linearly with initial additions of the inert diluents. However, near the limit composition, the ratio of the maximum explosion pressure to the initial pressure drops rapidly to a value of 1·5 and thereafter gradually fall towards unity. The limit composition for flammability was taken as that composition at which the maximum slope of the curve cuts the abscissa at $P_E/P_{IT} = 1$. The error involved in obtaining this limit composition was estimated to be within ± 1%.

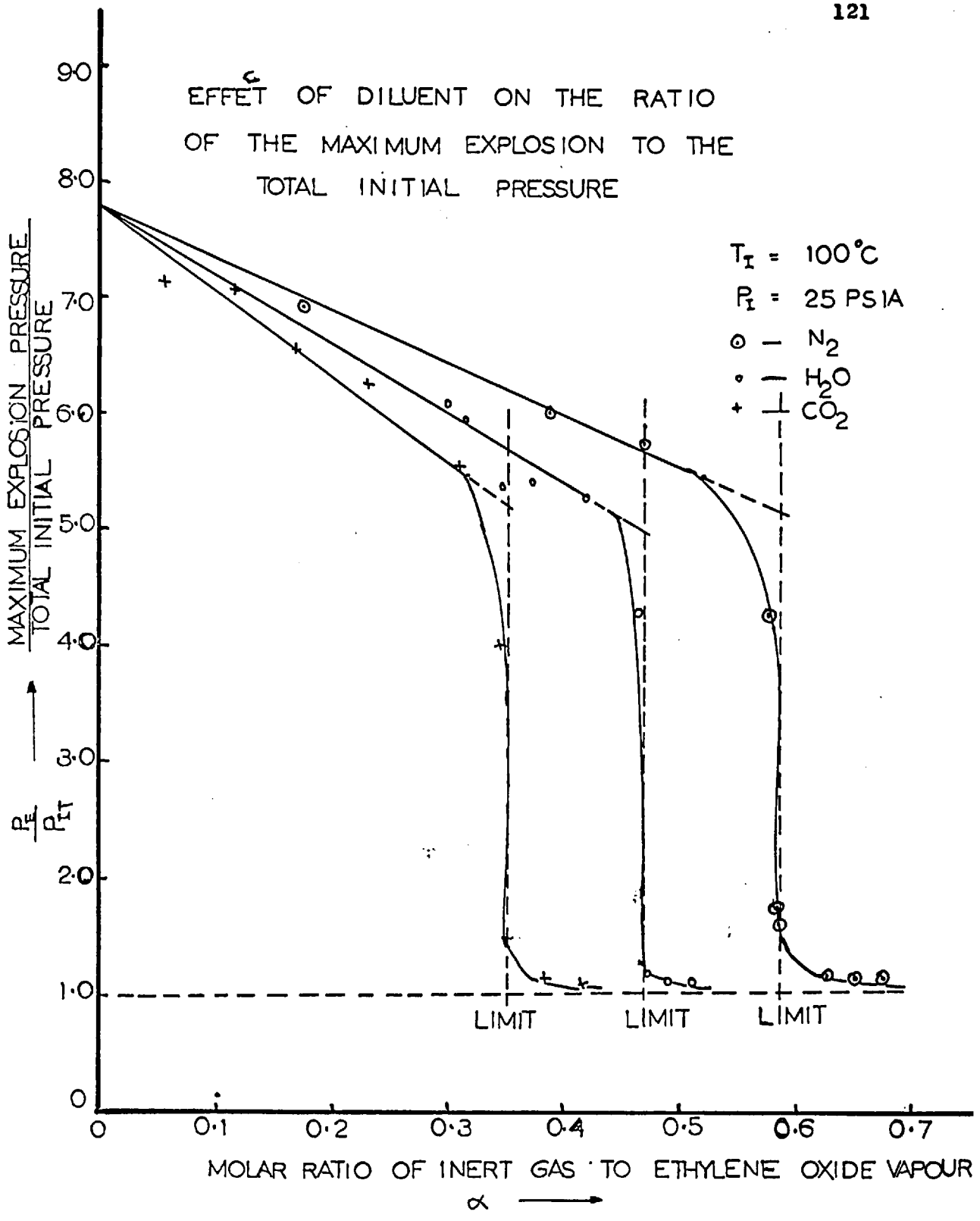
EFFET OF DILUENT ON THE RATIO
OF THE MAXIMUM EXPLOSION TO THE
TOTAL INITIAL PRESSURE
T_I = 100°C
P_I = 25 PSIA
⊙ — N_2
∘ — H_2O
+ — CO_2
MAXIMUM EXPLOSION PRESSURE / TOTAL INITIAL PRESSURE
P_E / P_{IT}
9·0
8·0
7·0
6·0
5·0
4·0
3·0
2·0
1·0
0
0·1
0·2
0·3
0·4
0·5
0·6
0·7
LIMIT
LIMIT
LIMIT
MOLAR RATIO OF INERT GAS TO ETHYLENE OXIDE VAPOUR
α

FIGURE 32

The propagation of a flame depends on the transfer of energy from the burnt gas to the neighbouring unburnt gas, and in a limit mixture the amount of energy for transfer is only just enough to maintain flame propagation. Therefore, anything that reduces the available energy will affect the limits and, it is necessary to make observations in vessels wide enough so that wall cooling effects are negligible. The limit compositions for the propagation of the ethylene oxide decomposition flame was studied in vessels of internal diameters 4·5 ins., 3·75 ins. and 1·5 ins. and the results are shown in Table 8.

TABLE 8

Effect of vessel Diameter on the flammability limit.

T_I	P_I	VESSEL		LINER I		LINER II	
		D = 4·5"	L/D = 2·25	D = 3·75"	L/D = 2·25	D = 1·5"	L/D = 6·76
°C	PSIA	PERCENTAGE NITROGEN BY VOLUME					
60	14·7	24		24		20	
60	25	28		29		23	
100	14·7	33		34		27	
100	25	37		37		29	

The amount of nitrogen required to suppress the explosive decomposition of the etnylene oxide vapour was found to be little affected by vessel size for vessels having internal diameters larger than 3·75 inches. However, for vessels having internal diameters less than 3·75 inches, wall quenching of the flame is likely to alter the limit composition as is the case, shown in Table 8, for a vessel of 1·5 inches internal diameter. It was concluded therefore that the limit determinations should be carried out in the vessel having an internal diameter of 4·5 inches.

VII B Results:-

B (1) Products of decomposition:-

The products of the explosive decomposition of ethylene oxide vapour in the presence of inert diluents such as nitrogen, steam and carbon dioxide were analysed and the results are shown in Figures 33, 34 and 35 respectively. It may be seen that the presence of an inert gas tends to increase methane and to decrease hydrogen and carbon formation in the final decomposition products. On approaching the flammability limit, the amount of methane formed per mole of ethylene oxide decomposed begins to decrease sharply with subsequent increase in ethylene formation to a limiting value. Although flame propagation did not occur on the lean side of the limit composition, about 5% ethylene oxide vapour was found to have decomposed.

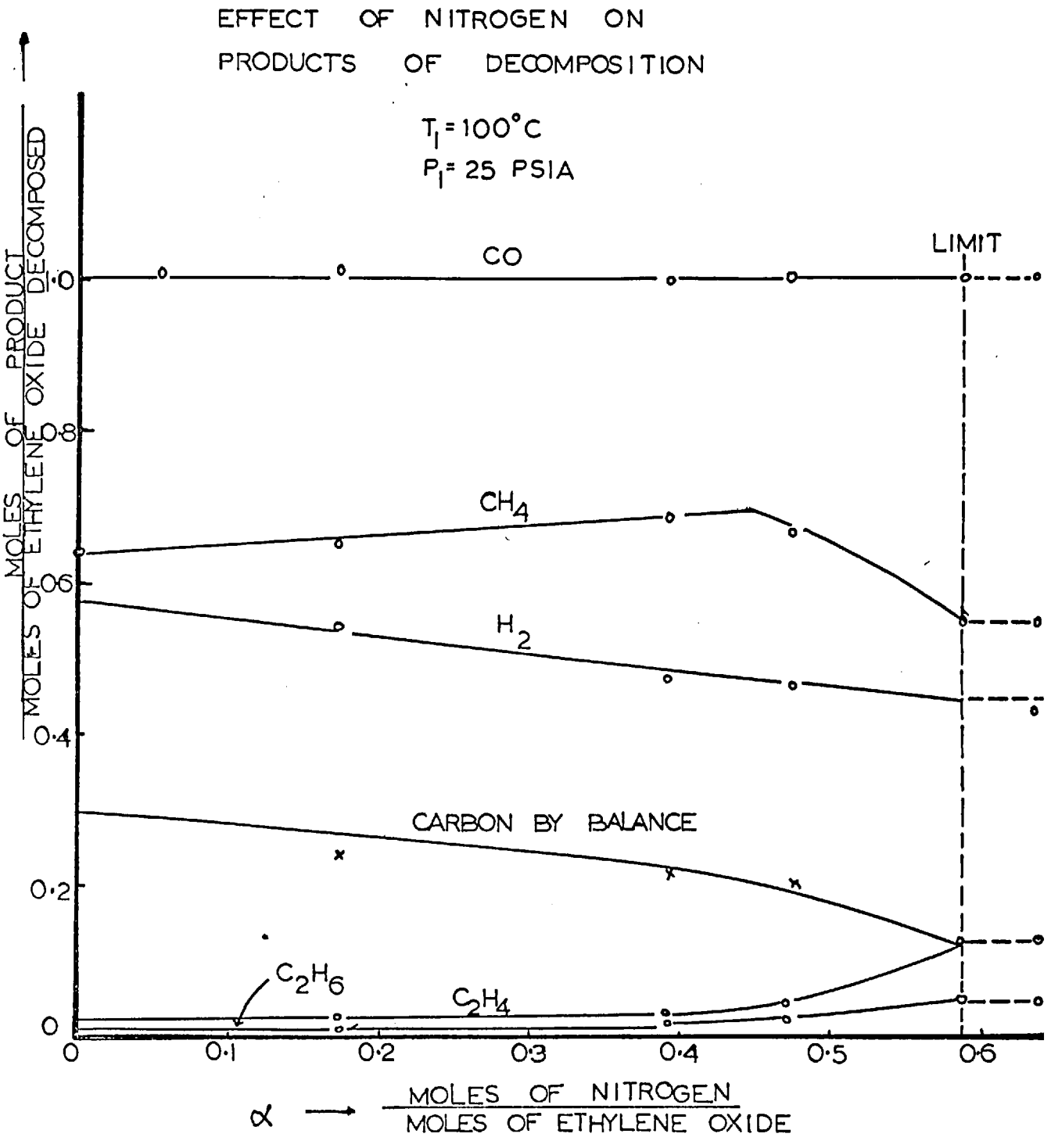
EFFECT OF NITROGEN ON
PRODUCTS OF DECOMPOSITION
$T_1 = 100°C$
$P_1 = 25$ PSIA
MOLES OF PRODUCT / MOLES OF ETHYLENE OXIDE DECOMPOSED
CO
LIMIT
CH_4
H_2
CARBON BY BALANCE
C_2H_6
C_2H_4
1.0
0.8
0.6
0.4
0.2
0
0
0.1
0.2
0.3
0.4
0.5
0.6
$\alpha \longrightarrow$ MOLES OF NITROGEN / MOLES OF ETHYLENE OXIDE

FIGURE 33

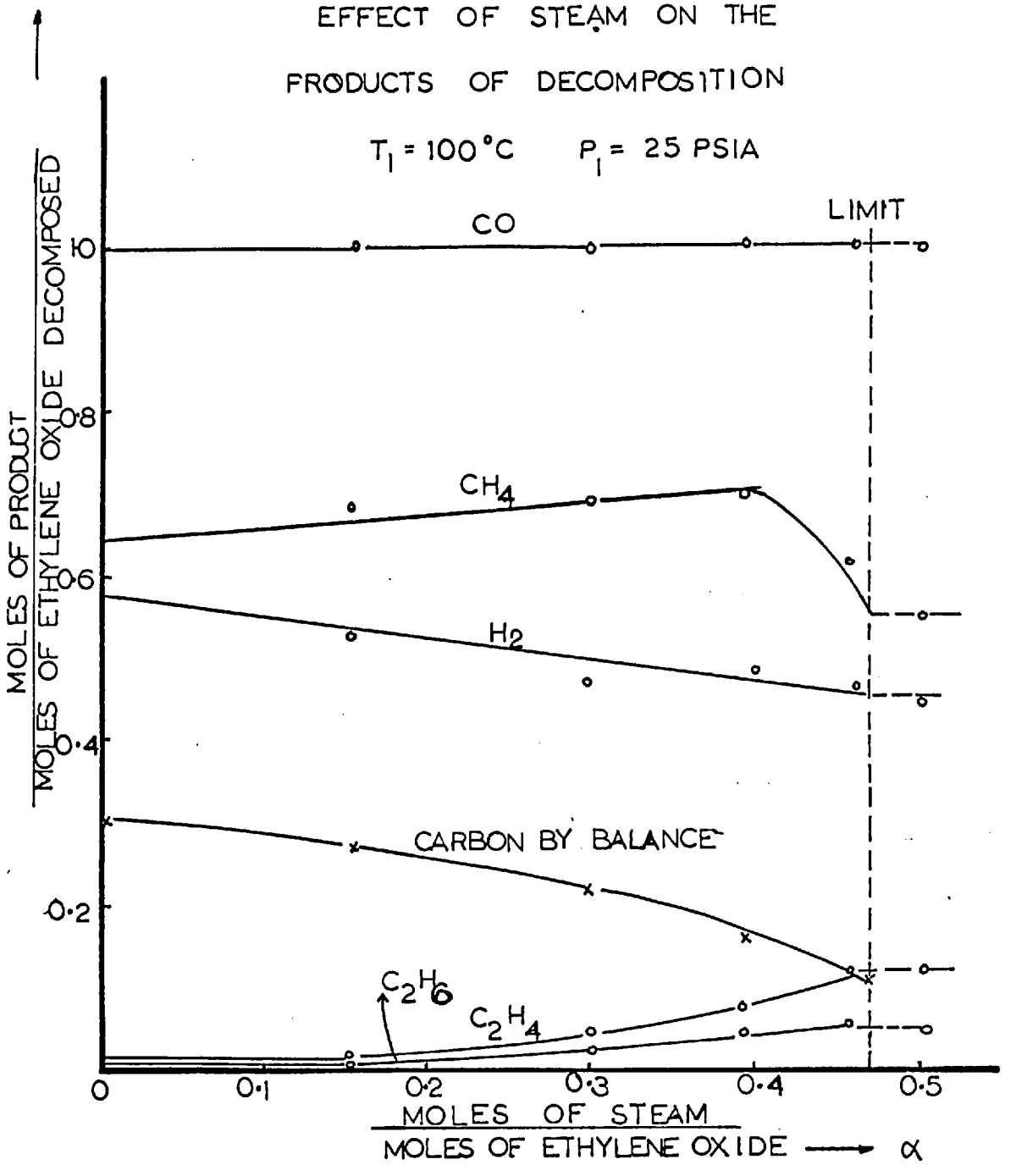
EFFECT OF STEAM ON THE
PRODUCTS OF DECOMPOSITION
T_1 = 100 °C P_1 = 25 PSIA
LIMIT
CO
CH_4
H_2
CARBON BY BALANCE
C_2H_6
C_2H_4
MOLES OF PRODUCT / MOLES OF ETHYLENE OXIDE DECOMPOSED
1·0
0·8
0·6
0·4
0·2
0
0·1
0·2
0·3
0·4
0·5
MOLES OF STEAM / MOLES OF ETHYLENE OXIDE → α

FIGURE 34

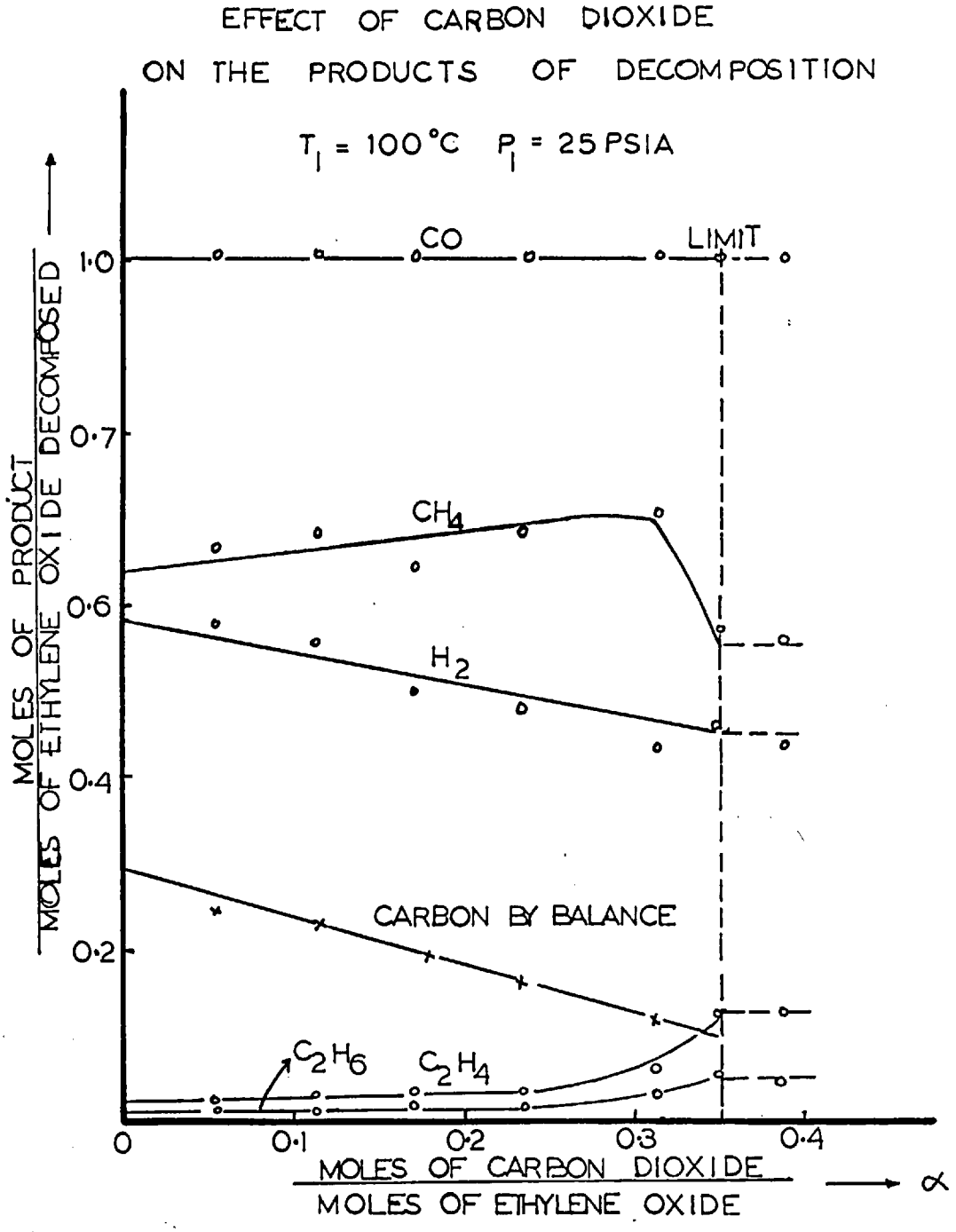
EFFECT OF CARBON DIOXIDE
ON THE PRODUCTS OF DECOMPOSITION
T_1 = 100 °C P_1 = 25 PSIA
MOLES OF PRODUCT / MOLES OF ETHYLENE OXIDE DECOMPOSED
1·0
0·7
0·6
0·4
0·2
CO
LIMIT
CH_4
H_2
CARBON BY BALANCE
C_2H_6
C_2H_4
0
0·1
0·2
0·3
0·4
MOLES OF CARBON DIOXIDE / MOLES OF ETHYLENE OXIDE
α

FIGURE 35

Since an error of 1% in the analysis of undecomposed ethylene oxide would have led to an error of about 20% in determining the amount of ethylene oxide decomposed, it was necessary to adopt an alternative procedure to estimate the moles of product per mole of ethylene oxide decomposed. If it is assumed that one mole of carbon monoxide is always formed per mole of ethylene oxide decomposed, then the products formed per mole of ethylene oxide decomposed on the lean side of the limit can be expressed relatively accurately. It may be seen from the results shown in Figures 33, 34 and 35 that at the flammability limit the same product composition, given in Table 9, is obtained in the presence of each of the three inert diluents.

TABLE 9 Decomposition products at the flammability limit.

P_I = 25 PSIA T_I = 100°C

$\frac{CO}{C_2H_4O}$	$\frac{CH_4}{C_2H_4O}$	$\frac{H_2}{C_2H_4O}$	$\frac{C_2H_4}{C_2H_4O}$	$\frac{C_2H_6}{C_2H_4O}$	'unbalanced' carbon
1·0	0·55	0·45	0·13	0·05	0·09

B (2) Flammability Limits:-

The amounts of various inert gases required to suppress the explosive decomposition of an ethylene oxide vapour is shown in Table 10.

TABLE 10 Limit Composition of different inert gases.

P_I = 25 PSIA T_I = 100°C

Diluent	Limit Composition	
	% diluent ± 1%	α
N_2	37	0·588
$H_2O(g)$	32	0·471
CO_2	26	0·352

The effect of temperature on the amount of inert diluents required to suppress the decomposition has been studied in the temperature range 20°C to 100°C and the results obtained for various initial partial pressure of the vapour are shown in Figure 36. It is apparent that an increasing amount of inert diluent is required to suppress the explosion

EFFECT OF INITIAL TEMPERATURE ON THE AMOUNT OF DILUENT REQUIRED FOR SUPRESSION OF ETHYLENE OXIDE DECOMPOSITION EXPLOSION

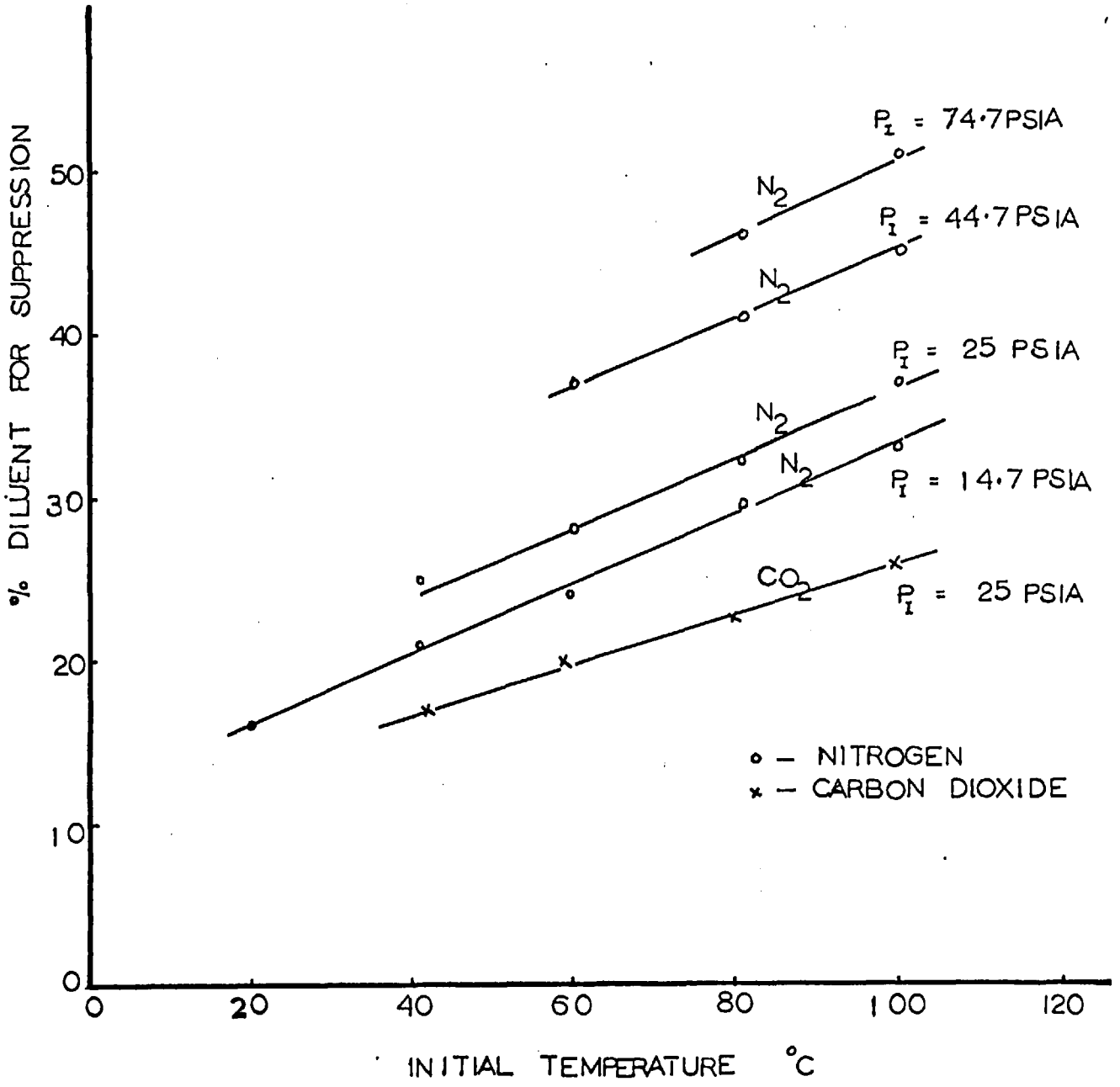

FIGURE 36

when the initial temperature is increased from 20 to 100°C. For example, at an initial partial pressure of the ethylene oxide vapour of 14·7 PSIA, 16% nitrogen was required at 20°C to suppress the decomposition explosion compared with 33% at 100°C.

The effect of the initial partial pressure on the amount of nitrogen required to suppress the decomposition explosion is shown in Figure 37. It may be seen that more nitrogen is required at higher pressures.

VII C Discussion on Results.

(i) Products of decomposition:-

Figures 33, 34 and 35 show that the addition of different inert diluents increases the formation of methane to a maximum quantity of 0·7 moles per mole of ethylene oxide decomposed and that at the flammability limit the composition of the decomposition products is the same irrespective of the diluent. It is therefore apparent that the different inert diluents employed in this work all have the same influence on the decomposition mechanism of the ethylene oxide vapour and that its adiabatic limit flame temperature is not influenced by the nature of the inert diluents. In support of this view, Figure 32 shows that each inert gas reduces the ratio of the maximum explosion pressure to the total initial pressure to a limit value of 5·1, which corresponds to a mean

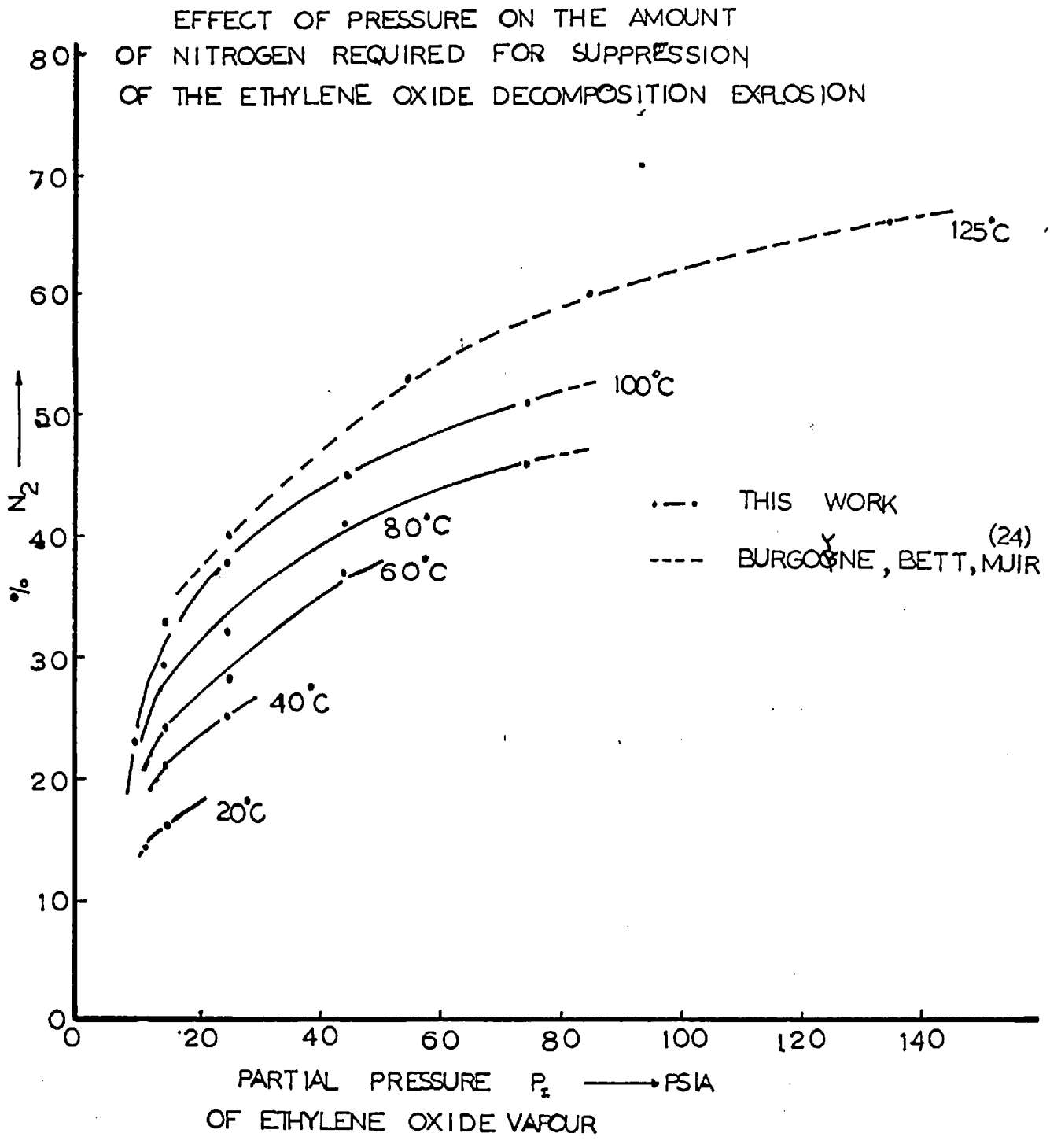
EFFECT OF PRESSURE ON THE AMOUNT
OF NITROGEN REQUIRED FOR SUPPRESSION
OF THE ETHYLENE OXIDE DECOMPOSITION EXPLOSION
% N2
80
70
60
50
40
30
20
10
0
0
20
40
60
80
100
120
140
125°C
100°C
80°C
60°C
40°C
20°C
THIS WORK
BURGOYNE, BETT, MUIR (24)
PARTIAL PRESSURE Pε ——→ PSIA
OF ETHYLENE OXIDE VAPOUR

FIGURE 37

maximum explosion temperature of 950°K, below which flame propagation fails. The increase in methane concentration and the simultaneous decrease in carbon and hydrogen concentrations in the decomposition products when an inert gas is present are probably associated with the complex process of pyrolysis of ethane and ethylene to give carbon, methane and hydrogen.

VII C (2) Effect of various inert diluents on flammability limit:-

It has been established in the previous section that the limit flame temperature of the ethylene oxide decomposition is little affected by various inert diluents. Now according to equation III (23) which gives the limit flame temperature, T_{fL} as

$$T_{fL} = \left[T_I + \frac{\Delta H_D}{\bar{C}_p + \alpha \bar{C}_{pN}} \right] \eta \qquad \text{III (23)}$$

Since T_{fL}, T_I, ΔH_D and $\bar{C}_p$ are all constant, then

$$\alpha \bar{C}_{pN} = \text{constant} \qquad \text{VII (1)}$$

A plot of the molar specific heat of the diluent gas, C_{pN}, against the reciprocal of the molar ratio of the inert gas to ethylene oxide vapour, $\frac{1}{\alpha}$, is shown in Figure 38 which gives a straight line through the origin and confirms the validity of equation VII (1). Other evidence in support

EFFECT OF SPECIFIC HEAT OF DIFFERENT INERT DILUENTS ON THE LIMIT

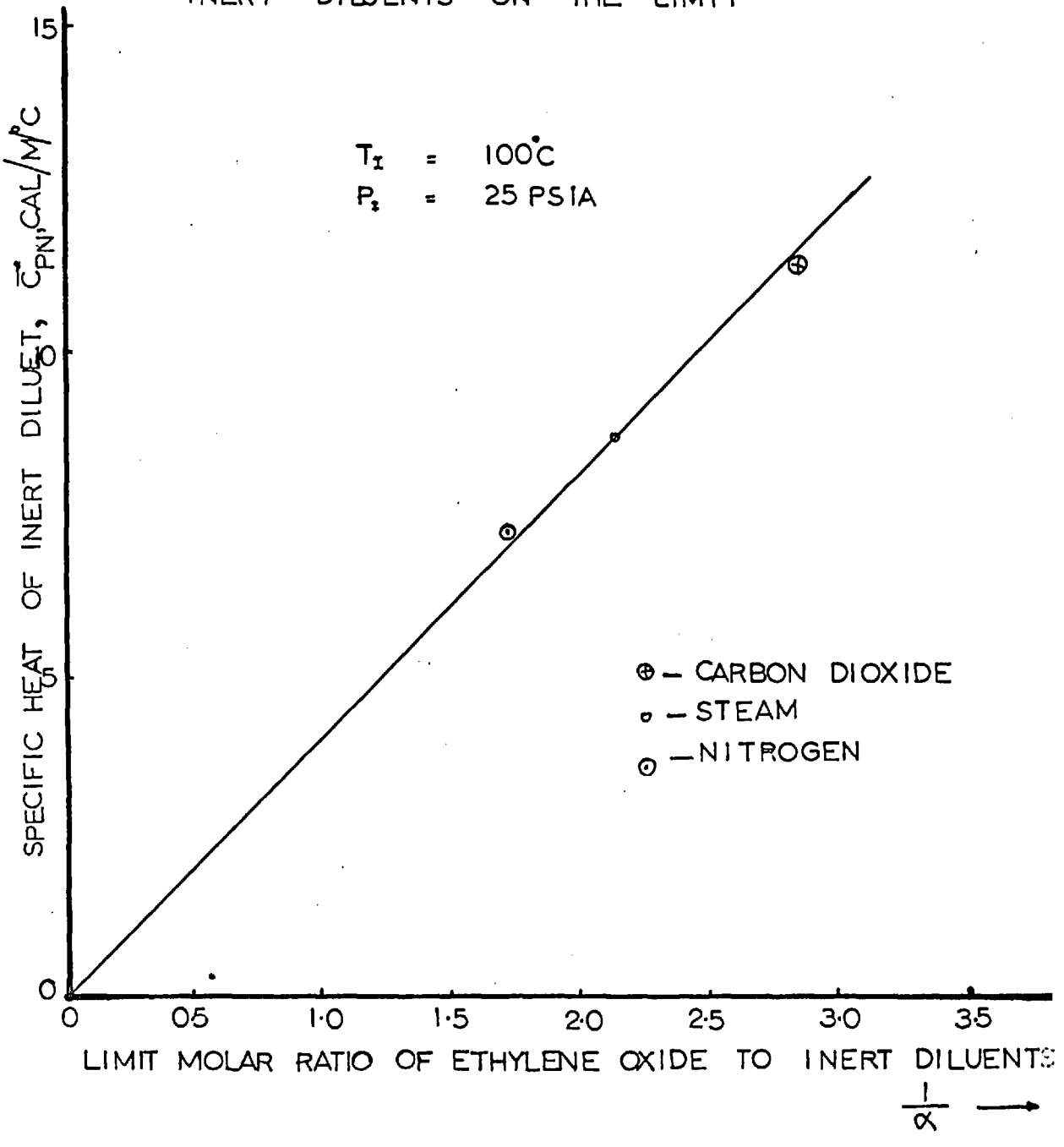

FIGURE 38

for the assumption that the adiabatic limit flame temperature is little affected by inert diluent was provided by Egerton and Powling [53] in their study on the flammability limits for hydrocarbon-oxygen-diluent systems. However, these workers reported that when helium was used as an inert diluent, the adiabatic limit flame temperature of a particular fuel mixture was greatly increased. Egerton and Powling [53] attributed this effect to the high thermal conductivity of the helium gas which increases the heat loss from the flame and therefore raises the adiabatic limit flame temperature since additional fuel must be added to the corresponding lower limit mixture to obtain a propagating flame. Nevertheless, equation VII (1) can be used as a guide to estimate whether or not a mixture of an inert gas and ethylene oxide vapour will propagate a flame, provided the thermal conductivity of the inert gas is similar to those of nitrogen, steam and carbon dioxide. As can be seen from Figure 28, inert diluents of high specific heat will have the greatest effect in suppressing an ethylene oxide decomposition explosion.

VII C (3) Effect of initial temperature on the flammability limit.

Figure 36 shows that the amount of inert diluent required to suppress the ethylene oxide decomposition explosion is temperature dependent. In view of this result, it is surprising to find that the two previous sets of workers, Hess and Tilton [26] and Burgogne et al [24] assumed that the

amount of nitrogen required to suppress the explosive decomposition of the ethylene oxide vapour was independent of temperature. However, in correlating the results of Hess and Tilton[26] at 30° - 40°C and Burgogne et al [24] at 125°C with this work, it can be seen in Figure 39 that all the results agree fairly well. It is therefore concluded that the original discrepancy between the results of Hess and Tilton [26] and Burgogne et al [24] arose, not as a result of the use of different igniting sources, but because the amount of nitrogen needed is temperature dependent. Hess and Tilton [26] worked at a temperature range of 30° - 40°C and this was too narrow a working temperature range for them to assume that the amount of inert diluent required was independent of temperature. Burgogne et al [24] studied the effect of temperature over the range of 89°C to 184·5°C but found that the amount of nitrogen needed to suppress the explosive decomposition of the ethylene oxide vapour under a partial pressure of 85 PSIA was constant to within ± 2%. The only plausible explanation for their result is that polymerisation of the ethylene oxide vapour occurred at the higher temperature and pressure during the half hour which was allowed for the mixture of ethylene oxide and nitrogen to mix before ignition. A reduction in the amount of ethylene oxide originally present would have reduced the amount of nitrogen needed to suppress the decomposition. Polymerisation of the ethylene oxide vapour has been reported by Walters and Smith [38] to occur at a measurable rate at 135°C.

COMPARISON OF LIMIT DATA

WITH PREVIOUS WORKERS

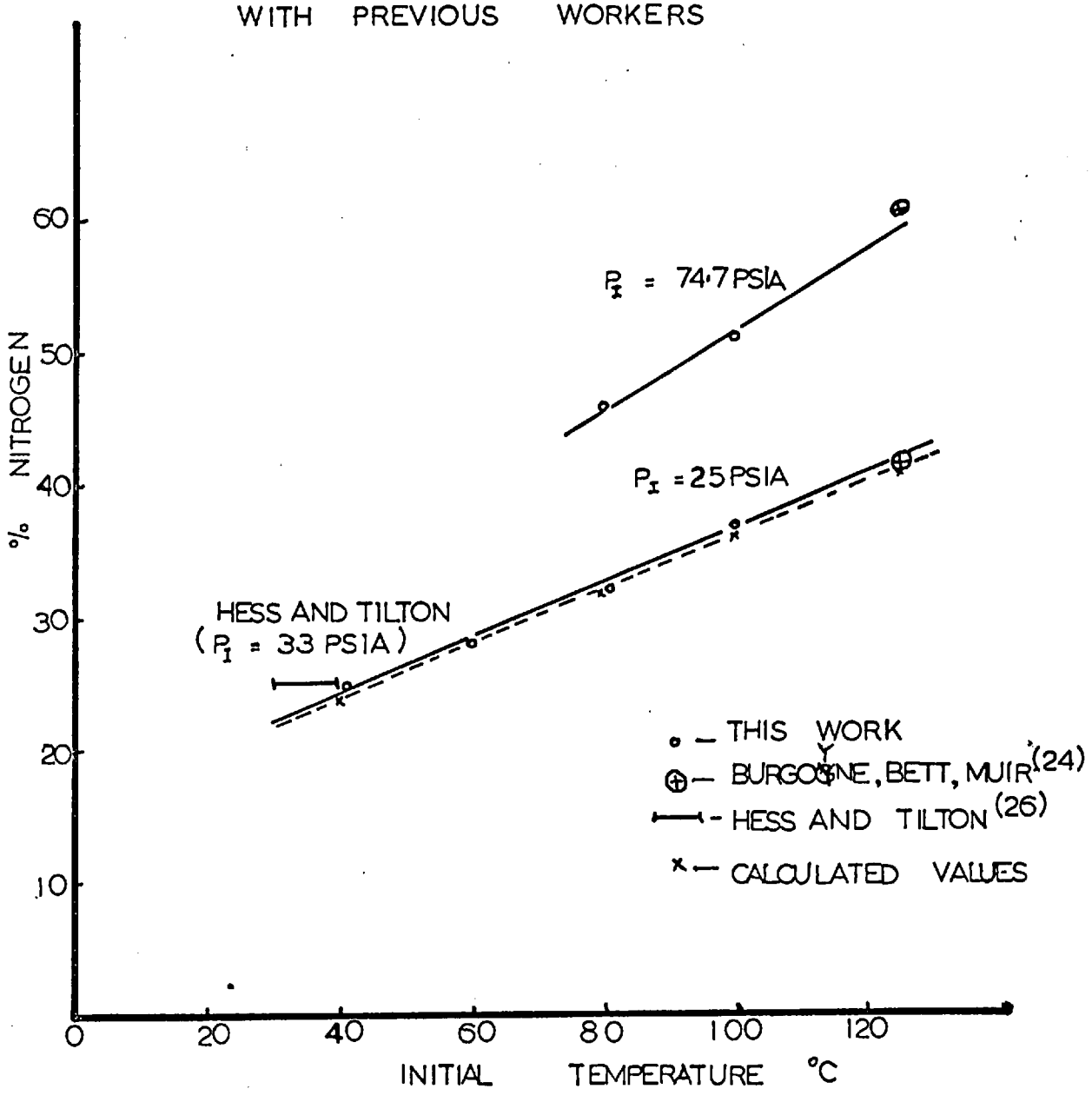

FIGURE 39

If it is assumed that the flame temperature for a limit composition is independent of the initial temperature, then the relation between the flammability limit and temperature can be expressed as

$$\alpha_2 = \left[\frac{1}{\frac{1}{C+\alpha_1} - \frac{\bar{C}_{pN}}{\Delta H_D}(T_2 - T_I)} - C \right] \qquad \text{III (25)}$$

where

$$C = \frac{\bar{C}_p}{\bar{C}_{pN}} \qquad \text{III (26)}$$

The values of $\bar{C}_p$ and ΔH_D in equation III (25) were calculated from the product of decomposition at the flammability limit, (see Table 9), which gave $\bar{C}_p$ = 22.65 cal/mole and ΔH_D = 23200 cals/mole. The corresponding limit flame temperature being 1230°K ± 10°. By substituting the values of $\bar{C}_p$ and ΔH_D in equation III (25) and taking T_I = 60°C and α_1 = 0.389, the values for α_2 as a function of temperature T_2 were calculated as shown in Figure 39. Although the results are in agreement at the lower temperatures, the calculated values of α_2 at higher temperatures are slightly lower than the observed values. This is attributed to the fact that the observed values of α_2 were based on constant partial pressures of the ethylene oxide vapour whereas the calculated values of α_2 is based on the constant total

initial pressure. It is shown in Figure 40 that increasing the total initial pressure will reduce the limit flame temperature and thus more nitrogen will be required to suppress the ethylene oxide decomposition explosion. If this pressure effect were to be taken into account, it is believed that a better agreement between the observed and the calculated values of α_2 would be obtained at higher initial temperatures. It is therefore concluded that a knowledge of one limit composition at a specified temperature and pressure, enables the limit composition at any other temperature but at the same pressure to be estimated by equation III (25). Similar procedures have been employed by Pechkin [52] and White [58].

VII C 4. Effect of Pressure on the limit Composition:-

Figure 37 shows that as the partial pressure of the ethylene oxide vapour increases, an increasing amount of nitrogen is required to suppress the ethylene oxide decomposition explosion. This result is in agreement with the findings of Burgogne et al [24], hence the assumption made by Hess and Tilton [26] that the amount of inert gas required for the suppression of the decomposition explosion is independent of pressure is incorrect. The increase in the amount of nitrogen required to suppress the explosive decomposition of the ethylene oxide vapour at higher partial pressures may be accounted for by two factors. Firstly, it has been shown

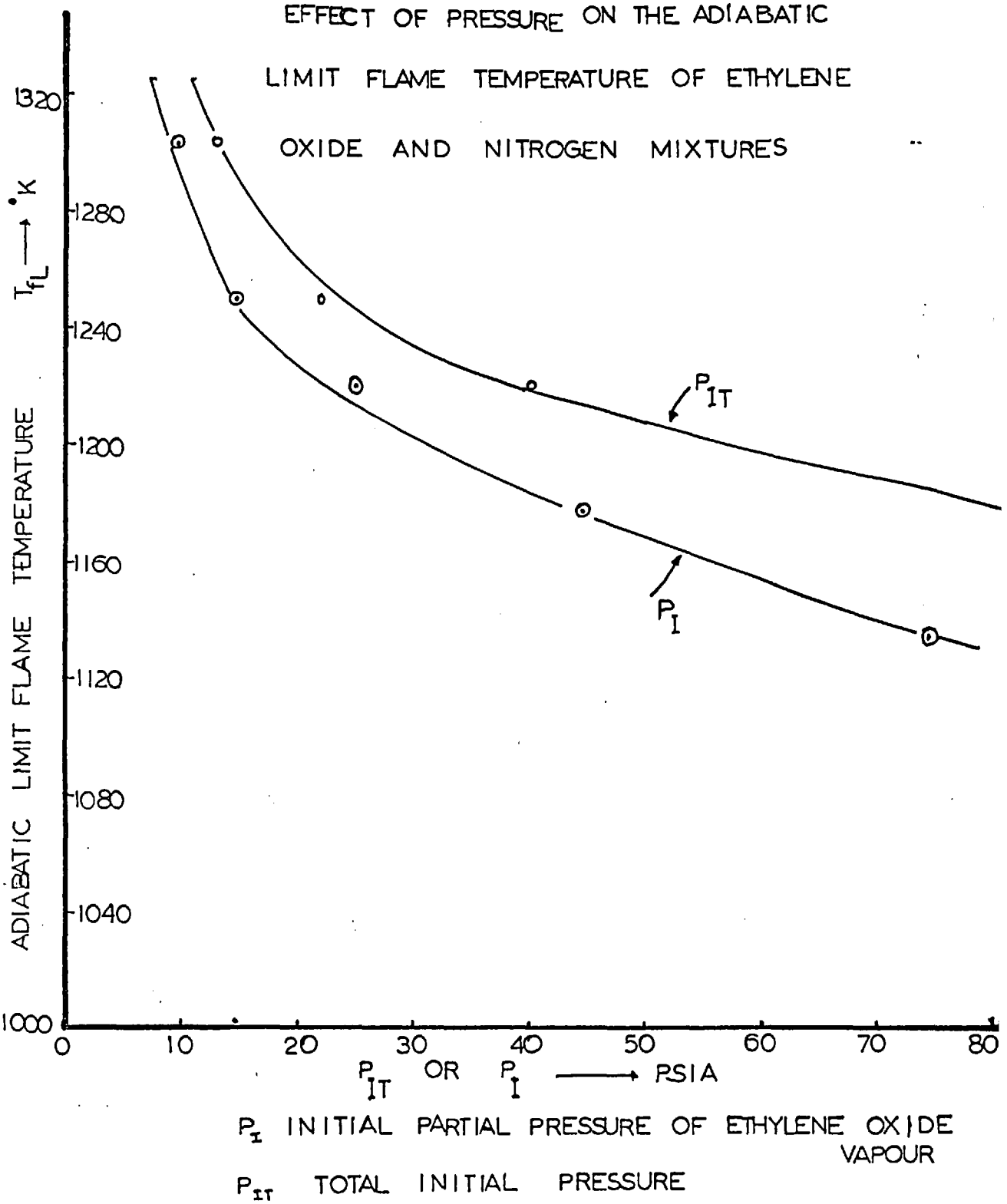
EFFECT OF PRESSURE ON THE ADIABATIC
LIMIT FLAME TEMPERATURE OF ETHYLENE
OXIDE AND NITROGEN MIXTURES
ADIABATIC LIMIT FLAME TEMPERATURE T_{fL} → °K
1320
1280
1240
1200
1160
1120
1080
1040
1000
0
10
20
30
40
50
60
70
80
P_{IT}
P_I
P_{IT} OR P_I → PSIA
P_I INITIAL PARTIAL PRESSURE OF ETHYLENE OXIDE VAPOUR
P_{IT} TOTAL INITIAL PRESSURE

FIGURE 40

in Chapter VI B that at higher initial ethylene oxide partial pressures an increasing amount of heat is liberated per mole of gas decomposed and consequently more nitrogen will be required to reduce the flame temperature to the limit flame temperature. Secondly, an increase in pressure is thought to reduce the limit flame temperature and thus increase the amount of nitrogen required to suppress the ethylene oxide decomposition explosion. If it is assumed that the amount of heat liberated per mole of ethylene oxide decomposed at the limit composition, ΔH_D, is approximately constant and is independent of initial pressure, then it is possible to estimate the adiabatic flame temperature of the limit mixtures at various pressures by using the data in Table 9 and applying equation III (23). Figure 40 shows that the effect of pressure on the adiabatic limit flame temperature is greatest at low pressures. Similar conclusions were drawn by Zabetakis et al [53] in their study on the effect of pressure on the adiabatic flame temperatures for lower limit compositions of natural gas and air mixtures. It is therefore apparent that there exists no simple mathematical relationship between the limits of flammability and pressure, but the general trend is that an increase in pressure always increases the amount of inert diluent required to suppress the ethylene oxide decomposition explosion.

The calculated adiabatic limit flame temperature of 1284°K at a total initial pressure of 14·7 PSIA is low compared to the value of 1750 ± 20°K [54] for most hydrocarbon-air mixtures, and according to Egerton and Powling [53], the adiabatic flame temperature of low limit mixtures in air increases from 1628°K to 1973°K for the corresponding increase in the paraffin series from methane to iso-octane. However, it is difficult to compare data obtained by various investigators because they are governed by the type of apparatus used; nevertheless, each investigation may give consistent results. It is therefore concluded that the adiabatic limit flame temperature of 1284° K obtained in this work cannot be regarded as an absolute value for estimating limit mixtures of ethylene oxide and an inert diluent under different experimental conditions, such as a flat flame burner. However, the limit, as determined by various apparatii vary little, and therefore the results obtained in this investigation will serve as a useful guide for assessing hazards involved in the safe handling of the ethylene oxide vapour. A summary of the results on the flammability limits of ethylene oxide vapour is shown in Table A 9 in the Appendix.

VII D. Conclusion.

The amount of inert diluent required to suppress the explosive decomposition of the ethylene oxide vapour was found to depend on both the

initial temperature and pressure and the results obtained agree well with those obtained by the previous workers. [24][26] The disagreement between the results of Hess and Tilton [26] and Burgoyne et al [24] may therefore be explained by the fact that both these workers assumed that the flammability limit was independent of the initial temperature. The assumption that the limit composition was also independent of pressure made by Hess and Tilton [26] was therefore also in error. Since Shell Chemicals [63] based their chart for the safe handling of ethylene oxide data on the limit results obtained by Hess and Tilton [26], it has been revised as shown in Figure 41 in the light of the results obtained in this investigation. It may be seen from Figure 41 that the 35% N_2 recommended by Shell on the basis of Hess and Tilton's result is insufficient to suppress the decomposition at high temperatures and pressures. This revised chart, if accepted by the Chemical Industry, should reduce the hazards involved in the handling of ethylene oxide.

The adiabatic flame temperature of limit mixtures of ethylene oxide vapour and inert gases has been found to be relatively independent of the initial mixture temperature and the type of inert gas used. From these observations, a simple mathematical relationship has been derived for the effect of temperature and the specific heat of various inert gases on the limit composition. Increasing pressure reduces the limit flame temperature in a complex way and no simple relationship between the calculated adiabatic limit flame temperature and pressure was found.

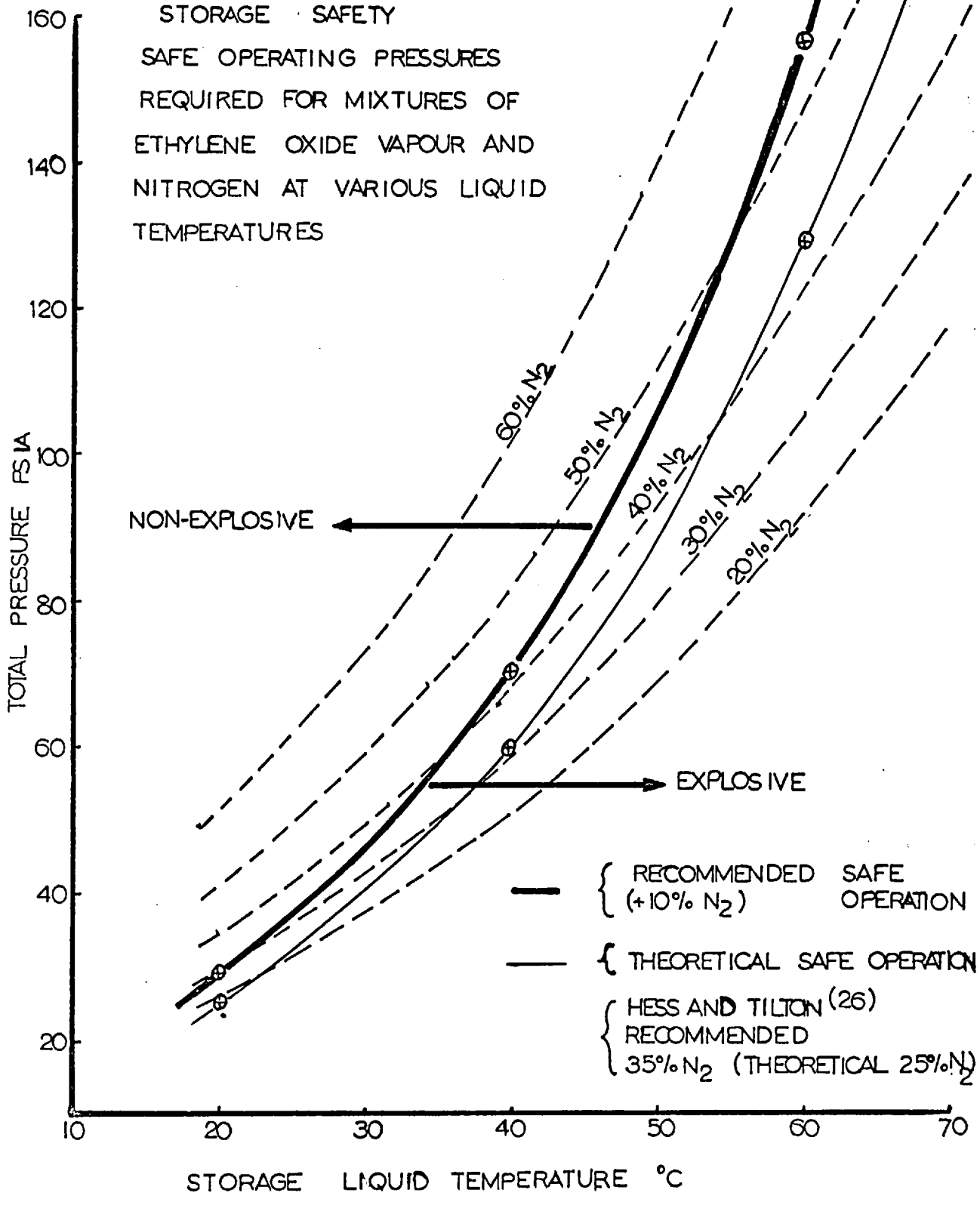
STORAGE SAFETY
SAFE OPERATING PRESSURES REQUIRED FOR MIXTURES OF ETHYLENE OXIDE VAPOUR AND NITROGEN AT VARIOUS LIQUID TEMPERATURES
TOTAL PRESSURE PS IA
160
140
120
100
80
60
40
20
10
20
30
40
50
60
70
STORAGE LIQUID TEMPERATURE °C
60% N2
50% N2
40% N2
30% N2
20% N2
NON-EXPLOSIVE
EXPLOSIVE
RECOMMENDED SAFE OPERATION (+10% N2)
THEORETICAL SAFE OPERATION
HESS AND TILTON (26) RECOMMENDED 35% N2 (THEORETICAL 25% N2)

FIGURE 41

CHAPTER VIII

ADDITION OF VOLATILE DILUENTS

VIII A Introduction:-

The primary object of this work was to study the hazards involved in the handling of volatile mixtures of ethylene oxide and various substances that are of importance in industrial practice. For this reason, the flammability limit compositions for mixtures of ethylene oxide/methanol, ethylene oxide/propylene oxide, and ethylene oxide/ammonia were determined at an initial vessel temperature of 100°C, the partial pressure of the ethylene oxide vapour in the mixtures being maintained at 25 PSIA. Each mixture was tested first to see whether or not the volatile diluents reacted with the ethylene oxide vapour before ignition. This was done by allowing a 25% diluent mixture to stand in the vessel for an hour so as to observe any pressure drop that occurred. It was found that with ethylene oxide mixtures with methanol and propylene oxide, there was no observable change in the pressure. However, in the case of a 25% ammonia mixture the total pressure decreased 11% after an hour. In view of this, only five minutes was allowed for the ethylene oxide/ammonia system to mix before ignition instead of the usual half-an-hour.

The secondary object of this work was to study the effect of these volatile diluents on the limit temperature for the ethylene oxide decomposition flame. It is known that methanol [59] and propylene oxide [8][14] undergo thermal decomposition at temperatures above 400°C; hence it was thought that each of these diluents would play a chemically active part in the ethylene oxide decomposition flame and would influence the limit flame temperature depending on whether the decomposition product have an inhibiting or promoting influence on the flame propagation mechanism.

VIII (B) Results:-

The products of the explosive decomposition of the ethylene oxide vapour with methanol, propylene oxide and ammonia are shown in Figures 42, 43 and 44 respectively. The analysis of the products of decomposition on the lean side of the limit composition has also been carried out and the result at the flammability limit is given in Table 11.

TABLE 11: Products of decomposition at the flammability limit for various volatile diluent with ethylene oxide vapour.

P_I = 25 PSIA T_I = 373°K

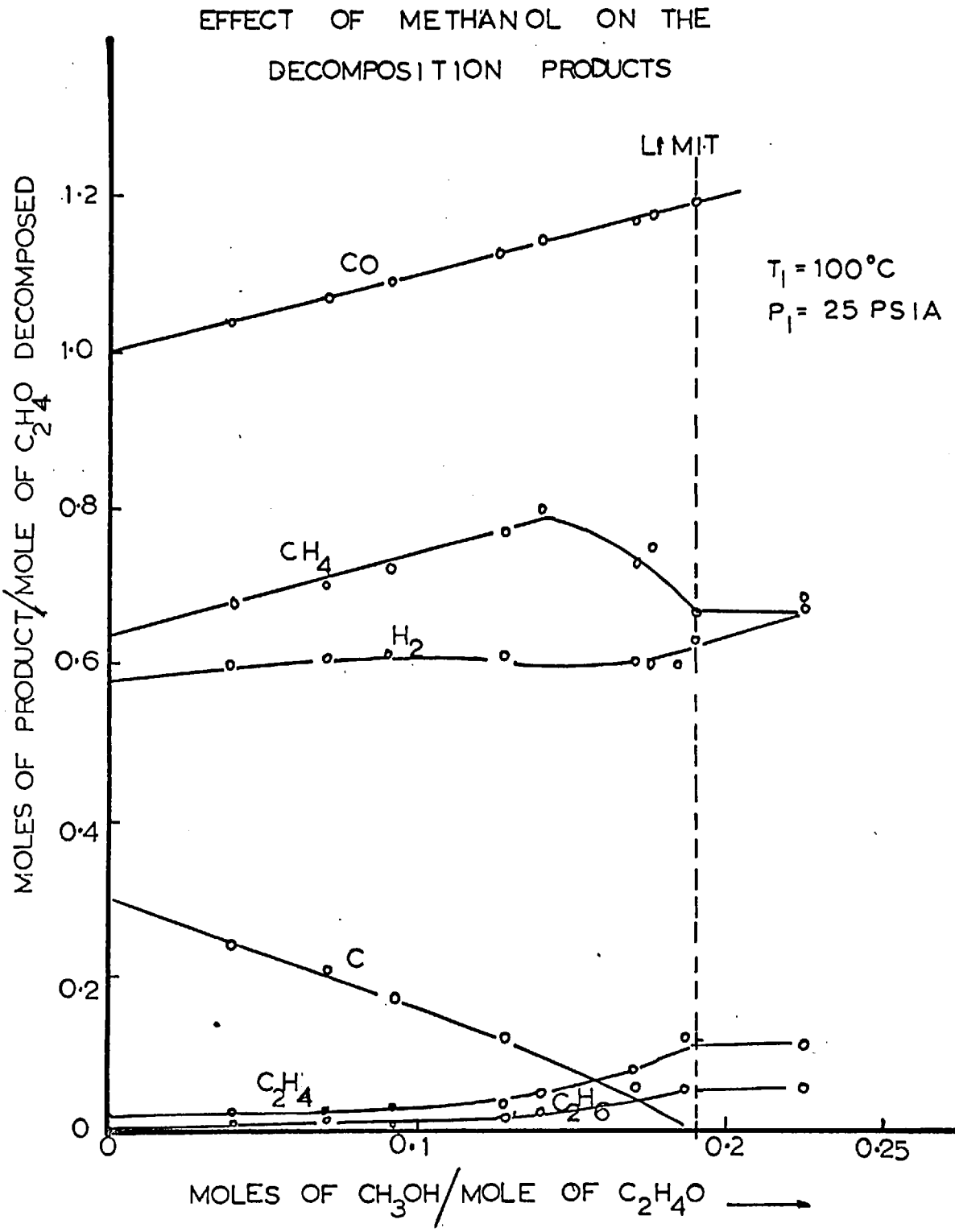
EFFECT OF METHANOL ON THE
DECOMPOSITION PRODUCTS
LIMIT
CO
CH4
H2
C
C2H4
C2H6
T1 = 100°C
P1 = 25 PSIA
MOLES OF PRODUCT/MOLE OF C2H4O DECOMPOSED
1·2
1·0
0·8
0·6
0·4
0·2
0
0
0·1
0·2
0·25
MOLES OF CH3OH/MOLE OF C2H4O

FIGURE 42

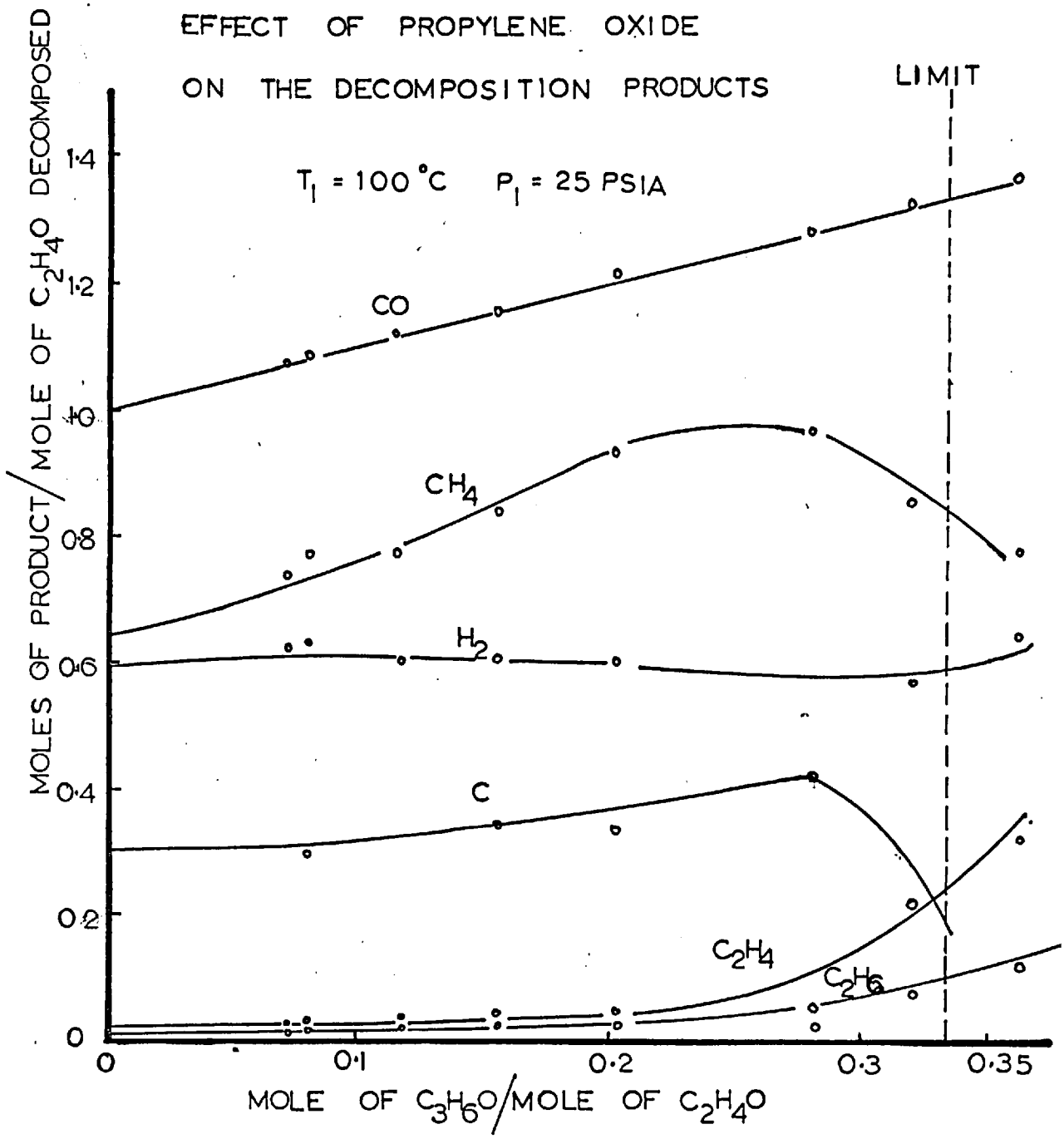
EFFECT OF PROPYLENE OXIDE
ON THE DECOMPOSITION PRODUCTS
T_1 = 100 °C P_1 = 25 PSIA
LIMIT
CO
CH_4
H_2
C
C_2H_4
C_2H_6
MOLES OF PRODUCT/MOLE OF C_2H_4O DECOMPOSED
1·4
1·2
1·0
0·8
0·6
0·4
0·2
0
0
0·1
0·2
0·3
0·35
MOLE OF C_3H_6O/MOLE OF C_2H_4O

FIGURE 43

EFFECT OF NH_3 ON THE DECOMPOSITION PRODUCTS

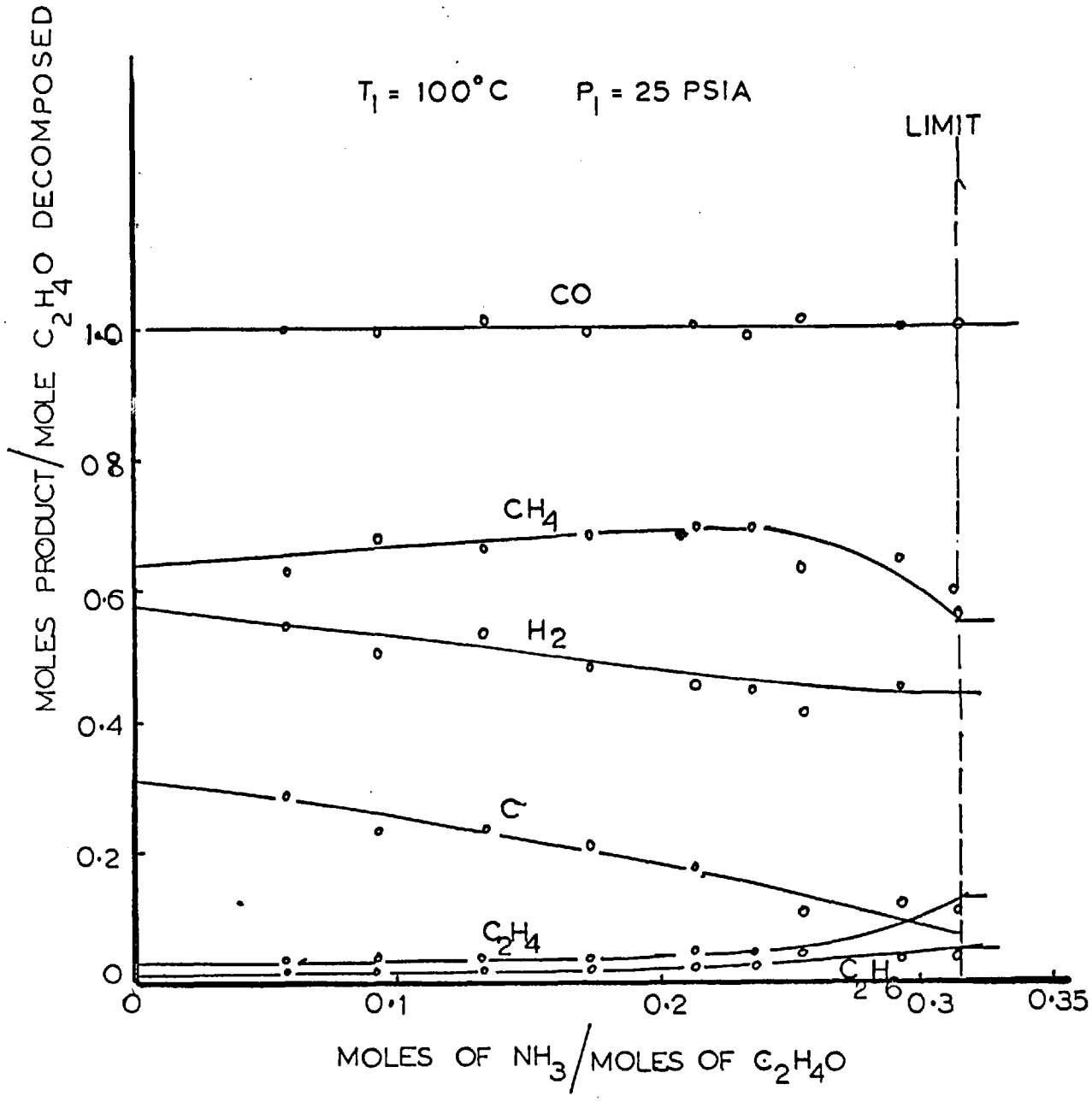

FIGURE 44

Diluent	Limit Composition		Product per mole of mixture					
	$\frac{\text{Diluent}}{C_2H_4O}$	% diluent	CO	CH_4	H_2	C_2H_4	C_2H_6	unbalanced C
CH_3OH	0·1904	16	1·0	0·56	0·53	0·1	0·04	-
$CH_3 \cdot CH\ CH_2$ (epoxide)	0·333	25	1·0	0·62	0·41	0·18	0·08	0·11
NH_3	0·316	24	0·76	0·418	0·342	0·1	0·038	0·068

VIII (C) Discussion on Results:-

VIII (C)1. Flammability limit composition:-

The results in Table 11 shows that vapour mixtures of ethylene oxide/methanol, ethylene oxide/propylene oxide, and ethylene oxide/ammonia containing more than 16%, 25% and 24% of the respective diluent are not flammable. In industrial practice, these mixtures are usually employed in the liquid state and it is of interest to consider the corresponding liquid phase which might in certain circumstances produce flammable vapour mixtures. Two such circumstances will be considered.

(1) - The vapour mixture composition is the same as the liquid mixture composition; this condition will arise if the liquid mixture is allowed to evaporate rapidly.

(2) - The vapour mixture is in equilibrium with the liquid mixture; this condition will occur when the liquid mixtures are confined in a closed vessel.

Case 1 is straightforward since the limit diluent/ethylene oxide vapour ratios can be used to determine the corresponding limit liquid mixture ratios. Thus, the limit ratio of liquid volumes can be represented as

$$\left(\frac{V_D}{V_E}\right)_{LIQ.} = \alpha \frac{M_D}{M_E} \frac{\rho_E}{\rho_D} \qquad \text{VIII (1)}$$

where α is the limit diluent/ethylene oxide vapour ratio, and M_D/M_E and ρ_D/ρ_E are the ratios of the molecular weights and densities respectively, of the liquid diluent and ethylene oxide. It is not suggested that a liquid phase mixture having the composition given by equation VIII (1) is capable of being ignited in the liquid phase, but that a mixture of this composition will produce a vapour of limit composition.

The assumption is made for case (2) that the partial pressure of the vapour above a liquid mixture can be expressed by Raoult's Law which gives

$$P_x = N_x P^o_x \qquad \text{VIII (2)}$$

where N_x is the mole fraction of component 'x' in the mixture, and P_x^o is the vapour pressure of the pure liquid 'x' at the temperature of the solution. Under these conditions, the limit ratio of liquid volumes of diluent/ethylene oxide can be expressed as

$$\left(\frac{V_D}{V_E}\right)_{LIQ.} = \propto \frac{M_D}{M_E} \cdot \frac{\rho_E}{\rho_D} \cdot \frac{P_E^o}{P_D^o} \qquad \text{VIII (3)}$$

By comparing equations VIII (1) and VIII (3) for case (1) and case (2) the following relation is obtained,

$$\left(\frac{V_D}{V_E}\right)_{LIQ.2} = \frac{V_D}{V_E}_{LIQ.1} \times \frac{P_E^o}{P_D^o} \qquad \text{VIII (4)}$$

where the subscripts 1, and 2 represents cases 1 and 2. The data for the two cases are summarised in Table 12

TABLE 12: Limit Compositions of Vapour and Liquid Mixtures.

Mixture	$\frac{M_D}{M_E}$	$\frac{\rho_E(60)}{\rho_D}$	$\frac{P_E^o}{P_D^o}$ 100°C	$\propto$	$\frac{V_D}{V_E}$ LIQ. 1	LIQ. 2
C_2H_4O - CH_3OH	0·71	1·098	3·75 (62)	0·1904	0·148	0·555
C_2H_4O - $CH_3 \cdot CH \cdot CH_2$	1·319	1·07	2·12 (61)	0·333	0·47	0·995
C_2H_4O - NH_3	0·386	1·392	0·214 (60)	0·316	0·17	0·0314
C_2H_4O - H_2O	0·409	0·898	13·28 (60)	0·471	0·173	0·23

The result for steam is included in the above table because liquid ethylene oxide and water mixtures occur in practice in the manufacture of ethylene glycol. The order of volatility of the compounds studied is $NH_3 > C_2H_4O > C_3H_6O > CH_3OH > H_2O$. A comparison of the amount of diluent required for rapid and slow vaporisation (Case 1 and 2, respectively) shows that for diluents which are less volatile than ethylene oxide, more diluent is required to form non-flammable mixtures if these mixtures are vaporised slowly than if they are vaporised rapidly. Conversely, ammonia is more volatile than ethylene oxide and therefore less ammonia is required to form non-flammable mixtures if these mixtures are vaporised slowly than if they are vaporised rapidly. Care must be taken in practice to ensure that vapour mixtures originally classed as non-flammable do not become flammable as a result of condensation enriching the ethylene oxide content of the vapour mixture; this may occur in the case of ethylene oxide mixtures with methanol, or propylene oxide or steam. Also non-flammable equilibrium vapour mixtures of ethylene oxide/ammonia above their liquids may become flammable if the liquid mixture is allowed to vaporise rapidly.

VIII (C) 2 Products of Decomposition.

Figure 42 shows that for each quantity of methanol added to the ethylene oxide vapour, there is a corresponding increase in the amount of carbon monoxide and methane formed per mole of ethylene oxide vapour

decomposed. It is therefore apparent that for every mole of methanol decomposed one mole of carbon monoxide is produced and that the methane must have come from the interaction between a methyl radical and the methanol molecule. A tentative proposal for some of the radical reactions involved in the decomposition of methanol is shown as follows:-

$$R + CH_3OH \longrightarrow RH + CH_2OH \qquad \text{VIII (5)}$$

$$CH_2OH \longrightarrow H{\cdot}CHO + H \qquad \text{VIII (6)}$$

$$H\,CHO \longrightarrow H + CHO \qquad \text{VIII (7)}$$

$$CHO \longrightarrow CO + H \qquad \text{VIII (8)}$$

where R represents a CH_3 radical or H atoms present in the ethylene oxide decomposition flame. It can be seen that the decomposition of one molecule of methanol produces three hydrogen atoms which are available for further radical reactions of the type

$$H + C_2H_4O \longrightarrow H_2 + \dot{C}_2H_3O \qquad \text{VIII (9)}$$

$$H + CH_3OH \longrightarrow H_2 + \dot{C}H_2OH \qquad \text{VIII (10)}$$

The presence of larger quantity of hydrogen in the decomposition products compared to the case when inert diluents were added, (see Figure 33), supports the proposed reaction mechanisms. Near the flammability limit, the drop in methane concentration is due to the fact that less ethylene is being pyrolysed, (see Chapter VI).

In the case of ethylene oxide/propylene oxide mixtures, Figure 43 shows that for each quantity of propylene oxide added to the ethylene oxide vapour, an equivalent amount of carbon monoxide is produced in the decomposition products. However, the increase in the methane formation was found to be larger than the equivalent amount of propylene oxide added. For example, an addition of 0·2 moles of propylene oxide to one mole of ethylene oxide vapour was found to increase the amount of carbon monoxide and methane by 0·2 moles and 0·29 moles respectively per mole of ethylene oxide decomposed. It is also shown in Figure 43 that an increased amount of unbalanced carbon is formed as the propylene oxide content of the vapour increases. It is known that propylene oxide decomposes [8] in the following manner:-

hence, the results can be explained on the basis that the following reactions take place in the ethylene/oxide decomposition flame:-

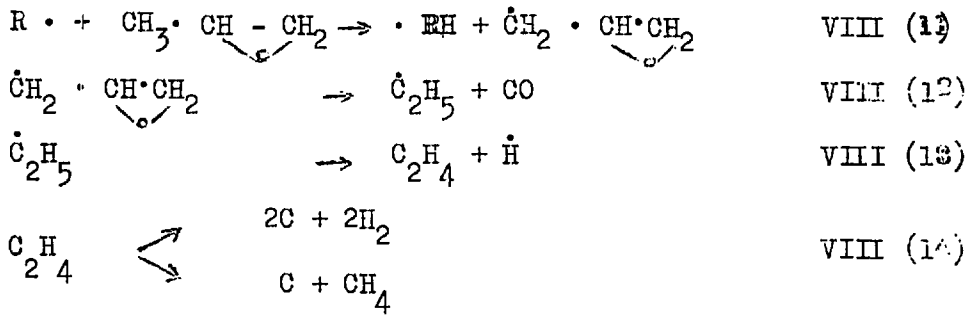

The larger quantity of ethylene found in the decomposition products near the flammability limit compared with systems containing an inert gas (see Figure 33) support the proposed reaction mechanism.

The analysis of the products of the explosive decomposition of mixtures of ethylene oxide vapour and ammonia showed that all the ammonia remained undecomposed at the end of the explosion. The products formed per mole of ethylene oxide decomposed shown in Figure 44, are similar to the results obtained with ethylene oxide/inert gas mixtures, (see Figure 33), and it is concluded that ammonia acts solely as an inert diluent. If this is so, the flammability limit of an ethylene oxide/ammonia mixture can be predicted from Figure 38. By taking the mean specific heat of ammonia at 800°K to be 12·1 cals/mole/°C, the predicted flammability limit is 23% NH_3 as compared with the observed value of 24% NH_3.

The adiabatic limit flame temperatures of mixtures of ethylene oxide with methanol, propylene oxide and ammonia have been calculated from the products of decomposition at the flammability limit given in Table 11. A summary of the results are given in Table 13.

TABLE 13

Limit Flame temperature of ethylene/volatile diluent mixture.

Diluent	limit composition		Adiabatic limit flame temp. ^{o}K
	α	% Diluent	
CH_3OH	0·1904	16	1170 ± 10
$CH_3 \cdot CH\,CH_2$ (O)	0·333	25	1420 ± 10
NH_3	0·316	24	1230 ± 10

Ammonia behaves as an inert diluent, hence the adiabatic limit flame temperature remains constant at 1230°K. Methanol reduces whereas propylene oxide raises the adiabatic limit temperatures of the ethylene oxide decomposition flame. These results can be explained on the basis that the limit flame temperature is influenced by two major factors. Firstly, a physical factor is involved in that the volatile diluent may produce products which have a higher thermal conductivity than the inert gases, in which case more heat will be conducted from the flame to the unburnt gas and consequently higher flame temperatures must be attained for flame propagation.

The presence of a larger quantity of hydrogen molecules in the decomposition products of ethylene oxide/methanol and ethylene oxide/propylene oxide mixtures (see Figures 42, 43,) compared with ethylene oxide/ammonia mixtures (Figure 44) suggests that the higher limit flame temperatures for the former mixtures are due to the high thermal conductivity of the hydrogen molecule. Secondly, a chemical factor is involved, in that the additives take part in the flame reactions and may produce a higher concentration of active radicals, e.g. H atoms, which are responsible for flame propagation. The flame temperature must therefore be sufficiently high to maintain a critical rate of diffusion of these active radicals from the flame to the unburnt gas where reactions are initiated. Hence, flames with higher concentration of active radicals will have a lower limit flame tempeature. Equations 5 to 8 shows that for every mole of methanol decomposed three hydrogen atoms are produced. It is to be expected, therefore, that from chemical considerations, a lower limit flame temperature will result for the ethylene oxide/methanol mixture. Thus, the physical factor tends to increase the limit flame temperature, whilst the chemical factor tends to reduce it; the balance of the two effects probably accounts for the fact that the calculated adiabatic limit flame temperature for the ethylene oxide/methanol mixture (1170°K) is only slightly lower than that for the inert diluent mixtures. The higher calculated adiabatic limit flame temperature for an ethylene oxide/propylene oxide mixture (1420°K) probably arises because of the thermoconductivity effect; since the decomposition

mechanism of propylene oxide is similar to that of ethylene oxide and no effective chemical factor is involved.

Conclusion:-

It is concluded that mixtures of ethylene oxide/methanol, ethylene oxide/propylene oxide, ethylene oxide/ammonia containing more than 16%. 25% and 24% of their respective diluent are non-flammable. Ammonia was found to behave as an inert diluent. Methanol and propylene oxide have been shown to be chemically active in the ethylene oxide decomposition flames; the adiabatic limit flame temperature using methanol as the volatile diluent is about 60°K lower than the corresponding limit for an inert diluent whereas that using propylene oxide is about 190°K higher.

CHAPTER IX

MECHANISM OF THE EXPLOSIVE DECOMPOSITION OF ETHYLENE OXIDE VAPOUR.

IX A Determination of the burning velocity in closed vessels:-

Marvin, Caldwell and Roeder [44] assumed that the compression of the reactant and the products during an explosion in a closed vessel to be adiabatic and derived a relation for the burning velocity for the explosive mixture to be

$$S_u = \left[1 - \frac{R^3 - r_f^3}{3_p \gamma_u r_f^2} \cdot \frac{d_P}{d r_f} \right] \left[\frac{d r_f}{d_t} \right] \qquad \text{IX (1)}$$

where R is the radius of a spherical vessel and r_f that of the spherical flame at a time 't' when the pressure is P. A source of inaccuracy in equation IX (1) lies in the fact that the second term in the bracket is very close to unity (0·85 to 0·95) during most of the explosion. This means that an error of 1% in this term will lead to an inaccuracy of 10% in the calculated value of S_u. Also in order to apply the above equation a knowledge of 'r_f' as a function of time is required. Lewis and von Elbe [1] have attempted to overcome these difficulties by assuming that during the explosion, the ratio of the specific heats of the burnt and unburnt gas

remain constant and that the change in the number of molecules resulting from the chemical reaction remains constant. On this basis, an approximate equation was derived which shows that the fraction of gas burnt is equal to the fraction of total pressure rise, i.e.

$$N = \frac{P - P_I}{P_E - P_I} \qquad \cdots\cdots \qquad IX\ (2)$$

for small values of N.

Before ignition, N occupies a volume v_i at a radius r_i,

$$\therefore \quad \frac{r_i}{R} = \left(\frac{P - P_I}{P_E - P_I} \right)^{1/3} \qquad \cdots\cdots \qquad IX\ (3)$$

After ignition, N occupies 'v_b' at a radius r_b, i.e.

$$v_b = V \cdot n_i\ (1 - N) \frac{RT_u}{P} \qquad \cdots\cdots \qquad IX\ (4)$$

$$\text{whence} \quad \left(\frac{v_b}{V} \right)^{1/3} = \frac{r_b}{R} = \left\{ 1 - \frac{n_i\ (1-N)\ RT_u}{V \qquad P} \right\}^{1/3} \quad \cdots \qquad IX\ (5)$$

from equation IX (2) noting that

$$P_I V = n_i RT_I,$$

equation IX (5) becomes

$$\frac{r_f}{R} = \left[1 - \frac{P_I}{P} \cdot \frac{T_u}{T_I} \cdot \frac{P_E - P}{P_E - P_I} \right]^{1/3} \quad \ldots\ldots \quad \text{IX (6)}$$

where dr_f/dt is the flame speed.

For adiabatic compression,

$$T_u = T_I \left(\frac{P}{P_I} \right)^{\frac{\gamma_u - 1}{\gamma_u}} \quad \ldots\ldots \quad \text{IX (7)}$$

The volume of an element before ignition $= 4\pi r_i^2 \, dr_i$

The volume of an element after ignition $= 4\pi r_i^2 \, dr_i \cdot \frac{T_u}{T_I} \cdot \frac{P_I}{P}$ $\ldots\ldots$ IX(8)

Since the thickness of the element $= S_u \, dt$

then the volume of the element $= 4\pi r_f^2 \, S_u \, dt$ ... IX (9)

Combining equations IX (7), (8), (9), the burning velocity at any instant is given by

$$S_u = \frac{dr_i}{dt} \left(\frac{r_i}{r_f} \right)^2 \left(\frac{P_I}{P} \right)^{\frac{1}{\gamma_u}} \quad \ldots\ldots \quad \text{IX (10)}$$

The procedure used for calculating the burning velocity was to plot values of 'r_i' obtained from equation IX (3) as a function of time from the pressure-time record so as to enable the slope $\frac{dr_i}{dt}$ to be determined at any instant. Values of 'r_b' were calculated from equation IX (6) from which the burning velocity could be estimated with the aid of equation IX (10).

Although the determination of burning velocities from the pressure-time record of an explosion in a closed vessel with central ignition have been proved reliable [45], the method has scarcely been tested [46] for slow burning mixtures. The reason is that for slow burning mixtures, convection causes early contact of the flame with the wall of the vessel and this results in excessive heat loss and distortion of the shape of the pressure-time record. In order to avoid these difficulties, it is necessary to confine the observations of pressure to the early stages of the explosion process during an interval of time in which the pressure rise is small.

The method employed in this work for determining the burning velocity of the pure ethylene oxide decomposition flame was similar to that employed by Manton, Lewis and von Elbe, [45] but in addition, a heat loss correction was applied to the pressure-time record. In order to make the correction it was assumed that the heat loss rate increased linearly from zero at the ignition point to a maximum at the end of the

explosion. Hence the pressure drop due to heat loss at any instant during the explosion is given by

$$\Delta P' = \Delta P'_T \left(\frac{t}{t_t} \right)^2 \qquad \text{IX (11)}$$

Therefore the true pressure at any instant during the explosion will be given by

$$P = P_I + \Delta P' + \Delta P \qquad \text{IX (12)}$$

where $\Delta P'$ is the pressure drop due to heat loss and ΔP is the pressure rise as the result of the explosion.

IX B Results:-

Figure 45 shows a plot of the radius of the burning surface, r_b, against time for a typical ethylene oxide decomposition explosion at an initial pressure of 84·7 PSIA. It may be seen that after a short deceleration period, the radial displacement of the flame front was uniform until it reached a radius of 5·55 cms, but thereafter the flame speed decreases owing to the compression of the products of decomposition and possibly contact of the flame with the vessel wall. The measurements used for the calculation of the burning velocity of the ethylene oxide decomposition flame were confined to the initial stages of the explosion where $P/P_I = 1{\cdot}25$ which corresponded to a flame radius, r_b, of approximately 4·0 cms. A specimen calculation for the burning velocity is given in

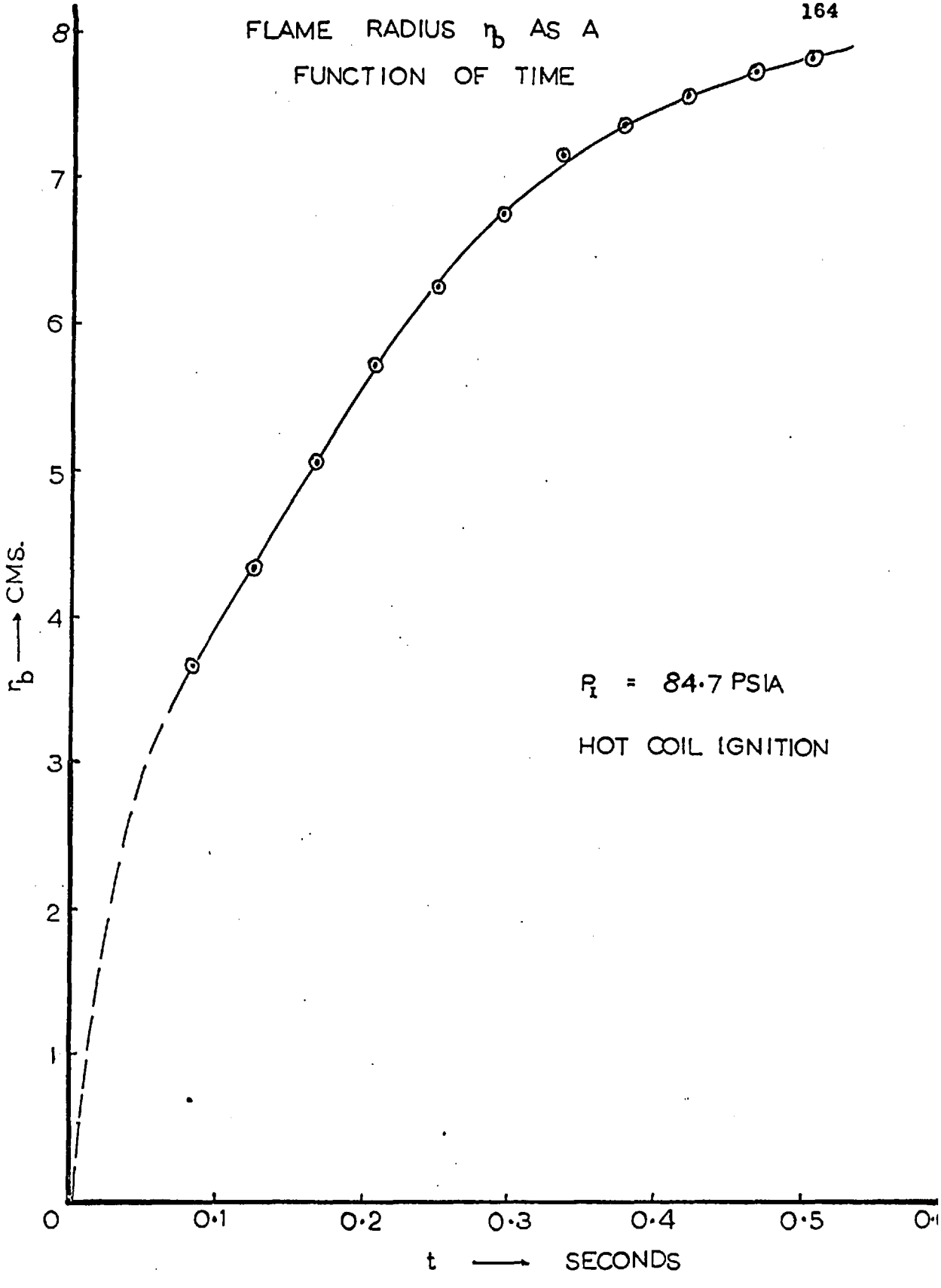
FLAME RADIUS r_b AS A FUNCTION OF TIME
r_b ⟶ CMS.
8
7
6
5
4
3
2
1
0
0·1
0·2
0·3
0·4
0·5
t ⟶ SECONDS
P_I = 84·7 PSIA
HOT COIL IGNITION

FIGURE 45

Appendix 3; it is estimated that the error involved in the determination of the burning velocity is ±5%. Figure 46 shows that the burning velocity of the ethylene oxide decomposition flame is not affected by changes in pressure from 3·0 atms. to 10 atms. The rapid fall of the burning velocity for pressures below 3·0 atms. is probably due to the limiting conditions of the apparatus for the decomposition flame to propagate.

IX C Discussion:-

Friedman and Burke [22][23], in their flat flame burner studies, were able to stabilise the ethylene oxide decomposition flame at pressures as low as 0·2 atmospheres and found that the burning velocity decreases as the pressure is increased from 0·2 to 1·5 atms. according to

$$S_u \propto P^{-\frac{1}{4}} \qquad \text{IX (13)}$$

On extrapolating their result to pressures and temperature corresponding to this work, it may be seen from Figure 46 that the burning velocities obtained in this work are of the same orders of magnitude as those determined by Friedman and Burke [22][23]. The burning velocity value of 12·5c/s as determined by Gerstein et al [17] in their tube method at 20°C and atmospheres pressure seems high and is unlikely to be reliable.

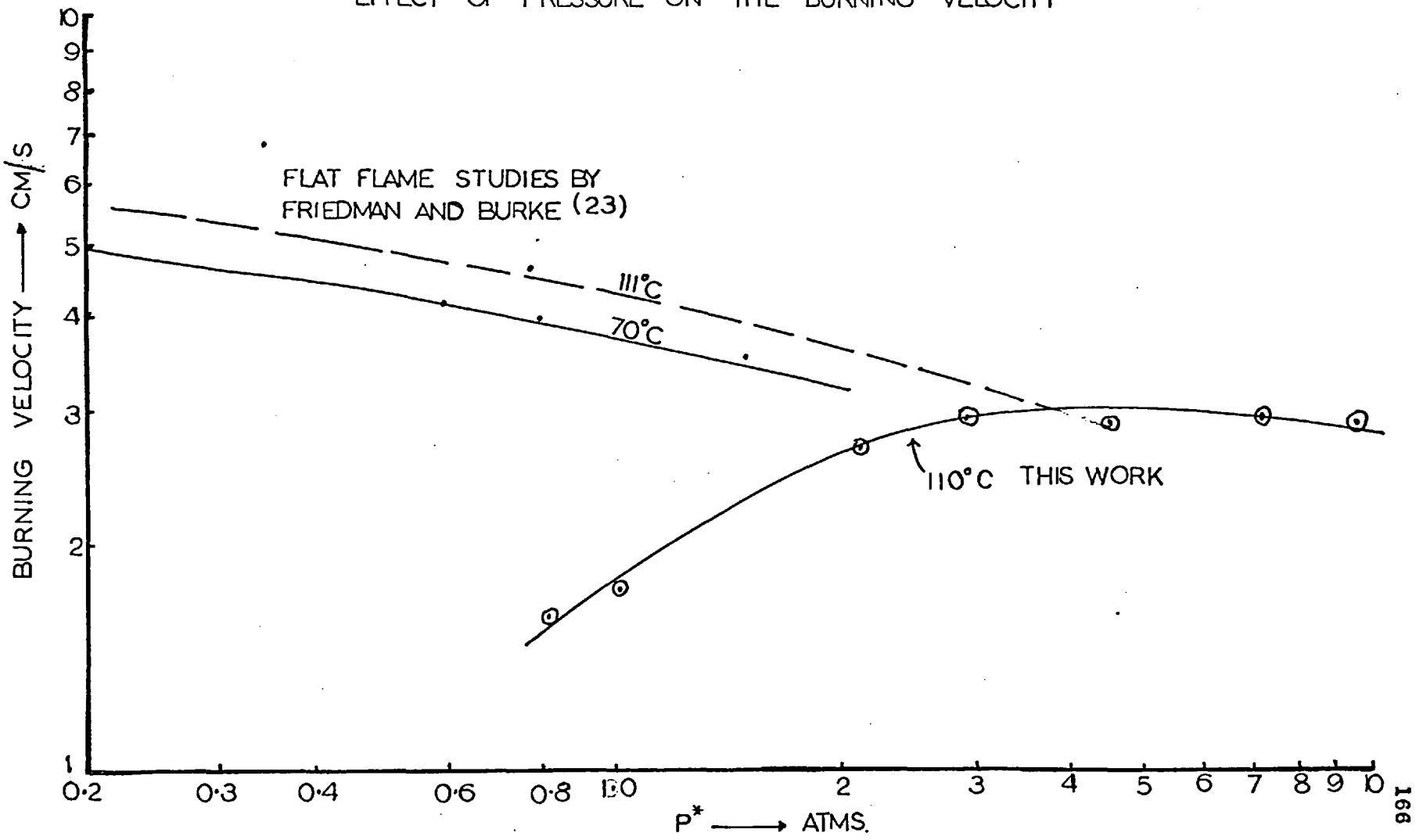
EFFECT OF PRESSURE ON THE BURNING VELOCITY
BURNING VELOCITY ——→ CM/S
10
9
8
7
6
5
4
3
2
1
FLAT FLAME STUDIES BY
FRIEDMAN AND BURKE (23)
111°C
70°C
110°C THIS WORK
0·2
0·3
0·4
0·6
0·8
1·0
2
3
4
5
6
7
8
9
10
P* ——→ ATMS.
168

FIGURE 46

The results obtained in this work indicate that for pressures above 3 atms., the burning velocity of the ethylene oxide decomposition flame is little affected by pressure. Now, according to the theory of flame propagation discussed in Chapter III, for simple flames of ideal gases, the burning velocity is given by

$$S_u \propto P^{\frac{n-2}{2}} \qquad \text{III (17)}$$

where 'n' is the overall order of the reaction. Therefore the measured burning velocity data suggests that the overall order for the decomposition flame reaction is a second order process. This is contrary to the findings in the low temperature kinetic work which concluded that the decomposition is a first order process. This discrepancy may be explained in the following way.

The burning velocity of an ethylene oxide decomposition flame can also be calculated from the thermal theories [18] of flame propagation given by the equations III (18), (19). However, these equations refer to conditions of the flame at constant pressures and the products at the end of the decomposition explosion in a closed vessel cannot be used to estimate the adiabatic flame temperature under constant pressure conditions. If the products of decomposition from a constant pressure burner [23] are used to estimate the adiabatic flame temperature and using the method given in Appendix 3 (b), the results as a function of flame temperature are as shown

in Figure 47. The calculated burning velocity of 6·45 c/s at 111°C and atmospheric pressure is high compared with the values of 4·5 c/s obtained by Friedman and Burke [23]. This discrepancy is not surprising considering the large number of assumptions that have had to be made to compute the burning velocity from the low temperature first order kinetics data. The interesting aspect of the calculated burning velocities shown in Figure 47 is that they are very sensitive to the flame temperature. Hence, should there be an increase in the flame temperature as the pressure is increased, the burning velocity will tend to increase. The effect of pressure on the products of decomposition of ethylene oxide has already been discussed in Chapter VI B and it was concluded that increasing amounts of methane will be formed as the initial pressure is increased. Inspection of Figure 15 shows that as the initial pressure is increased from 2 to 9 atms., there is an increase in methane formation per mole of ethylene oxide decomposed of about 0·06 moles. If it is assumed that the same increase in methane formation occurs in a constant pressure process, then this will lead to an increase in the flame temperature of about 50°K which according to Figure 47 will raise the burning velocity from 6·45 c/s to 10·0 c/s, (i.e. an increase of 3·55 c/s). But according to the first order rate equation, $S_u \propto P^{-\frac{1}{2}}$, a pressure increase from 2 atms. to 9 atms., will decrease the burning velocity from 6·45 c/s to 3·01 c/s., (i.e. a decrease of 3·44 c/s).

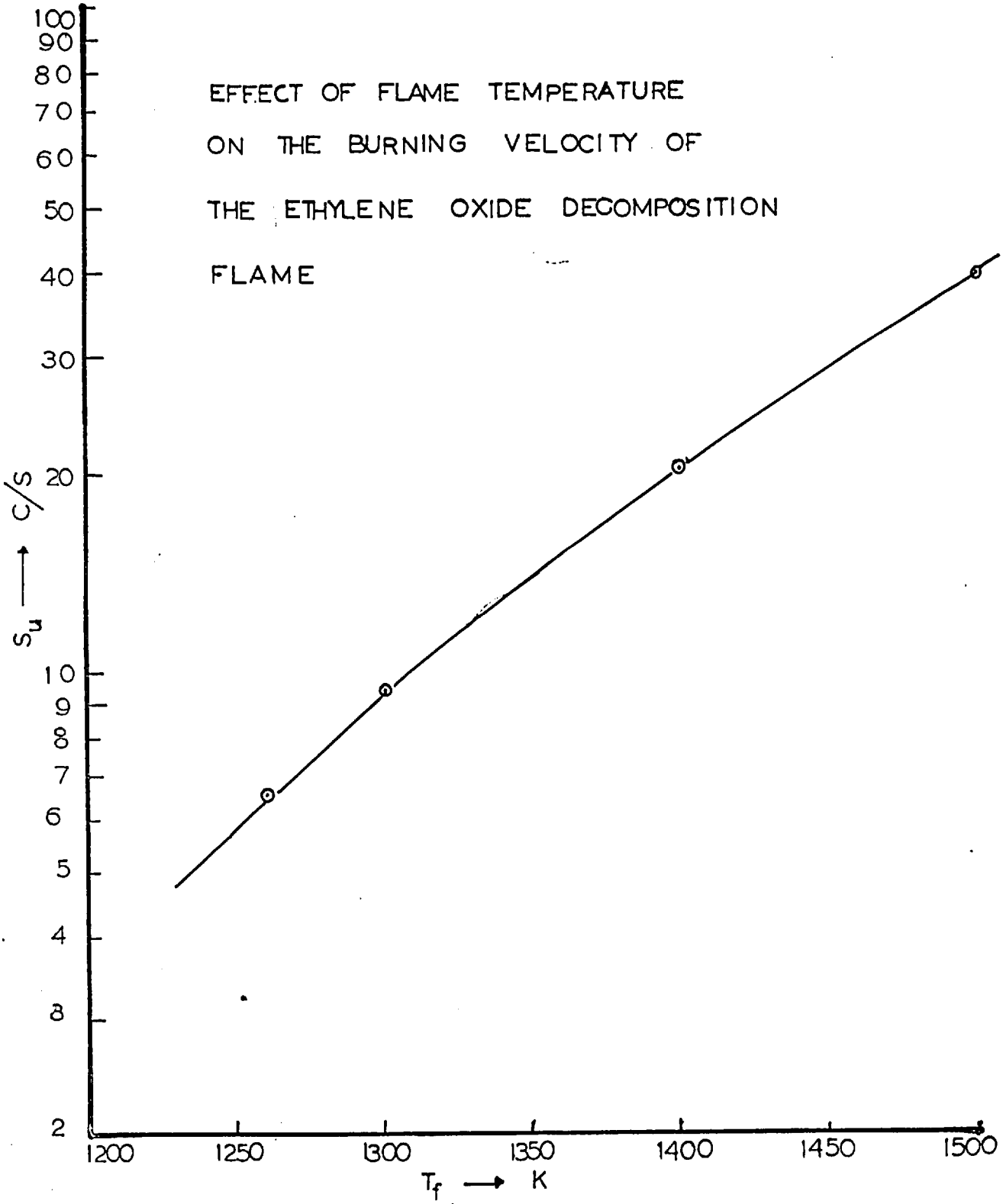
EFFECT OF FLAME TEMPERATURE
ON THE BURNING VELOCITY OF
THE ETHYLENE OXIDE DECOMPOSITION
FLAME
100
90
80
70
60
50
40
30
20
10
9
8
7
6
5
4
8
2
S_u ⟶ C/S
1200
1250
1300
1350
1400
1450
1500
T_f ⟶ K

FIGURE 47

It is therefore apparent that the decrease in burning velocity for a first order rate reaction is counterbalanced by its increase due to the increase in the flame temperature as the pressure is increased. In view of this, it may be concluded that the burning rate for the ethylene oxide decomposition flame is governed by the same first order reaction as that which governs the low temperature decomposition, but the temperature of the subsequent flame reactions depend on the pressure.

The effect of temperature on the burning velocity of the decomposition flame has not been studied in this work because an accurate knowledge of the flame temperature is required to deduce the activation energy of the overall process. However, Friedman and Burke [22][23] have studied this and obtained an overall activation energy of 14 kcals/mole which is not in agreement with the value of 52·7 kcals/mole employed for computing the burning velocity of the flame. These workers explained this discrepancy on the basis that pre-heating increases the flame temperature, favours the less exothermic reactions, with the result that the increase in the adiabatic flame temperature is small. (This topic was discussed in Chapter II B). Experimental evidence obtained in this work supports this view. For example it may be seen in Figure 14 that increasing the initial temperature from 20 to 100°C does in fact reduce the methane formation slightly. Also, if it is assumed that the presence of inert diluents in the flame merely acts as heat sinks and reduces the flame temperatures, then

Figures 33, 34, 35 shows that increasing amount of methane is formed which tends to favour flame reactions of the more exothermic type.

It is therefore apparent that kinetic information, such as the overall order of the reaction and its activation energy, obtained from the thermal theory of flame propagation [18] needs careful interpretation since some of the flame reactions are influenced by changes in pressure and pre-heat temperature.

IX D Tentative proposal for the explosive decomposition mechanism of the ethylene oxide vapour.

It has been shown that the rate controlling reaction in the decomposition flame is the same as that which governs the low temperature decomposition. Furthermore, the presence of large quantities of methane and hydrogen suggests that methyl radicals and hydrogen atoms play an important role in the explosive decomposition mechanism of the ethylene oxide vapour. On the basis of this information the following free radical reactions are proposed:-

$$\text{Initiation} \begin{cases} C_2H_4O \longrightarrow (CH_3 \cdot CHO)^{*} & \text{IX (14)} \\ (CH_3CHO)^{*} \longrightarrow \dot{C}H_3 + \dot{C}HO & \text{IX (15)} \end{cases}$$

$$\dot{C}HO \longrightarrow CO + H \qquad \text{IX (16)}$$

$$CH_3 + C_2H_4O \longrightarrow CH_4 + \dot{C}_2H_3O \qquad \text{IX (17)}$$

	$H + C_2H_4O$	$\longrightarrow$	$H_2 + \dot{C}_2H_3O$	IX 18
	$\dot{C}_2H_3O$	$\longrightarrow$	$C\ O + \dot{C}H_3$	IX 19
	$\dot{C}H_3 + \dot{C}H_3$	$\rightleftharpoons$	C_2H_6	IX 20
	$\dot{C}H_3 + C_2H_6$	$\longrightarrow$	$CH_4 + \dot{C}_2H_5$	IX 21
	$\dot{C}_2\dot{H}_5$	$\longrightarrow$	$C_2H_4 + H$	IX 22
	$\dot{C}H_3 + \dot{C}_2H_5$	$\longrightarrow$	C_3H_8	IX 23
termination	$\dot{C}_2H_5 + \dot{C}_2H_5$	$\longrightarrow$	C_4H_{10}	IX 24
	$\dot{C}H_3 + H$	$\longrightarrow$	CH_4	IX 25

Propane and butane have not been detected in the decomposition products; this may be due to the fact that under the decomposition flame conditions, they are unstable and decompose to give carbon and hydrogen. It has been shown in Chapter VI B that ethane is also unstable under the decomposition flame conditions and decomposed by the reverse of equation IX 20. In fact equations IX 20 to 25 merely represent the pyrolysis of ethane and give methane, ethylene and hydrogen. Ethylene being further pyrolysed to give carbon and hydrogen.

IX E Conclusion:-

The burning velocities of the ethylene oxide decomposition flame obtained from the pressure-time record were found to be in agreement with those obtained by Friedman and Burke [23]. Also the burning velocity

computed from Zeldovich-Frank-Kamenetsky's equation using the low temperature, first order reaction kinetics data of Mueller and Walters[10] agreed well with the experimental result. It was therefore concluded that the burning rate of the ethylene oxide decomposition flame is controlled by the same reaction that governs the low temperature decomposition rate. This rate controlling reaction is attributed to the isomerisation of ethylene oxide to acetaldehyde.

CHAPTER X

CONCLUSION.

The following conclusions can be drawn as a result of this investigation:-

(1) Pure ethylene oxide vapour will undergo explosive decomposition in the temperature range 20 to 100°C and pressures higher than 4·16 PSIA.

(2) The formation of methane in the decomposition products is favoured at initial pressures exceeding 30 PSIA, and that of ethylene is favoured at initial pressures below 30 PSIA.

(3) The products of decomposition are little affected by changes in the initial temperature between 20° to 100°C.

(4) Carbon is formed as a result of the pyrolysis of ethane and ethylene and not from methane.

(5) The maximum explosion pressure during the decomposition explosion is greatly influenced by heat losses from the flame to the surrounding walls of the vessel; this is particularly so for initial pressures of the ethylene oxide vapour below 30 PSIA.

(6) No simple relation between P_E/P_I and S/V ratio of the vessel was found to exist.

(7) N_2, H_2O, CO_2 and NH_3 act as inert diluents in suppressing the decomposition explosion and the amount of each required is governed by the relation that the product of its mean specific heat and the amount of diluent required per mole of ethylene oxide is constant at a fixed temperature and pressure.

(8) The amount of inert diluent required to suppress the decomposition explosion is a function of both the initial temperature and pressure.

(9) It is shown that the discrepancy between the results of Hess and Tilton [26] and Burgoyne et al [24] is due to the incorrect assumption that the amount of inert diluent required is independent of temperature.

(10) Methanol and propylene oxide also suppress the decomposition explosion but act as chemically active diluents; whereas methanol lowers the adiabatic limit flame temperature, propylene oxide increases it.

(11) The burning velocity of the decomposition flame obtained in this investigation is in agreement with previous worker made with a flat flame burner.

(12) The rate controlling reaction in the decomposition flame is the same as that which governs the low temperature decomposition, i.e. the isomerisation of ethylene oxide to an excited acetaldehyde molecule.

APPENDICES

Appendix (1)

Purity of materials:-

It is known that ethylene oxide may polymerise to acetaldehyde during storage. Although each 50 pound cylinder was renewed every three months by Shell Chemicals Ltd., aldehyde content in the ethylene oxide bottle was periodically analysed by the bisulphite method.[40] During each three months, the aldehyde content was found to be within the suppliers specifications. A summary of the purities of the other materials used in this investigation is given in Table A1.

Appendix (2)

2 (a) Estimation of the overall heat transfer coefficient 'h'.

The overall heat transfer coefficient 'h' during the cooling process following the decomposition explosion was estimated from the cooling curve which gave

$$\log \left\{ \frac{P_E^* - P_F^*}{P^* - P_F} \right\} = \frac{h S}{n_e C_v 2{\cdot}303} . t \qquad \text{VI (16)}$$

A plot of L.H.S. against 't' is shown in Figure 22 to give a straight line whose slope, B', is given by

$$B' = \frac{h\,S}{n_e\,\bar{C}_v\,2{\cdot}303} \qquad A\ (1)$$

Now, according to the ideal gas law,

$$P^{*}\,V = n_e R T_E \qquad A\ (2)$$

Combining equations A (1) and A (2).

$$B' = \frac{h}{\bar{C}_v} \cdot \frac{S}{V} \cdot \frac{R\,T_E}{2{\cdot}303\,P_E^{*}} \qquad A\ (3)$$

where $\bar{C}_v$, is the mean specific heat of the product, 9·5 cals/m/^{o}K

S/V, is the surface/volume ratio of vessel, 0·421 cm^{-1}

R, is the gas constant 82·06/g mole

Table A_2 gives the results for B' and h at various initial and final explosion pressures.

2 (b) Estimation of the total pressure drop due to heat loss during the explosion period.

The drop in pressure equivalent to the heat loss during the explosion is given by

$$\Delta P' = \tfrac{1}{2} \left(\frac{-dP^*}{dt}\right)_{MAX} t_t \text{ atms.} \qquad \text{VI (22)}$$

where $$\left(\frac{-dP^*}{dt}\right)_{MAX} = \frac{h\,S}{n_e\,\bar{C}_v} \left(P_E^* - P_F^*\right) \qquad \text{VI (15)}$$

The overall heat transfer coefficient 'h' is correlated with the maximum explosion pressure by the following equations

$$h = 0.66 \times 10^{-3} \left(P_E^*\right)^{0.6}, \text{ exploding wire ignition,} \qquad \text{VI(17)}$$

$$h = 0.52 \times 10^{-3} \left(P_E^*\right)^{0.6}, \text{ hot coil ignition,} \qquad \text{VI(18)}$$

By combining equations VI (15), VI (17) and A (2), the maximum rate of pressure drop due to heat loss for an explosion initiated by an exploding wire can be expressed as

$$\left(\frac{dP^*}{dt}\right)_{MAX} = 2.4 \times 10^{-3}\, T_E \left(P_E^* - P_F^*\right)\left(P_E^*\right)^{-0.4} \text{ atms/s} \qquad \text{A(4)}$$

from which $\Delta P'$ can be calculated. A summary of the results is given in Table A3.

A 2 (c) Estimation of $(P_E/P_I)_o$ for 100% decomposition:-

For any gaseous explosion in a closed vessel, the mean maximum temperature attained is given by

$$T_E - T_I = \frac{\eta \beta \Delta U_D}{\beta \Sigma n_j \bar{C}_{vj} + (1-\beta)\bar{C}_{vi}} \qquad A\ (5)$$

where η : fraction of heat lost;

β fraction of ethylene oxide decomposed,

ΔU_D heat of decomposition, cal/mole.

$\bar{C}_{vj}$ mean molar specific heat for product, species 'j'.

n_j moles of product 'j' per mole of ethylene oxyde decomposed.

$\bar{C}_{vi}$ mean molar specific heat for ethylene oxide

Similarly, for 100% decomposition,

$$T_{EO} - T_I = \frac{\eta \Delta U_D}{\Sigma n_j \bar{C}_{vj}} \qquad A\ (6)$$

Combining equations A (5) and A (6)

$$\frac{T_{EO} - T_I}{T_E - T_I} = 1 + \frac{(1-\beta)\bar{C}_{vi}}{\beta \Sigma n_j \bar{C}_{vj}} \qquad A\ (7)$$

According to the gas law,

$$P_{EO}/P_E = \frac{n_{eo}}{n_e} \cdot \frac{T_{EO}}{T_E} \qquad A\ (8)$$

where the subscript (o(represents 100% decomposition. From equations A (7) and A (8) the maximum explosion pressure, P_{EO}, for 100% decomposition can be calculated. The result is shown in Table A4.

Appendix 3.

A (3) (a) Calculation for S_u from the P - t curve:-

The calculation for the burning velocity S_u of an ethylene oxide decomposition flame for a typical explosion with an initial temperature of 100°C and pressure at 35 PSIA using a hot coil ignition source is as follows:-

P'_E,	maximum explosion pressure corrected for heat loss	= 333 PSIA
P_I,	initial pressure	= 35 PSIA
$\Delta P'_T$,	total pressure due to heat loss	= 51.8 PSIA
t_t,	total explosion time	= 0·35 s.
R,	radius of vessel, (equivalent volume)	= 8·11 cms.
γ_u,	ratic of specific heats for ethylene oxide	= 1·16

Pressure drop due to heat loss at any instant during the explosion is given by

$$\Delta P' = \Delta P'_T \left(\frac{t}{t_t} \right)^2 \qquad \text{IX (11)}$$

Hence the true pressure during the explosion,

$$P' = P_I + \Delta P' + \Delta P \qquad \text{IX (12)}$$

where $\Delta P'$ is the pressure drop due to heat loss,

ΔP is the pressure rise due to explosion.

Now, before ignition, the radius of unburnt element, r_i, is given

$$\frac{r_i}{R} = \left\{ \frac{P' - P_I}{P'_E - P_I} \right\}^{1/3} \qquad \text{IX (3)}$$

After ignition,

$$\frac{r_b}{R} = \left\{ 1 - \frac{P_I}{P} \cdot \frac{T_u}{T_I} \cdot \frac{P'_E - P'}{P'_E - P_I} \right\}^{1/3} \qquad \text{IX (6)}$$

The burning velocity S_u is given as

$$S_u = \frac{dr_i}{dt} \cdot \left(\frac{r_i}{r_b}\right)^{1/\gamma_u} \qquad \text{IX (10)}$$

Values for r_i and t are given in Table A6 and the slope dr_i/dt at any instant may be obtained from Figure A1.

At the instant when $P/P_I = 1{\cdot}25$, $r_i = 2{\cdot}5$ cms., $r_b = 4{\cdot}75$ cms. and $dr_i/dt = 12{\cdot}62$ c/s., then,

$$S_u = 12{\cdot}62 \times \left(\frac{2{\cdot}5}{4{\cdot}75}\right)^2 \times (0{\cdot}8)^{0{\cdot}862} = 2{\cdot}89 \text{ c/s.}$$

A summary of the burning velocities for the ethylene oxide decomposition flame under various conditions is given in Table A7.

3 (b) Computation of S_u from the thermal theory of flame propagation.

From the theories of Zeldovich, Frank-Kamenetsky and Semenov discussed in Chapter III, the following equation was derived,

$$2 \log S_u = \log B + 2 \log T_I + 4 \log T_f - 2 \log (T_f - T_I) \frac{-E}{2{\cdot}303\, RT_f} \qquad \text{III (20)}$$

where $B = \dfrac{2\lambda'_f}{(273)^2 \rho_{io}} \dfrac{A\, C_{pf} \cdot n_I \cdot R^2}{\ddot{C}_p^2 \cdot n_f \quad E^2}$ III (19)

The products of decomposition under constant pressure conditions [23] gives the adiabatic flame temperature as 1260°K. Now,

ρ_{io}, density of ethylene oxide vapour at 0°C(1atm.press) = $1{\cdot}965 \times 10^{-3}$ g/cc.

λ'_f, thermal conductivity of products at 0°C = $1{\cdot}288 \times 10^{-4}$ cal/cm/°K

$\bar{C}_{pf}$, mean specific heat of products (800°K) = 1·285 cal/g/°C

C_p, specific heat of product at flame temperature = 1·362 cal/g/°C

Using the low temperature kinetics data of Walters and Mueller [10], i.e.

$$k = 1{\cdot}5 \times 10^{13} \; e^{\frac{-52700}{RT}} \qquad \text{II (7)}$$

then the calculated value for B is 0·128, from which the burning velocity can be computed for given values of T_I and T_f. Table A 8 gives the effect of flame temperature on the computed burning velocity of the ethylene oxide decomposition flame.

TABLE AI PURITY OF CHEMICALS EMPLOYED

MATERIAL	SUPPLIER	FURTHER PURIFICATION	PURITY % by weight	CHIEF IMPURITIES
Ethylene Oxide	Shell Petrochemicals	None	> 99·5	Acetaldehyde Water
Propylene Oxide	B.D.H.	Distilled over N_2 (34°C)	> 99·9	-
Methanol	H & W (Analar)	None	> 99·8	Aldehydes Ketones
Ammonia	I.C.I.	None	> 99·9	-
Nitrogen (O_2 Free)	B.O.C.	None	> 99·9	-
Carbon Dioxide	B.O.C.	None	> 99·9	-
Water	College Distilled Water	None	> 99·9	-

TABLE A2 OVERALL HEAT TRANSFER COEFFICIENT

EXPLODING WIRE IGNITION $T_I = 100^{\circ}C$

P_I PSIA	P_E PSIA	P_E^* ATMS	P_F^* ATMS	T_E $^{\circ}K$	B' -	$h \times 10^3$ cal/m/cm^2
4.66	22.2	1.63	0.654	935	0.87	0.96
6.92	36.4	2.96	0.970	1140	0.723	1.19
14.7	100.7	6.85	2.08	1240	0.604	2.11
25.0	206.5	14.00	3.57	1280	0.514	3.55
28.7	218.0	14.80	4.40	1282	0.471	3.44
44.7	329.5	25.40	8.38	1410	0.356	4.06
74.7	669.7	45.50	12.22	1465	0.198	3.90
HOT COIL IGNITION						
9.7	58.7	4.0	1.36	1002	0.519	1.31
12.2	79.2	5.4	1.73	1050	0.456	1.49
35.0	283.0	19.3	5.40	1350	0.320	2.90
54.7	483.0	32.8	8.90	1400	0.237	3.55
84.7	817.0	55.5	14.23	1397	0.151	3.80
114.7	1127.0	76.7	30.4	1430	0.112	3.81

TABLE A 3 COMPARISON OF P_E/P_I, P_F/P_I and $\left(\frac{P_E}{P_I}\right)_c$

EXPLODING WIRE IGNITION $T_I = 100^oC.$

P_I PSIA	P_E^* ATMS	P_F^* ATMS	P_F/P_I -	N_F/N_I -	T_E ^oK	$(P_E^*)^{-0.4}$ -
4.17	1.37	0.58	2.05	2.04	883	0.88
4.66	1.63	0.65	2.06	2.05	935	0.82
6.92	2.96	0.97	2.06	2.05	1140	0.65
6.96	2.83	0.98	2.06	2.05	1087	0.66
14.70	6.85	2.08	2.08	2.06	1240	0.46
25.0	14.0	3.57	2.20	2.10	1280	0.35
28.7	15.5	4.40	2.25	2.21	1340	0.33
28.7	14.8	4.40	2.25	2.21	1282	0.34
44.7	25.4	8.38	2.28	2.21	1410	0.27
74.7	45.5	12.22	2.41	2.28	1465	0.22
74.7	43.8	11.90	2.35	2.22	1460	0.22
104.7	65.2	17.80	2.50	2.30	1485	0.19
134.7	86.4	24.00	2.62	2.30	1530	0.17

TABLE A 3 Continued

$(\frac{dP}{dt})_{MAX}$	$\Delta P'$	t_t	P_E/P_I	P'_E/P_I	$(P_E/P_I)_c$
PSI/S	PSI	s.	-	-	-
25.0	7.4	0.685	4.83	6.61	7.27
27.0	3.4	0.260	5.14	5.95	7.27
46.0	8.4	0.324	6.28	7.75	-
54.0	13.6	0.578	5.98	7.91	7.72
95.0	20.2	0.318	6.85	8.22	8.32
150	28.6	0.355	7.20	9.39	-
159	28.5	0.324	7.96	8.96	9.64
146	42.0	0.571	7.6	9.05	9.60
178	52.6	0.454	8.35	9.51	9.70
304	53.0	0.283	8.95	9.70	9.95
296	66.5	0.368	8.61	9.50	9.69
364	56.5	0.241	9.16	9.71	10.05
430	53.0	0.188	9.42	9.85	10.05

TABLE A4 ESTIMATION OF $(P_E/P_I)_o$ FOR 100% DECOMPOSITION

$T_I = 100^oC.$

P_I PSIA	S/V cm^{-1}	P_E/P_I -	T_E ^oK	$\Sigma n_j \bar{C}_{vj}$ cals/^oK	$\bar{C}_{vi}$ cals/M/^oK	β -	$\beta(\Sigma n_j \bar{C}_{vj})$ cal/^oK
14.7	0.421	6.85	1220	18.4	25.0	0.981	18.03
14.7	0.540	5.95	1058	17.5	23.4	0.873	15.28
14.7	1.655	3.50	764	15.2	19.0	0.658	10.00
25.0	0.421	7.7	1305	18.9	25.8	0.981	18.52
25.0	0.540	6.92	1160	18.1	24.4	0.89	16.10
25.0	1.655	3.66	772	15.8	22.5	0.604	9.55
45.0	0.421	8.35	1380	19.3	26.3	0.99	19.10
45.0	0.540	7.65	1290	17.9	24.0	0.877	15.70
45.0	1.655	3.84	779	15.9	20.3	0.51	8.10

TABLE A4 Continued

$(1-\beta)\,\bar{C}_{vi}$ cal/°K	π_e/π_I -	π_{eo}/N_I -	π_{eo}/π_e -	T_{EO} °K	$\frac{T_{EO}-T_I}{T_E-T_f}$ -	T_{EO}/T_E -	$(P_E/P_I)_o$
0.487	2.06	2.082	1.001	1243	1.027	1.02	7.0
2.985	2.06	2.082	1.011	1192	1.196	1.13	6.8
6.500	1.71	2.082	1.218	1018	1.650	1.33	5.67
0.308	2.220	2.23	1.005	1319	1.017	1.01	7.81
2.680	2.217	2.23	1.007	1292	1.166	1.11	7.77
8.910	1.768	2.23	1.261	1144	1.934	1.48	6.85
0.263	2.215	2.30	1.012	1393	1.014	1.01	8.54
2.960	2.21	2.30	1.04	1340	1.189	1.04	8.28
9.950	1.792	2.30	1.282	1238	2.23	1.59	7.83

TABLE A 5 VALUES OF $(P_E/P_I)_o$ AND 'X'.

$T_I = 100^oC$

P_I	$(P_E/P_I)_o$	P^*_{EO}	$(P^*_{EO})^{-0.4}$	S/V	t_t	X
PSIA	-	ATMS	-	CM^{-1}	S.	-
14.7	7.0	7.0	0.460	0.421	0.318	4.67
14.7	6.8	6.8	0.464	0.540	0.253	4.72
14.7	5.67	5.67	0.499	1.655	0.200	2.08
25.0	7.81	13.3	0.354	0.421	0.318	6.10
25.0	7.77	13.2	0.356	0.540	0.218	7.05
25.0	6.85	11.62	0.374	1.655	0.199	2.68
45.0	8.54	26.1	0.272	0.421	0.454	5.94
45.0	8.28	25.3	0.274	0.540	0.391	5.50
45.0	7.83	24.0	0.280	1.655	0.193	3.65

TABLE A 6 VALUES FOR 'r_i' and t.

P_I = 84.7 PSIA T_I = 100°C. HOT COIL IGNITION

ΔP PSI	$\Delta P'$ PSI	$(P'-P_I) = (\Delta P + \Delta P')$ PSI	$\frac{P'-P_I}{P'_E-P_I}$ -	$\left\{\frac{P'-P_I}{P'_E-P_I}\right\}^{1/3}$ -	r_i cms.	t S.
0	0	0	0	0	0	0
1.99	0.146	2.14	0.0072	0.193	1.570	0.045
3.84	0.585	4.43	0.0149	0.246	1.995	0.090
8.11	1.32	9.43	0.0316	0.316	2.56	0.135
14.51	2.34	16.85	0.0565	0.384	3.12	0.180
21.62	3.64	25.26	0.0846	0.439	3.57	0.226
30.60	5.29	35.89	0.1183	0.491	3.99	0.271
43.0	7.15	50.15	0.1682	0.552	4.48	0.316
57.5	9.38	66.88	0.224	0.606	4.91	0.361
73.4	11.92	85.32	0.286	0.660	5.35	0.406
91.1	14.66	105.8	0.354	0.706	5.73	0.451
108.3	17.60	125.9	0.422	0.750	6.09	0.496

TABLE A 7 BURNING VELOCITY OF ETHYLENE OXIDE

HOT COIL IGNITION $P/P_I = 1.25$, $T_u/T_I = 1.03$, $T_u = 384\ ^oK$

P_I PSIA	P^* ATMS.	S_u c/s
9.7	0.825	1.59
12.2	1.038	1.74
25.0	2.12	2.68
35.0	2.98	2.89
54.7	4.65	2.86
84.7	7.20	2.91
114.7	9.75	2.89

TABLE A 8 CALCULATED BURNING VELOCITY FROM ZELDOVICH, FRANK-KAMENETSKY; SEMENOV'S EQUATION

$T_I = 484^oK.$ $B = 0.128$

T_f ^oK	2 log T_I -	4 log T_f -	2 log(T_f-T_I) -	$\frac{E}{2.303RT_f}$ -	2 log S_u -	S_u C/S
1260	5.166	12.400	5.888	9.15	1.632	6.55
1300	5.166	12.456	5.926	8.86	1.944	9.36
1400	5.166	12.586	6.014	8.24	2.606	20.1
1500	5.166	12.704	6.096	7.69	3.192	39.4
1600	5.166	12.816	6.170	7.20	3.650	65.5

TABLE A 9 RESULTS OF FLAMMABILITY LIMITS.

(a) NITROGEN:-

T_I	P_I	$\% N_2$
^oC	PSIA	-
20	14.7	16
41	14.7	21
41	25.0	25
60	14.7	24
60	25.0	28
60	44.7	37
81	14.7	29
81	25.0	32
80	44.7	41
80	74.7	46
100	14.7	33
100	25.0	37
100	44.7	45
100	74.7	51

(b) CARBON DIOXIDE

T_I	P_I	% N_2
°C	PSIA	-
42	25	17
59	25	20
80	25	23
100	25	26

(c)

T_I = 100°C P_I = 25 PSIA

DILUENT	% DILUENT
Steam	32
Methanol	16
Ammonia	24
Propylene Oxide	25

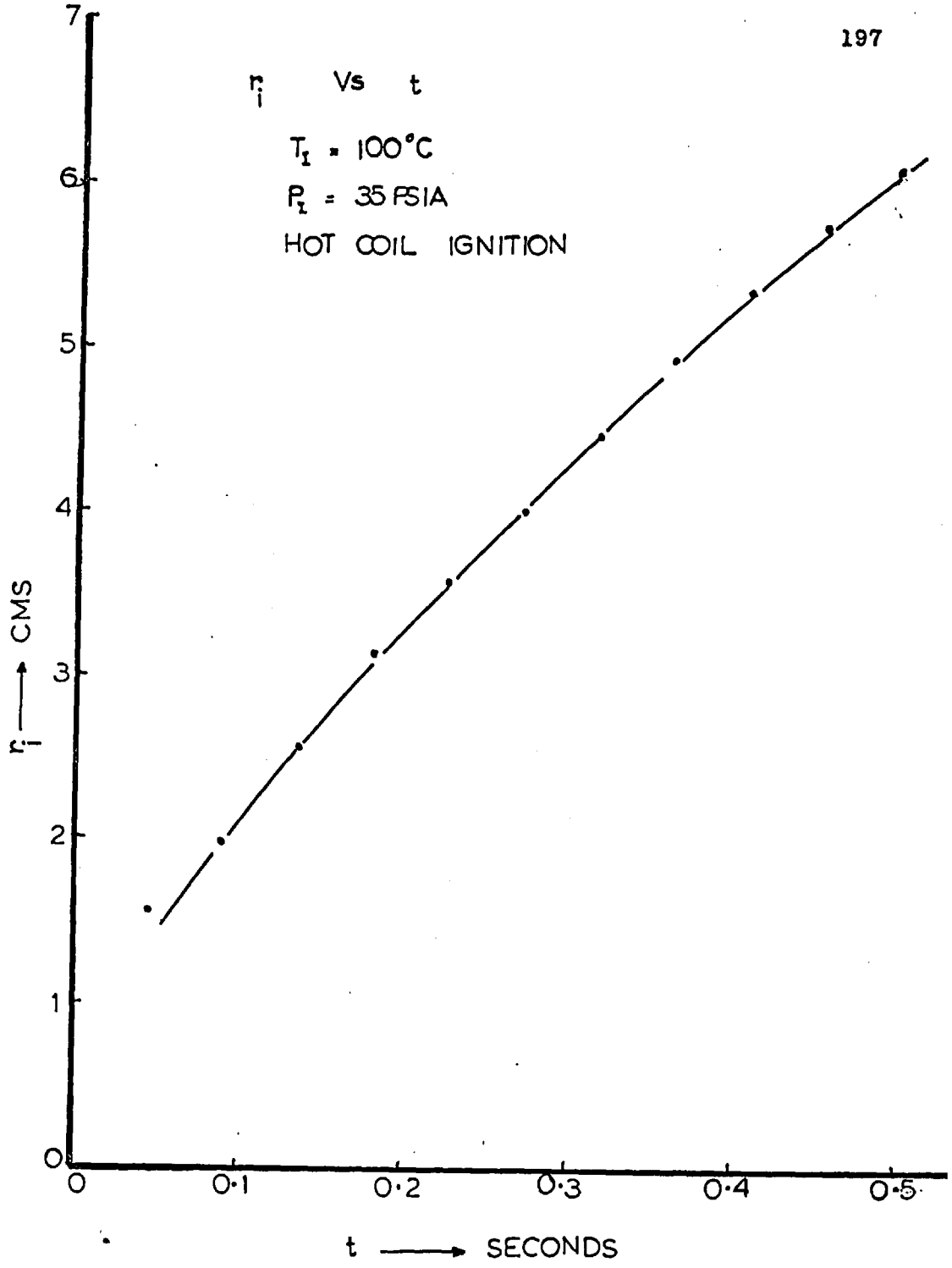
r_i Vs t
T_I = 100°C
P_I = 35 PSIA
HOT COIL IGNITION
r_i ⟶ CMS
t ⟶ SECONDS
0
1
2
3
4
5
6
7
0
0·1
0·2
0·3
0·4
0·5

FIGURE A1

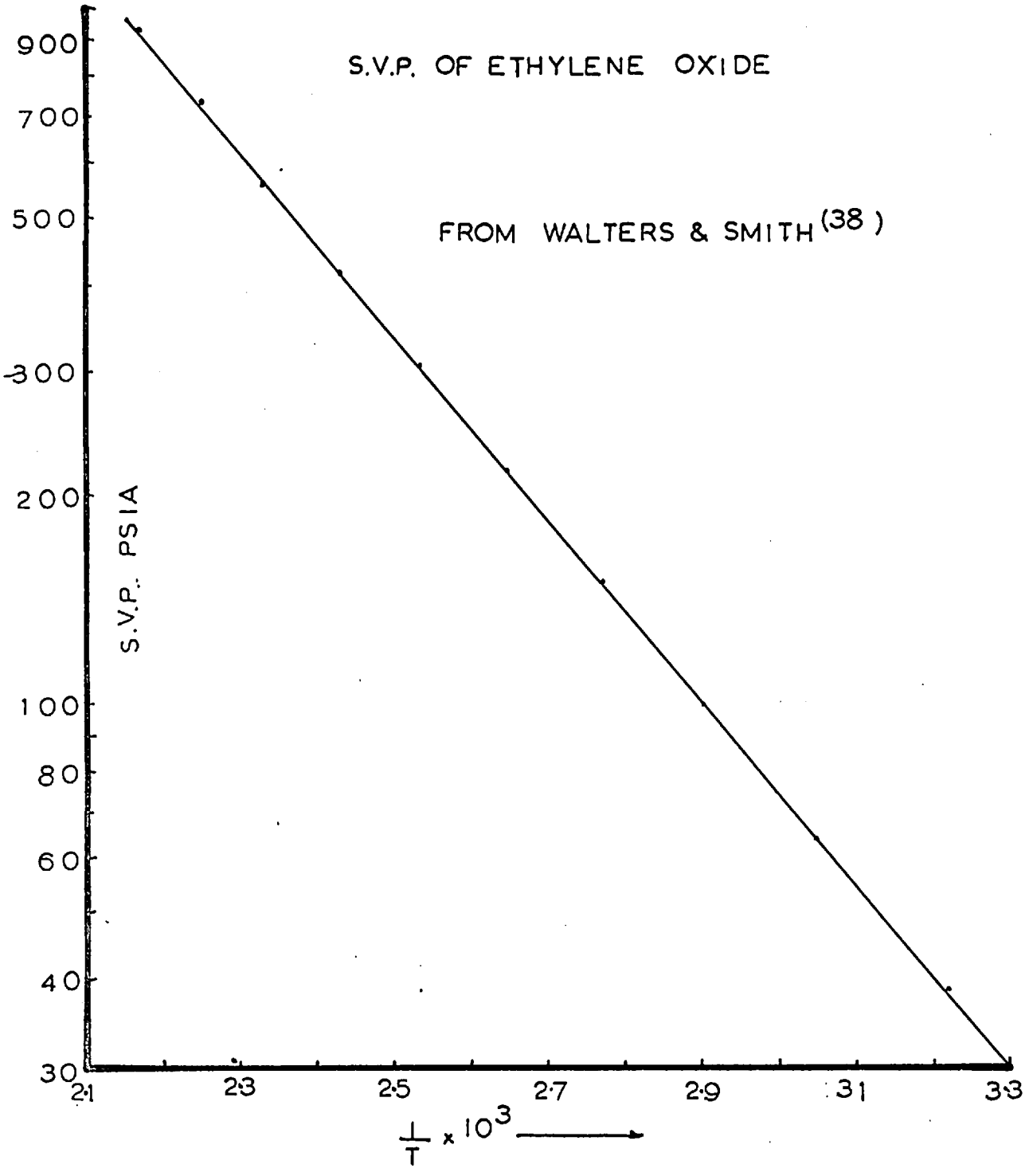
S.V.P. OF ETHYLENE OXIDE
FROM WALTERS & SMITH (38)
S.V.P. PSIA
900
700
500
300
200
100
80
60
40
30
2·1
2·3
2·5
2·7
2·9
3·1
3·3
1/T x 10^3

FIGURE A 2

References

1. Lewis, B., von Elbe, G., Combustion, flames and explosions of gases, Academic Press.
2. Jost, W., Explosion and combustion processes in gases, McGraw-Hill.
3. Gaydon, A.G., Wolfhard, H.G., Flames, Chapman and Hall.
4. Stearcie, E.W.R., Atomic and free radical reactions, volumes (1) and (2)., Reinhold.
5. Heckert, W.W., Mack, E. Jr., J.A.C.S. 51, 2706, 1929.
6. Fletcher, C.J.M., J.A.C.S., 58, P1, 534, 1936.
7. Fletcher, C.J.M., Rollefson, G.K., J.A.C.S. 58, 2135, 1936.
8. Thompson, H.W., Meissner, M., Trans. Fara. Soc. 32, 1451, 1936.
9. Mueller, K.H. Walters, W.D., J.A.C.S. 73, 1458, 1951.
10. Muller, K.H. Walters, W.D., J.A.C.S. 76, 330, 1954.
11. Simard, G.L., Steger, J., et al, J. Chem. Phys. 16, 836, 1948.
12. Benson, S.W., J. Chem. Phys. 40, No. 1, 104, 1964.
13. Crocco, L., Glassman, I., Smith, I.E. J. Chem. Phys. 31, No. 2. 506, 1959.
14. Lossing, F.P., Ingold, K.U., Tickner, A.W., Diss. Fara. Soc. No. 14, 34, 1953.
15. Polanyi, J.C., Diss. Fara. Soc. No. 14, 115, 1953.
16. Burden, F.A., Burgoyne, J.H., Proc. Roy. Soc. A199, 328, 1949.

17. Gerstein, M., Mcdonald, G.E., Schalla, R.L., 4th Int. Sym.P.375

18. Zeldovich, Semenov, NA.C.A. T.M. 1084. 1946.

19. Boys, S.F., Corner, J., Proc. Roy. Soc. A 197, 90, 1949.

20. Adams, Univ. Wisconsin Naval Research Lab. C-F 957.

21. Hirchfelder, J.O., Curtis, C.F., 3rd Int. Sym. Combn. P.121.

22. Friedman, R., Burke, E., J. Chem. Phys. 21, 165, 1953.

23. - - 5th Int. Sym. Combn. P.596.

24. Burgoyne, J.H., Bett, K.E., Muir, R., Sym. on plant hazards. with reference to plant design, P.30-36, 1960.

25. Gordon, L.J., Green, S.H., J. Am. Rocket Soc. 27, 798, 1957.

26. Hess, L.G., Tilton, V.V., Ind. & Eng. Chem. June, 1251, 1950.

27. Jones, G.W., Kennedy, R.E., Ind. Eng. Chem. 22, 146, 1930.

28. Jones, R.M., Ind. Eng. Chem. 25, 394, 1933.

29. Peters, G., Gantes, W., Angew. Chem., 51, 29, 1938.

30. Litchfield, E.L., Combn. and Flame. 5, No. 3, P 235, 1961.

31. Chace., W.G., Exploding Wires, Chapman and Hall, 1959.

32. Stevens, D.R., Royal Aircraft Establishment, Farn., private communication.

33. Yang. J.Y., Wolf, A.P., J.A.C.S. 82, Pt.3, 4488, 1960.

34. Feigl, F., Spot tests; Elsevier Pub. Co. 1960.

35. Courtney, W.G., et. al. J. Am. Rock. Soc. 32, (10), 1530, 1962.

36. Coward, H.F., Jones, G.W., U.S. Bur. of Mines. Bullet. 503, 1952.

37. Egerton, A., Powling, J., Fuel. 28, 25, 1949.

38. Walters, C.J., Smith, J.M., Chem. Eng. Progress. 48, 337, 1952.

39. Kozlov, G.I., Knorre, V.G., Comb. and Flame. V.6. No. 4. P. 253. Dec. 1962.

40. Reid, V.W., Salmon, D.G., The analyst, 80, No. 953, 602, 1955.

41. Gottenberg, W.G., Olson, D.R., Best, H.W., Comb. & Flame, 7, 9, 1963.

42. Daniels, W.A., 6th Int. Sym. Combn. P. 886.

43. Friedman, R., Johnston,W.C., J. Appl. Physics., 21, 791, 1950.

44. Marrin, Coldwell, Roeder, N.A.C.A. Aero. report No. 682, 1940.

45. Manton, J., Lewis, B., von Elbe, G., 4th Int. Sym. Combn.P.358.

46. Gray, P., Lee, C.J., 7th Int. Sym. Combustion, P.61.

47. Kaye. G.W., Laby, T.H., Tables of Physical and Chem. Constants, Longmans.

48. Evans, M.W., Chem. Review, 51, 363, 1952.

49. Gray, P., Lee, C.J., 6th Int. Sym. Combn. P. 255.

50. Hicks, J.A., 8th Int. Sym. Combn. P.487.

51. Dixon-Lewis,G., Isles, G.L., 7th Int. Sym. Combn. P.475.

52. Pechkin, M.A., J. Phys. Chem. (U.S.S.R.), 28, 433, 1954.

53. Egerton, A., Powling, J., Proc. Roy. Soc. A 193, 190, 1948.

54. Egerton, A., Thabet, S.K., Proc. Roy. Soc. A 211, 445, 1952.

55. Zabetakis, M.G., Lamiris, S., Scott, G.S., 7th Int. Sym. Combn. P 484.

56. Dixon-Lewis, G., Linnet, J.W., Proc. Roy. Soc. A 210, 48, 1951-52.

57. Egerton, A., 4th Int. Sym. Combustion P.4.

58. White, A.G., J. Chem. Soc. 127, 672, 1925.

59. Fletcher, C.J.M., Proc. Roy. Soc., A 147, 119, 1934.

60. Int. Critical Tables.

61. Egloff, Reactions of hydrocarbon.

62. Dever, D.F., Finch, A., Grunwood, E., J. Phys. Chem. 59, 668, 1955.

63. Shell Chemicals, technical bulletin G.C./12.

64. Katzen, R., Petroleum Refiner, 39, No. 1. 167, 1960.

65. Collinswood, P.N., Mackintosh, C.F.M., Steiner, H., Petroleum Times, 61, 146, 1957.

66. Gupta, A.K., J. Soc. Chem. Eng. (Lond.) 68, 179, 1949.